

WINCO-1060  
NOVEMBER 1988

TRA Library C1  
Copy 2 of 2

MODELING HYPOTHETICAL GROUNDWATER TRANSPORT OF NITRATES,  
CHROMIUM, AND CADMIUM AT THE IDAHO CHEMICAL PROCESSING PLANT

T. R. Thomas

1	1	19
K. Jones	Plants	10-17-90
J. Jones	11/28/90	



**IDAHO NATIONAL ENGINEERING LABORATORY**

*Managed by the U.S. Department of Energy*

Prepared for the  
U.S. Department of Energy  
Idaho Operations Office  
Under DOE Contract No. DE-AC07-84ID12435



**Westinghouse Idaho Nuclear Company, Inc.**  
Idaho Falls, Idaho 83403

#### DISCLAIMER

This book was prepared as an account of work sponsored by an agency of the United States Government. Neither the United States Government nor any agency thereof, nor any of their employees, makes any warranty, express or implied, or assumes any legal liability or responsibility for the accuracy, completeness, or usefulness of any information, apparatus, product or process disclosed, or represents that its use would not infringe privately owned rights. References herein to any specific commercial product, process, or service by trade name, trademark, manufacturer, or otherwise, does not necessarily constitute or imply its endorsement, recommendation, or favoring by the United States Government or any agency thereof. The views and opinions of authors expressed herein do not necessarily state or reflect those of the United States Government or any agency thereof.

WINCO-1060

Distributed Under Category: UC-70  
Nuclear Waste Management

MODELING HYPOTHETICAL GROUNDWATER TRANSPORT OF NITRATES,  
CHROMIUM, AND CADMIUM AT THE IDAHO CHEMICAL PROCESSING PLANT

T. R. Thomas

November 1988



Westinghouse Idaho  
Nuclear Company, Inc.

PREPARED FOR THE  
**DEPARTMENT OF ENERGY**  
**IDAHO OPERATIONS OFFICE**  
UNDER CONTRACT DE-AC07-84ID12435

## ACKNOWLEDGMENTS

The author wishes to thank several individuals who provided input and support to this report. Neldon Marshall (EG&G, Scientific Computing Support) loaded and verified the operability of the TRACR3D Code on the INEL CRAY X-MP/24 computer, created batch files for expediting code operation, and taught the author how to manipulate the parameter, data, executable, and plot files of the code. Neldon is the INEL Site custodian of the TRACR3D Code and should be contacted by those who wish to use it. Bryan Travis (LANL, author of the code) assisted the author in setting up parameter and data files, code operation, and interpretation of data output. Mack Galusha (EG&G, User Support Group) set up the procedure for obtaining high quality contour plots from a Laser Jet Printer.

Brent Russell's hydrology group (EG&G) provided hydrogeologic support. Support tasks included an update of a 1974 geologic cross section under the ICPP (Jack Barraclough and Joel Renner) and building a hydrogeologic data base for the TRACR3D Code (Barraclough and Larry Hull). Nate Chipman (WINCO, Waste Processing Research) provided laboratory data on % composition and solubility of calcine constituents.

## FOREWORD

This report is one in a continuing series of studies to evaluate potential impacts of three alternative strategies being considered for the disposal of the Idaho Chemical Processing Plant (ICPP) high-level radioactive waste (HLW). One of the alternative strategies under evaluation is near-surface in-place disposal of the calcined waste presently stored in the Calcine Solids Storage Facilities (CSSF). This study along with others will serve as technical bases to recommend a reference strategy and process for the final disposal of ICPP HLW for future consideration by DOE.

The hypothetical transport of three non-radioactive constituents ( $\text{Cr}^{+6}$ ,  $\text{Cd}^{+2}$ , and  $\text{NO}_3^-$ ) from the calcine, due to rainwater recharge, was modeled. The approach was to assimilate the available hydrogeological data for the ICPP area and employ a state-of-the-art code to model potential solute transport from the calcine into the aquifer. The results of this study are intended to provide guidance for future modeling studies and identify areas where more laboratory and field data are needed.

## ABSTRACT

One of the alternative strategies under evaluation for long-term management of the Idaho Chemical Processing Plant (ICPP) high-level radioactive waste (HLW) is on-site near-surface disposal of HLW calcine. About 18 Calcine Solids Storage Facilities (CSSF) would contain a maximum of  $2.65 \times 10^4 \text{ m}^3$  of HLW calcine by the year 2034, if no other management strategy were selected.

The purpose of this study is to begin the documentation process which will be required for evaluation of the on-site near-surface option. The approach was to assimilate the available hydrogeological data for the ICPP area and employ a state-of-the-art code to model potential solute transport from the calcine into the aquifer. The results of this study are intended to provide guidance for future modeling studies and identify areas where more laboratory and field data are needed.

For the study, a three-dimensional code called TRACR3D, which is applicable to solute transport in both unsaturated and saturated media was used. The hypothetical transport of three non-radioactive constituents ( $\text{Cr}^{+6}$ ,  $\text{Cd}^{+2}$ , and  $\text{NO}_3^-$ ) from the calcine in one CSSF, due to rainwater recharge, to and downgradient in the aquifer was modeled up to 10,000 years. Based on the assumed parameters,  $\text{Cr}^{+6}$  is the only one of the three solutes modeled which potentially could approach National Drinking Water Standards in the aquifer. The peak  $\text{Cr}^{+6}$  levels predicted are a factor of 130 and 31 below the standards 5.0 km downgradient in the aquifer for the current and ten times the current rainwater recharge rates (1.25 and 12.5 cm/yr), respectively.

One of the parameters assumed for modeling was an instantaneous release at time zero of the  $\text{Cr}^{+6}$  inventory into the vadose zone water. In actuality, water infiltration into the calcine would begin slowly and increase to that of the surrounding alluvium over several hundred years once the integrity of the CSSF were breached by pinhole leaks. Therefore, a sensitivity study using more realistic release rate scenarios should be conducted for  $\text{Cr}^{+6}$ .

## SUMMARY

Calcined high-level radioactive waste (HLW) from reprocessing of government-owned spent nuclear fuel is generated and stored at the Idaho Chemical Processing Plant (ICPP). Recommendation of a reference strategy for the long-term management of ICPP HLW will not be made until the 1990s. One of the alternative strategies under evaluation is on-site near-surface disposal of HLW calcine. About 18 Calcine Solids Storage Facilities (CSSF) would contain a maximum of  $2.65 \times 10^4 \text{ m}^3$  of HLW calcine by the year 2034, if no other management strategy were selected.

The purpose of this study is to begin the documentation process which will be required for evaluation of the on-site near-surface option. The approach was to assimilate the available hydrogeological data for the ICPP area and employ a state-of-the-art code to model potential solute transport from the calcine into the aquifer. The results of this study are intended to provide guidance for future modeling studies and identify areas where more laboratory and field data are needed.

For the study, a three-dimensional code called TRACR3D, which is applicable to solute transport in both unsaturated and saturated media was used. The hypothetical transport of three non-radioactive constituents ( $\text{Cr}^{+6}$ ,  $\text{Cd}^{+2}$ , and  $\text{NO}_3^-$ ) from the calcine in one CSSF, due to rainwater recharge, to and downgradient in the aquifer were modeled for up to 10,000 years. The predicted concentrations were compared to the standards given in the National Primary Drinking Water Regulations.

The geometrical configuration used for modeling is illustrated in Figure S-1. The small dot in the cylinder represents a single CSSF, the small cylinder represents the vadose zone, and the large rectangular wafer represents the aquifer zone that were modeled. The two black pentagons on the zero coordinate of the transverse direction represent the 0.5 and 5.0 km downgradient aquifer positions where solute concentration vs time was modeled in the greatest detail.

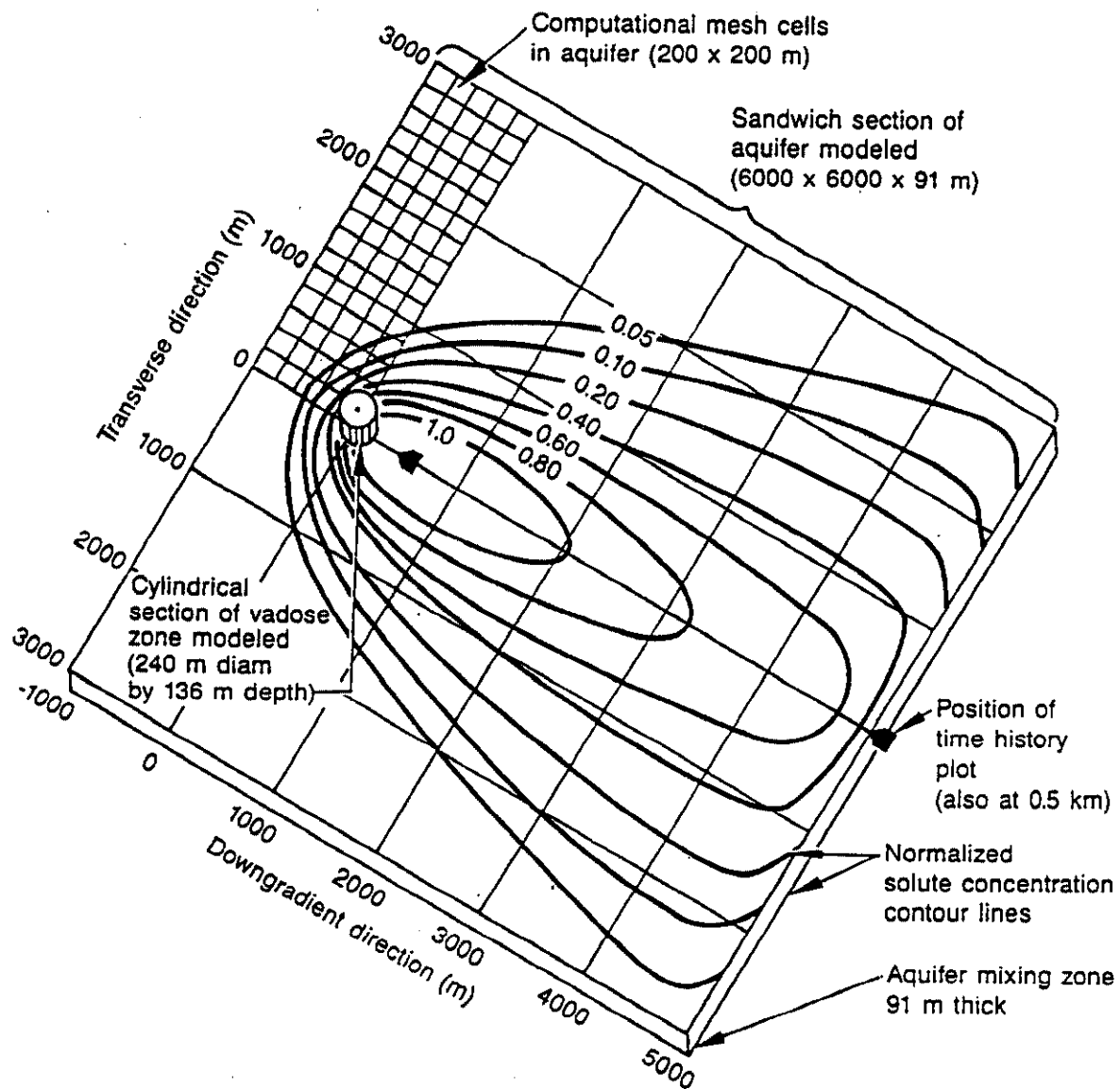


Figure S-1. Geometrical Configuration for Modeling Solute Transport



The rainwater recharge scenarios of 1.25 and 12.5 cm/yr were modeled. The smaller is based on the currently assumed recharge rate at ICPP and the larger a bounding parameter selected to examine the sensitivity of solute transport to a ten-fold increase in the current rate. The 5.0 km position was chosen for modeling because it is the maximum distance allowed in 40 CFR 191 from waste emplacement to the boundary of a high-level waste repository. At the boundary, the public would have access to well water. The 0.5 km position was modeled to examine the dilution capacity of the aquifer due to vertical and transverse mixing over a 10-fold downgradient distance from near the point of solute entry into the aquifer.

Table S.1 compares the National Primary Drinking Water Standards to the peak concentrations of the solutes in the source-term alluvial cylinder (which contains the contents of one CSSF), the vadose zone-aquifer interface directly below the cylinder, and the 0.5 and 5.0 km downgradient aquifer positions. The peak concentrations were predicted to occur 200-900 years after time zero for  $\text{Cr}^{+6}$  and  $\text{NO}_3^-$  and 7000 years for  $\text{Cd}^{+2}$ .

The results indicate that  $\text{Cd}^{+2}$  solute concentrations at 5 km downgradient in the aquifer would be a factor of about  $10^9$  and  $10^6$  below the drinking water standards for the smaller and larger rainwater recharge rates, respectively. Based on the hydrogeological parameters used in this model, any solute transport due to rainwater recharge from the ICPP calcine with a  $K_d$  of 100 or greater would probably be insignificant when compared to drinking water standards.

The peak  $\text{NO}_3^-$  levels predicted are about a factor of  $10^4$  and  $10^3$  below the drinking water standards at 5.0 km downgradient in the aquifer. Based on the hydrogeological parameters assumed, the  $\text{NO}_3^-$  levels would not exceed the drinking water standards even for a cluster of CSSF containing 13 times the amount of solute inventory modeled (i.e., the maximum projected inventory for the year 2034) from which a superposition of the contaminant plumes might conceivably increase the peak levels by a factor of ten.

Table S.1

Comparison of Model Results<sup>a</sup> to Drinking Water Standards

<u>1.25 cm/yr RAINWATER RECHARGE</u>	<u>Peak Solute Concentrations (g/mL)</u>		
	<u>NO<sub>3</sub><sup>-</sup></u>	<u>Cr<sup>+6</sup></u>	<u>Cd<sup>+2</sup></u>
Initial vadose source term	$3.7 \times 10^{-1}$	$3.7 \times 10^{-2}$	$3.0 \times 10^{-4}$
Vadose-aquifer interface	$4.5 \times 10^{-2}$	$4.5 \times 10^{-3}$	$8.2 \times 10^{-11}$
Aquifer 0.5 km downgradient	$2.2 \times 10^{-8}$	$2.2 \times 10^{-9}$	$2.1 \times 10^{-17}$
Aquifer 5.0 km downgradient	$4.0 \times 10^{-9}$	$4.0 \times 10^{-10}$	$3.9 \times 10^{-18}$
Drinking Water Limits	$4.4 \times 10^{-5}$	$5.0 \times 10^{-8}$	$1.0 \times 10^{-8}$
<u>Factor Below Drinking Water Limits</u>			
	<u>NO<sub>3</sub><sup>-</sup></u>	<u>Cr<sup>+6</sup></u>	<u>Cd<sup>+2</sup></u>
Aquifer at 0.5 km downgradient	$2.0 \times 10^3$	$2.3 \times 10^1$	$4.8 \times 10^8$
Aquifer at 5.0 km downgradient	$1.1 \times 10^4$	$1.3 \times 10^2$	$2.6 \times 10^9$
<u>Peak Solute Concentrations (g/mL)</u>			
<u>12.5 cm/yr RAINWATER RECHARGE</u>	<u>NO<sub>3</sub><sup>-</sup></u>	<u>Cr<sup>+6</sup></u>	<u>Cd<sup>+2</sup></u>
Initial vadose source term	$3.7 \times 10^{-1}$	$3.7 \times 10^{-2}$	$3.0 \times 10^{-4}$
Vadose-aquifer interface	$7.2 \times 10^{-2}$	$7.2 \times 10^{-3}$	$1.1 \times 10^{-7}$
Aquifer 0.5 km downgradient	$8.4 \times 10^{-8}$	$9.2 \times 10^{-9}$	$5.8 \times 10^{-14}$
Aquifer 5.0 km downgradient	$1.5 \times 10^{-8}$	$1.6 \times 10^{-9}$	$1.1 \times 10^{-14}$
Drinking Water Limits	$4.4 \times 10^{-5}$	$5.0 \times 10^{-8}$	$1.0 \times 10^{-8}$
<u>Factor Below Drinking Water Limits</u>			
	<u>NO<sub>3</sub><sup>-</sup></u>	<u>Cr<sup>+6</sup></u>	<u>Cd<sup>+2</sup></u>
Aquifer at 0.5 km downgradient	$5.2 \times 10^2$	5.4	$1.7 \times 10^5$
Aquifer at 5.0 km downgradient	$2.9 \times 10^3$	$3.1 \times 10^1$	$9.1 \times 10^5$

<sup>a</sup> Based on one 2000 m<sup>3</sup> capacity CSSF

Of the three solutes modeled,  $\text{Cr}^{+6}$  is the only one which potentially could approach drinking water standards in the aquifer based on the assumed parameters. The peak  $\text{Cr}^{+6}$  levels predicted are a factor 130 and 31 below drinking water standards: 5.0 km downgradient in the aquifer for 1.25 and 12.5 cm/yr rainwater recharge rates, respectively. If a cluster of CSSF containing 13 times the amount of solute inventory were modeled (i.e., the maximum projected inventory for the year 2034) with a configuration that would cause superposition of the contaminant plumes to increase solute concentrations by a factor of 10 (i.e., line the CSSF up parallel to the aquifer flow direction), the predicted peak  $\text{Cr}^{+6}$  levels would decrease to 13 and 3.1 below the drinking water standards, respectively.

For a given inventory, the most sensitive parameter for a highly soluble and non-adsorbing solute would be its release rate. Since an instantaneous release scenario was used for this study, further modeling of  $\text{Cr}^{+6}$  should incorporate realistic release rates based on water infiltration rates to the calcine which start slowly and increase with time. Based on corrosion data, the time for rainwater infiltration (i.e., recharge) to the calcine to equal that in the surrounding alluvium might take several hundred years once the integrity of the bin wall was breached by a pinhole leak.

Geochemical modeling to check for speciation or solubility limitations specific to the INEL groundwater would probably have little impact on the conclusions of this particular study. However for future modeling studies involving elements that could form solubility limited carbonates, bicarbonates or hydroxides or undergo speciation (e.g., Sr, Cs, Pu, and Am), use of a geochemical code is recommended.

## CONTENTS

ACKNOWLEDGEMENTS . . . . .	ii
FOREWORD . . . . .	iii
ABSTRACT . . . . .	iv
SUMMARY . . . . .	v
I. INTRODUCTION . . . . .	1-1
1. PURPOSE . . . . .	1-1
2. CALCINE WASTE MANAGEMENT . . . . .	1-2
2.1 ICPP Site Mission . . . . .	1-2
2.2 Calcine Properties and Inventories . . . . .	1-4
2.3 CSSF Design . . . . .	1-4
3. SELECTION AND INVENTORIES OF COMPOUNDS FOR MODELING . . . . .	1-8
II. HYDROGEOLOGIC PROPERTIES OF THE CSSF SUBSURFACE . . . . .	2-1
1. GEOLOGY OF THE INEL . . . . .	2-1
2. GEOLOGIC CROSS SECTIONS UNDER THE CSSF . . . . .	2-3
3. AQUIFER UNDER THE CSSF . . . . .	2-10
4. RAINFALL, RECHARGE, AND % WATER SATURATION . . . . .	2-13
5. HYDROGEOLOGIC PARAMETERS ASSUMED FOR MODELING . . . . .	2-14
III. SOURCE TERM ASSUMPTIONS FOR MODELING . . . . .	3-1
1. GROUNDWATER COMPOSITION . . . . .	3-1
2. INITIAL SOLUTE AND ADSORBED CONCENTRATIONS . . . . .	3-3
2.1 NO <sub>3</sub> <sup>-</sup> Solute . . . . .	3-4
2.2 Cr <sup>+6</sup> Solute . . . . .	3-4
2.3 Cd <sup>+2</sup> Solute . . . . .	3-5
IV. MODELING SOLUTE TRANSPORT . . . . .	4-1
1. SELECTION AND DESCRIPTION OF THE TRACR3D CODE . . . . .	4-1
2. GEOMETRY, SCALE, AND COMPUTATIONAL MESHES FOR MODELING . . . . .	4-3
V. TRACR3D CODE RESULTS . . . . .	5-1
1. NO <sub>3</sub> <sup>-</sup> SOLUTE . . . . .	5-1
1.1 1.25 cm/yr Rainwater Recharge . . . . .	5-1
1.2 12.5 cm/yr Rainwater Recharge . . . . .	5-8
2. Cr <sup>+6</sup> SOLUTE . . . . .	5-14
2.1 1.25 cm/yr Rainwater Recharge . . . . .	5-14
2.2 12.5 cm/yr Rainwater Recharge . . . . .	5-14

3. Cd <sup>2+</sup> SOLUTE . . . . .	5-16
3.1 1.25 cm/yr Rainwater Recharge . . . . .	5-16
3.2 12.5 cm/yr Rainwater Recharge . . . . .	5-22
VI. COMPARISON OF CODE RESULTS TO DRINKING WATER STANDARDS . . . .	6-1
VII. CONCLUSION AND RECOMMENDATIONS . . . . .	7-1
VIII. REFERENCES . . . . .	8-1

## FIGURES

S-1 Geometrical Configuration for Modeling Solute Transport . . .	vi
1-1 Location of ICPP . . . . .	1-3
1-2 Perspective of Bins and Vaults Used in the CSSF . . . . .	1-5
1-3 Schematic and Dimensions of the Nominal CSSF . . . . .	1-6
2-1 Relief Map of Idaho Showing the Location of the INEL, Snake River Plain, and Generalized Groundwater Flow Lines of the Snake River Plain Aquifer . . . . .	2-2
2-2 Location Map of Wells Used for Geologic Cross Section Analysis . . . . .	2-4
2-3a Geologic Cross Section A to A', North to South . . . . .	2-5
2-3b Geologic Cross Section B to B', Northwest to Southeast . . . .	2-6
2-3c Geologic Cross Section C to C', Semicircular Line of Wells South of ICPP . . . . .	2-7
2-4 Location Map of Wells Used for Fence Diagram, Wells Which Surround ICPP . . . . .	2-8
2-5 Geologic Cross Section Fence Diagram, Circular Line of Wells Which Surround ICPP . . . . .	2-9
2-6 Geologic Cross Section of the Test Reactor Area Showing Wells, Interbeds, Perched Water Bodies, and the Aquifer . . . .	2-11
2-7 Geologic Cross Section of the ICPP Area Showing Wells, Interbeds, Perched Water Bodies, and the Aquifer . . . . .	2-12
4-1 Geometrical Configuration for Modeling Solute Transport . . .	4-4
4-2 Computational Mesh for the ICPP Vadose Zone . . . . .	4-6
4-3 Computational Mesh for the ICPP Aquifer Zone . . . . .	4-7

5-1a	$\text{NO}_3^-$ Solute Transport (log conc. in g/mL) in the Vadose Zone 50-600 Years for 1.25 Rainwater Recharge . . . . .	5-3
5-1b	$\text{NO}_3^-$ Solute Transport (log conc. in g/mL) in the Vadose Zone 1000-4000 Years for 1.25 Rainwater Recharge . . . . .	5-4
5-2a	$\text{NO}_3^-$ Solute Transport (log conc. in g/mL) in the Aquifer 300-700 Years for 1.25 Rainwater Recharge . . . . .	5-5
5-2b	$\text{NO}_3^-$ Solute Transport (log conc. in g/mL) in the Aquifer 900-4000 Years for 1.25 Rainwater Recharge . . . . .	5-6
5-3	$\text{NO}_3^-$ Solute Concentration vs Time 0.5 and 5.0 km Down- gradient in the Aquifer for 1.25 cm/yr Rainwater Recharge . . .	5-7
5-4a	$\text{NO}_3^-$ Solute Transport (log conc. in g/mL) in the Vadose Zone 50-300 Years for 12.5 Rainwater Recharge . . . . .	5-9
5-4b	$\text{NO}_3^-$ Solute Transport (log conc. in g/mL) in the Vadose Zone 400-700 Years for 12.5 Rainwater Recharge . . . . .	5-10
5-5a	$\text{NO}_3^-$ Solute Transport (log conc. in g/mL) in the Aquifer 100-250 Years for 12.5 Rainwater Recharge . . . . .	5-11
5-5b	$\text{NO}_3^-$ Solute Transport (log conc. in g/mL) in the Aquifer 300-600 Years for 12.5 Rainwater Recharge . . . . .	5-12
5-6	$\text{NO}_3^-$ Solute Concentration vs Time 0.5 and 5.0 km Down- gradient in the Aquifer for 12.5 cm/yr Rainwater Recharge . . .	5-13
5-7	$\text{Cr}^{+6}$ Solute Concentration vs Time 0.5 and 5.0 km Down- gradient in the Aquifer for 1.25 cm/yr Rainwater Recharge . . .	5-15
5-8	$\text{Cr}^{+6}$ Solute Concentration vs Time 0.5 and 5.0 km Down- gradient in the Aquifer for 12.5 cm/yr Rainwater Recharge . . .	5-15
5-9a	$\text{Cd}^{+2}$ Solute Transport (log conc. in g/mL) in the Vadose Zone 200-10,000 Years for 1.25 Rainwater Recharge . . . . .	5-17
5-9b	$\text{Cd}^{+2}$ Adsorbed Distribution (log conc. in g/g) in the Vadose Zone 200-10,000 Years for 1.25 Rainwater Recharge . . . . .	5-18
5-10a	$\text{Cd}^{+2}$ Solute Transport (log conc. in g/mL) in the Aquifer 200-10,000 Years for 1.25 Rainwater Recharge . . . . .	5-19
5-10b	$\text{Cd}^{+2}$ Solute Transport (log conc. in g/mL) in the Aquifer 5000-10,000 Years for 1.25 Rainwater Recharge . . . . .	5-20
5-11	$\text{Cd}^{+2}$ Solute Concentration vs Time 0.5 and 5.0 km Down- gradient in the Aquifer for 1.25 cm/yr Rainwater Recharge . . .	5-21

5-12a	$\text{Cd}^{+2}$ Solute Transport (log conc. in g/mL) in the Vadose Zone 200-10,000 Years for 12.5 Rainwater Recharge . . . . .	5-24
5-12b	$\text{Cd}^{+2}$ Adsorbed Distribution (log conc. in g/g) in the Vadose Zone 200-10,000 Years for 12.5 Rainwater Recharge . . . . .	5-25
5-13a	$\text{Cd}^{+2}$ Solute Transport (log conc. in g/mL) in the Aquifer 300-2000 Years for 12.5 Rainwater Recharge . . . . .	5-26
5-13b	$\text{Cd}^{+2}$ Solute Transport (log conc. in g/mL) in the Aquifer 4000-10,000 Years for 12.5 Rainwater Recharge . . . . .	5-27
5-14	$\text{Cd}^{+2}$ Solute Concentration vs Time 0.5 and 5.0 km Down-gradient in the Aquifer for 12.5 cm/yr Rainwater Recharge . .	5-28

## TABLES

S.1	Comparison of Model Results to Drinking Water Standards . . .	viii
1.1	Vault and Bin Dimensions . . . . .	1-7
2.1	Hydrogeologic Parameters Used for Modeling . . . . .	2-15
3.1	Aquifer Composition Under the ICPP Area . . . . .	3-2
6.1	Comparison of Model Results to Drinking Water Standards . . .	6-2

## I. INTRODUCTION

### 1. PURPOSE

Calcined high-level radioactive waste (HLW) from reprocessing of government-owned spent nuclear fuel is generated and stored at the Idaho Chemical Processing Plant (ICPP). Recommendation of a reference strategy for the long-term management of ICPP HLW will not be made until the 1990s. Currently under evaluation are three alternative strategies<sup>1</sup>:

- (1) disposal of all immobilized HLW in a repository off-site,
- (2) disposal of all HLW in a near-surface facility onsite, or
- (3) disposal of annually produced HLW after FY 2010 in an immobilized form in a repository and disposal of existing calcined HLW in a near-surface facility onsite.

The purpose of this study is to begin the documentation process which will be required for evaluation of onsite disposal in alternatives (2) and (3) above. The approach was to assimilate the available hydrogeological data for the ICPP area and employ a state-of-the-art code to model potential solute transport from the calcine into the aquifer. The results of this study are intended to provide guidance for future modeling studies and identify areas where more laboratory and field data are needed.

For the study, a three-dimensional code called TRACR3D, which is applicable to solute transport in both unsaturated and saturated media was used. The hypothetical transport of three non-radioactive constituents ( $\text{Cr}^{+6}$ ,  $\text{Cd}^{+2}$ , and  $\text{NO}_3^-$ ) from the calcine, due to rainwater recharge, to and downgradient in the aquifer was modeled. The predicted concentrations were compared to the standards given in the National Primary Drinking Water Regulations.



## 2. CALCINE WASTE MANAGEMENT

### 2.1 ICPP Site Mission

The Idaho National Engineering Laboratory (INEL) is a government-owned, contractor-operated laboratory where experimental nuclear reactors are operated and defense nuclear fuel is reprocessed. It is administered by the Department of Energy (DOE). The semiarid  $2.3 \times 10^3$  km<sup>2</sup> tract of land comprising the INEL is located west of Idaho Falls, Idaho, along the northern edge of the eastern Snake River Plain. No permanent residents live on the site. The ICPP is located in the south central part of the INEL as indicated by Figure 1-1.

The purpose of the ICPP is to recover usable uranium in spent nuclear fuels generated by national defense programs. The recovery process begins by dissolving the spent fuel in acid. The acidic liquid waste remaining after uranium removal is characterized by relatively high levels of heat and penetrating radiation. After being allowed to cool three to five years through radioactive decay in underground stainless steel tanks, the liquid waste is converted to a solid through a process called calcination<sup>2</sup>. During the calcination process, as the liquid is evaporated, the dissolved material solidifies to form calcine which is a dry material with a sand-like texture. The calcine, which amounts to 15-20 percent of the original liquid volume, contains nearly all of the inert and radioactive material that was present in the liquid waste. It is stored in large stainless steel bins inside of the underground reinforced concrete vaults which are called Calcine Solids Storage Facilities (CSSF).

The calcining process used at the ICPP has proved to be a safe, effective means of managing the radioactive waste. The stainless steel bins and concrete vaults of the CSSF are expected to retain their integrity for at least 500 years; the adequacy of the present management strategy for this time period was confirmed in the Final Environmental Impact Statement on Waste Management Operations at the INEL<sup>3</sup>.

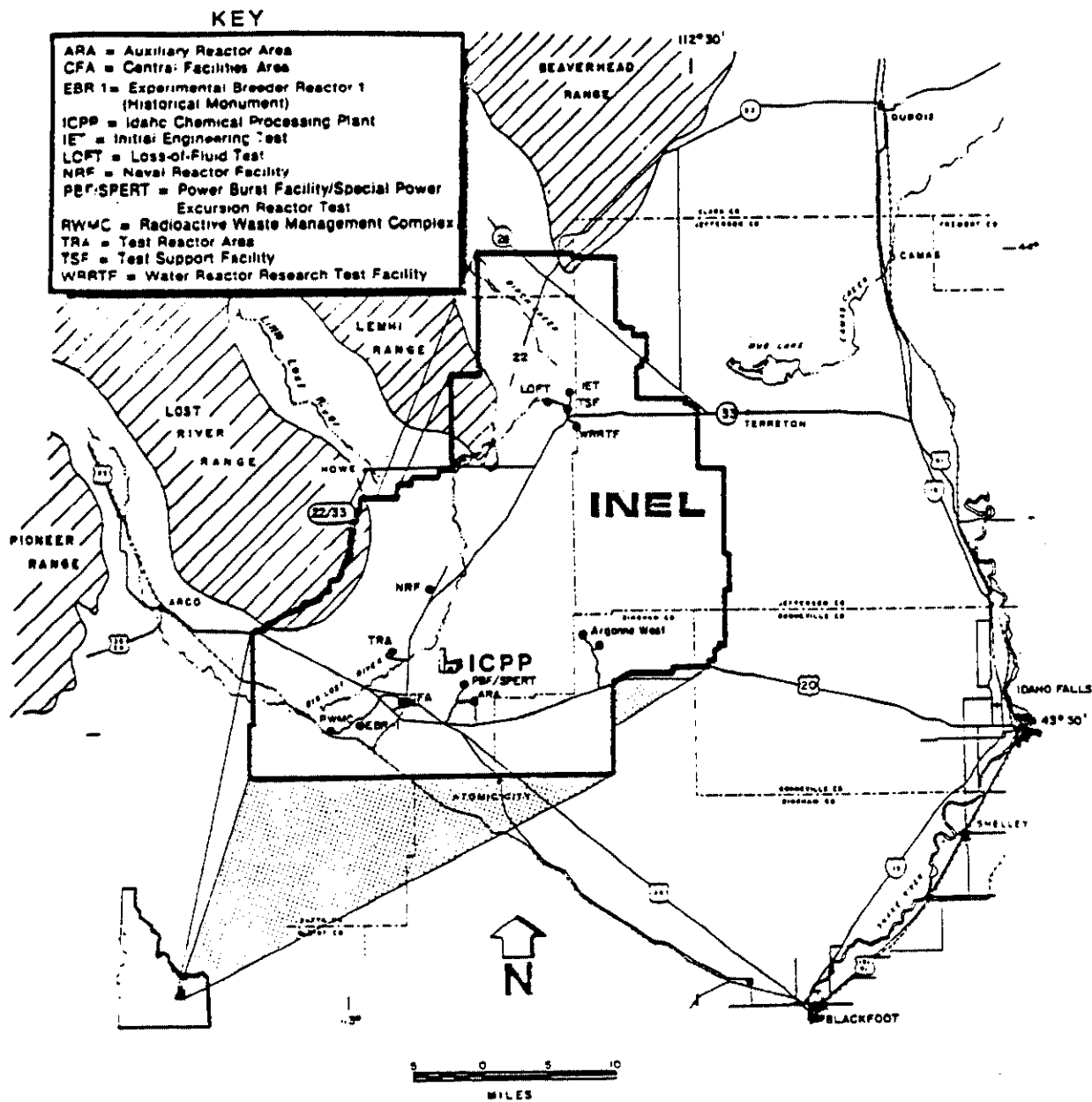


Figure 1-1. Location of ICPP

## 2.2 Calcine Properties and Inventories

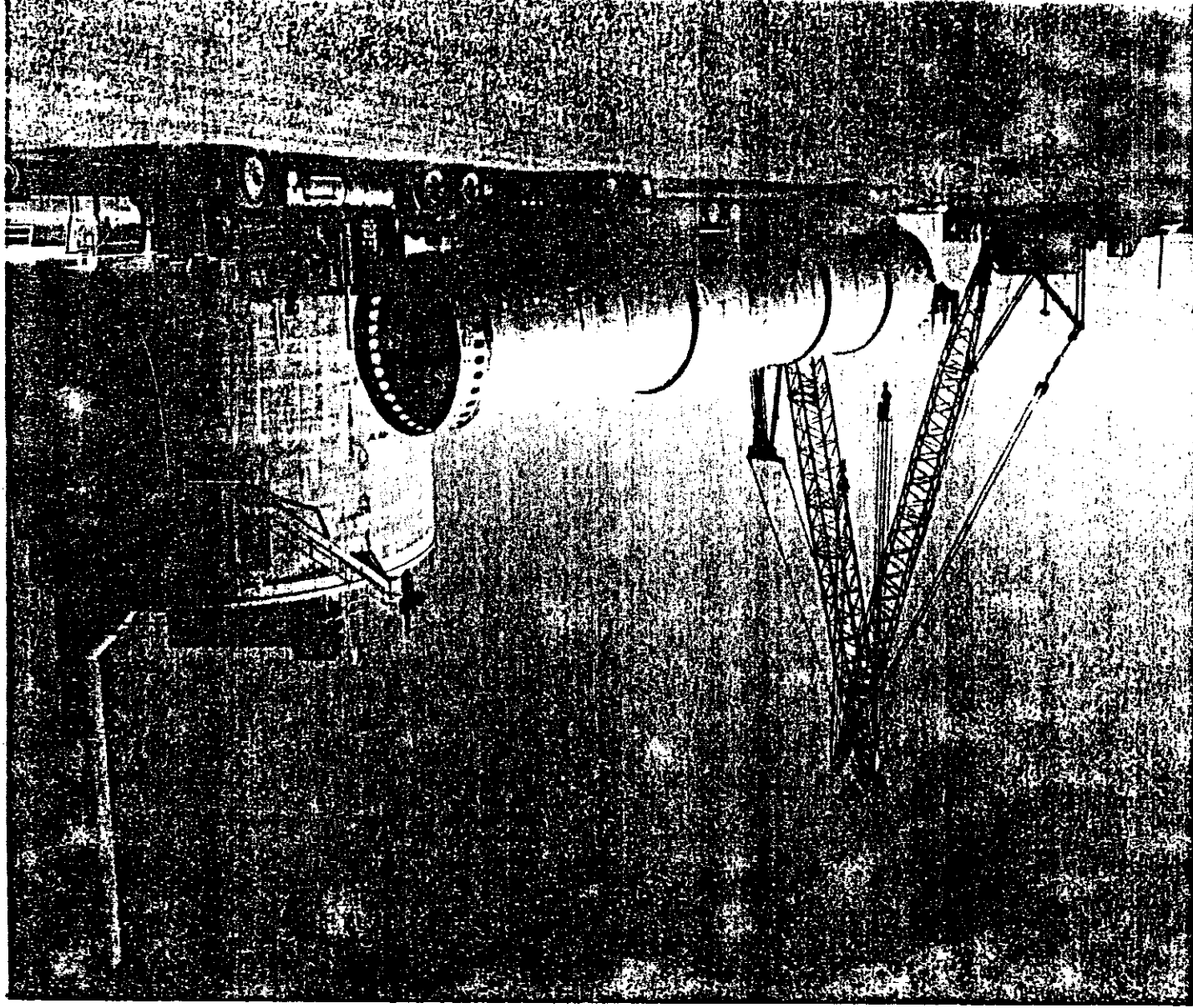
The ICPP HLW calcine is a mixture of granular solids (with diameters of 0.2 to 0.5 mm) and powdery fines with an average density of  $1.4 \text{ g/cm}^3$ . The main chemical constituents (in wt%) of future HLW calcines are projected to be  $\text{CaF}_2$  (about 43%), oxides of Zr, Al, Ca, Na, B (about 40%), nitrates, mainly as  $\text{NaNO}_3$  (about 10%), and  $\text{CdO}$  (about 6%). Minor constituents include radioactive fission products (less than 1%) and chromium oxide (less than 1%). The amount of calcined waste at the end of 1987 was about  $3.0 \times 10^3 \text{ m}^3$  which is projected to increase to  $2.65 \times 10^4 \text{ m}^3$  by the end of 2034<sup>1</sup>.

## 2.3 CSSF Design

The nominal design of the seventh and future CSSF is illustrated in Figures 1-2 and 1-3 and Table 1.1. Each CSSF is a cylindrical concrete vault containing seven stainless steel bins. The vault is about 18 m in diameter, extends 12.2 m into the ground and 20 m above, and is supported by 1.3 m thick walls and a 2 m thick base anchored in basalt bedrock. The seven bins within each vault extend 12.2 m below and 8.5 m above ground and provide  $1785 \text{ m}^3$  of storage capacity for the calcine. The vault volume to the inner ceiling is about  $5500 \text{ m}^3$ ; which leaves about  $3700 \text{ m}^3$  of void volume when the bin volume is subtracted.

The CSSF is designed for a service life of 500 years. The vault and bin configuration provides double containment against water intrusion into the calcine. If water were to penetrate and fill the vault, the stainless steel bins have sufficient corrosion resistance to ensure their water-tight integrity would be maintained for at least 500 years<sup>3</sup>. Data on the internal corrosion rate of the stainless steel bins filled with calcine predict a corrosion loss of  $1.25 \times 10^{-2} \text{ cm}$  internal wall thickness over 500 years<sup>4</sup>; this would amount to a 0.5 to 1.3% loss of wall thickness from the bottom to the top of the bin, respectively (i.e., the bin thickness varies from 2.5 to 0.95 cm, see Table 1.1). Data for stainless steel exposed to various tap and river waters near major industrial areas

Figure 1-2. Perspective of Rin and Vaults Used in the CSSF



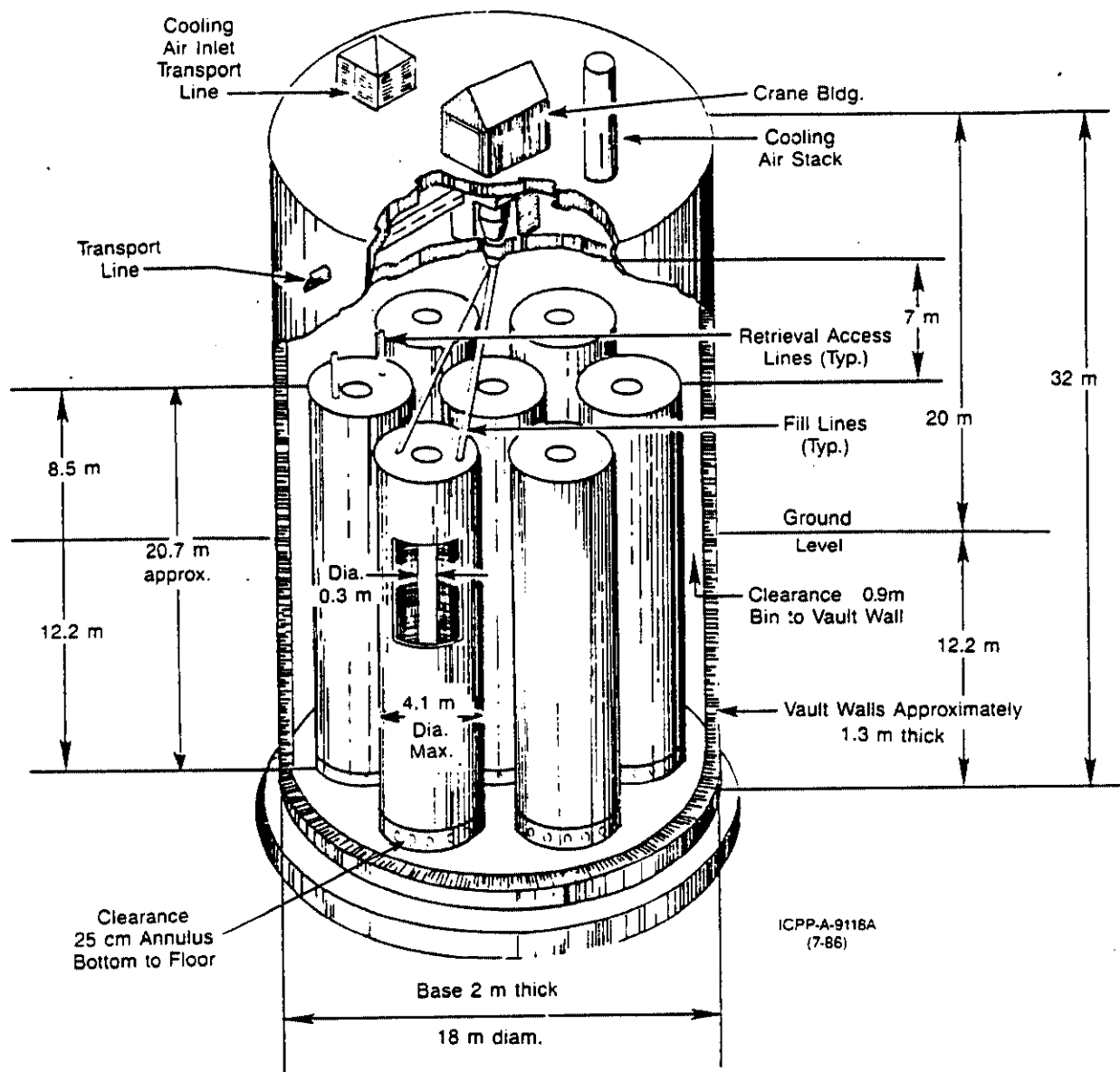


Figure 1-3. Schematic and Dimensions of the Nominal CSSF

Table 1.1

## Vault and Bin Dimensions

Item	Dimension	Comment
Bin		
wall thickness	2.5 to 0.95 cm	bottom to top; 304L S.S.
outside diam.	4.1 m	
annulus diam.	0.3 m	
height	20.7 m	extend 12.2 m below ground and 8.5 m above
volume/bin	255 m <sup>3</sup>	
number/vault	7	
total volume	1785 m <sup>3</sup>	available for calcine
Vault		
wall thickness	1.3 m	reinforced concrete
floor thickness	2 m	placed on grouted basalt
inner ceiling	2 m	reinforced concrete
outer ceiling	0.76 m	reinforced concrete
inside diam.	16 m	
outside diam.	18 m	
height	27.7 m	floor to first ceiling
volume	5490 m <sup>3</sup>	floor to first ceiling
total height	32 m	extend 12.2 m below ground

indicate corrosion rates are less than  $2.5 \times 10^{-4}$  cm/yr or 0.125 cm/500 yr.<sup>5</sup>

The external corrosion rates in the presence of water could be up to 10 times greater than the internal corrosion rate and 5 to 13% loss of external wall thickness might occur from constant exposure over 500 years. Based on these corrosion rates, the bins would most likely maintain their water-tight integrity beyond 1000 years even in the constant presence of water in the vault; loss of integrity would most likely be by pitting of the bin walls and gradual exposure of the calcine beyond a 1000 year period. However, because of the lack of long-term performance data on the vault structure and lack of external corrosion data on the bins, no attempt was made to construct a model for degradation of the CSSF integrity and rainwater infiltration vs time in this study.

### 3. SELECTION AND INVENTORIES OF COMPOUNDS FOR MODELING

Inorganic compounds of chromium, cadmium, and nitrates were selected for non-radioactive solute transport studies. The National Primary Drinking Water Regulations (40 CFR Part 141.11) lists maximum contaminant levels for nine elements when present as inorganic compounds<sup>6</sup>. Of these nine elements, only cadmium, chromium and nitrates are present in significant levels in the HLW calcine. As indicated in Section 2.2, the weight % of nitrates, CdO, and Chromium oxides are about 10, 6 and less than 1%, respectively. Actual weight % of these constituents may vary within bin sets depending on types of fuels processed and blending of different types of high-level liquid wastes during calcination. For modeling purposes, 10, 6, and 1% for the nitrate, cadmium and chromium ions, respectively, are assumed to represent upper bound levels for these constituents.

The inventories of the nitrate, cadmium, and chromium ions are estimated from the product of the calcine volume times the calcine density times the weight % of each constituent. The solute transport modeling was based on one CSSF and its  $1785 \text{ m}^3$  capacity was rounded to  $2000 \text{ m}^3$ .

Based on a density of  $1400 \text{ kg/m}^3$ , the inventories of the nitrate, cadmium, and chromium ions in one CSSF were estimated to be  $2.8 \times 10^8$ ,  $1.7 \times 10^8$ , and  $2.8 \times 10^7 \text{ g}$ , respectively. About 13 CSSF of  $2000 \text{ m}^3$  capacity each would be required to contain the projected amount of calcine ( $2.65 \times 10^4 \text{ m}^3$ ) for the year 2034. Because smaller capacity designs were used in construction of the first six CSSF, the actual number of CSSF required to hold  $2.65 \times 10^4 \text{ m}^3$  of calcine would be 18.



## II. HYDROGEOLOGIC PROPERTIES OF THE CSSF SUBSURFACE

### 1. GEOLOGY OF THE INEL

The INEL covers  $2.3 \times 10^3 \text{ km}^2$  of semiarid land on the Snake River Plain in southeastern Idaho. The eastern Snake River Plain is a large graben or downwarped structural basin  $3.1 \times 10^4 \text{ km}^2$  in area (see relief map in Figure 2-1). It has been filled to its present level with 800 m of thin basaltic flows and interbedded sediments formed from alluvial, lacustrine, and loess deposits.

Nearly all of the plain is underlain by a vast groundwater reservoir called the Snake River Plain aquifer which is depicted by water flow lines in Figure 2-1. The basaltic volcanic rocks and interbedded sediments composing the aquifer are all included in the Snake River Group of Quaternary age. The basement rocks are probably composed of older volcanic and sedimentary rocks in addition to any underlying crystalline rocks. Basalt is the principal aquifer medium. Water-bearing openings in the basalt are distributed throughout the rock system in the form of intercrystalline and intergranular pore spaces, fractures, cavities, interstitial voids, and interflow zones. The variety and degree of interconnection of openings complicate the direction of groundwater movement locally throughout the aquifer.

The Snake River Plain aquifer is estimated to contain  $1.2 \times 10^3 \text{ km}^3$  of water with a recharge of  $8 \text{ km}^3$  per year. Most of the recharge stems from rivers and streams feeding into the aquifer. The flow of the aquifer is principally to the southwest at 1.5 to 8 m/d with transmissivities in the range of  $10^4$  to  $10^6 \text{ m}^3/\text{d}/\text{m}$  of aquifer width perpendicular to the flow gradient. The above information and more details on INEL geology can be found in several U.S. Geological Survey reports.<sup>7-13</sup>

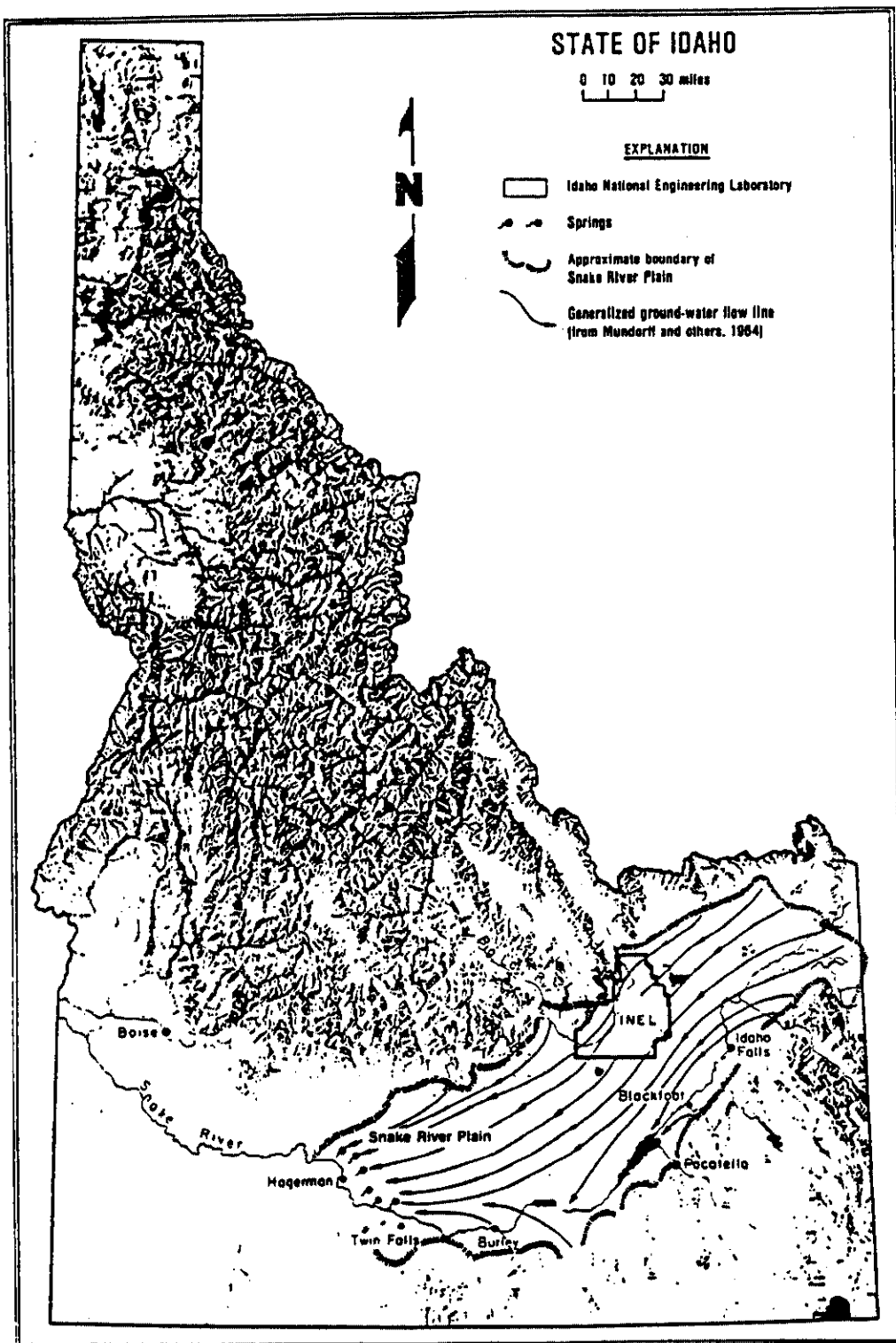


Figure 2-1. Relief Map of Idaho Showing the Location of the INEL, Snake River Plain, and Generalized Groundwater Flow Lines of the Snake River Plain Aquifer

## 2. GEOLOGIC CROSS SECTIONS UNDER THE CSSF

Figure 2-2 illustrates the location of wells located in the ICPP and TRA used to develop the geologic cross sections of the vadose zone illustrated in Figure 2-3 a, b, c, and d. The cross sections developed include:

- |                  |  |
|------------------|--|
| A to A'          | Line of wells about 5 km long running north to south from Fire Station #2 to well #20; geologic cross section shown in Figure 2-3a.        |
| B to B'          | Line of wells about 5 km long running northwest to southeast from well #19 to well #82; geologic cross section shown in Figure 2-3b.       |
| C to C'          | Semicircular line of wells about 2.5 km long south of the ICPP; geologic cross section shown in Figure 2-3c.                               |
| Line Around ICPP | Set of wells which enclose the ICPP and CSSF area Figure 2-4; three-dimension fence diagram of geologic cross section shown in Figure 2-5. |

Well log data from a total of 34 wells<sup>14,15</sup> were analyzed to produce the geologic cross section data. The data indicate that the aquifer lies about 136 m below the ICPP and that the vadose zone is predominantly basalt. In the vadose zone, the alluvial layer is about 12 m thick and the first continuous interbed occurs about 30 m below the ICPP which is about 12 m thick. Numerous interbed lenses occur down to the next apparent continuous interbed at about 115 m which is about 4 m thick. Most of the well log data in Figures 5-3a. through 5-3c. indicate interbed sediments exist at the lower level. The fence diagram in Figure 2-5, which maps the vadose zone in the immediate vicinity of the ICPP, indicates lower interbed materials were found in all wells (i.e., contour lines labeled 6 and 7).

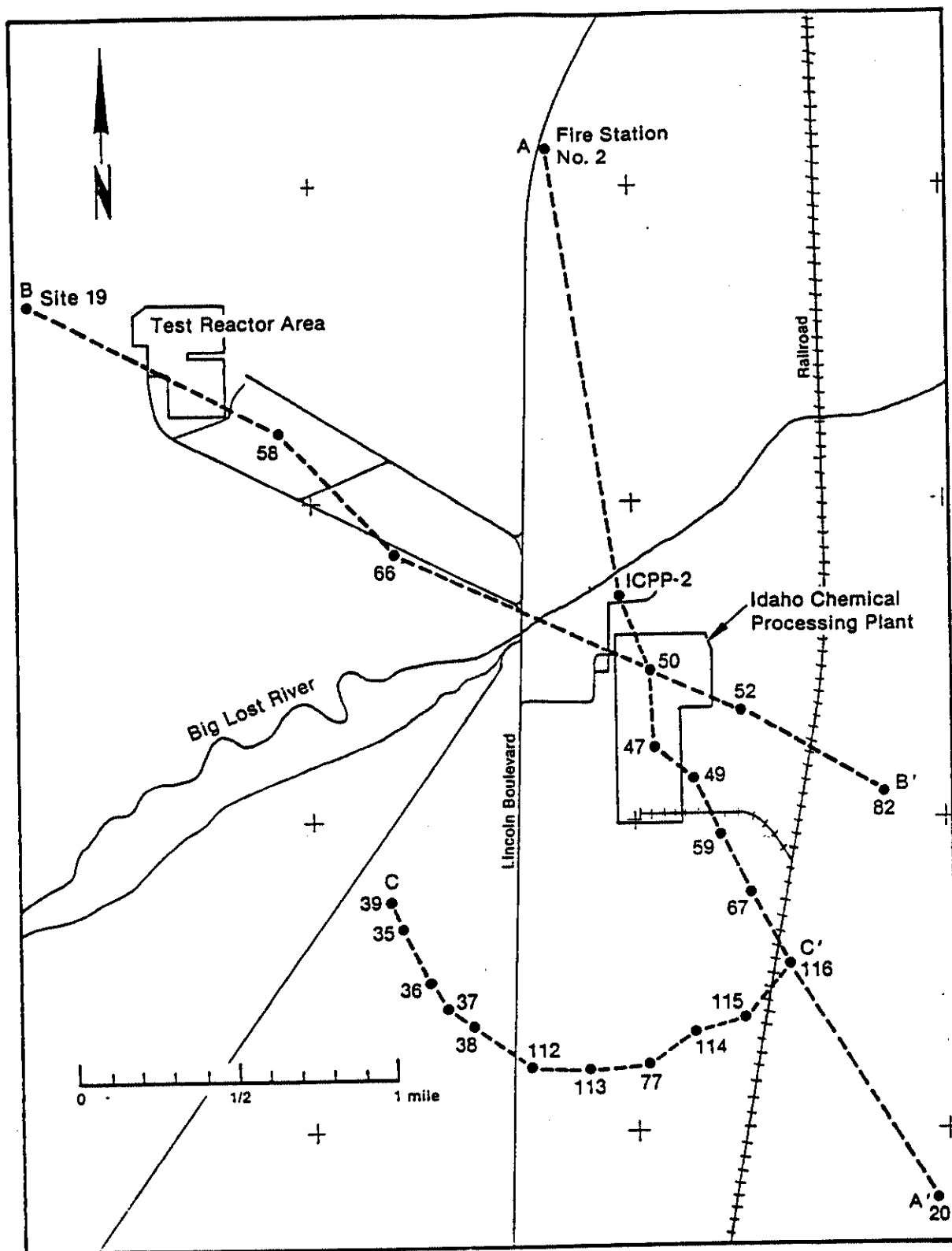


Figure 2-2. Location Map of Wells Used for Geologic Cross Section Analysis

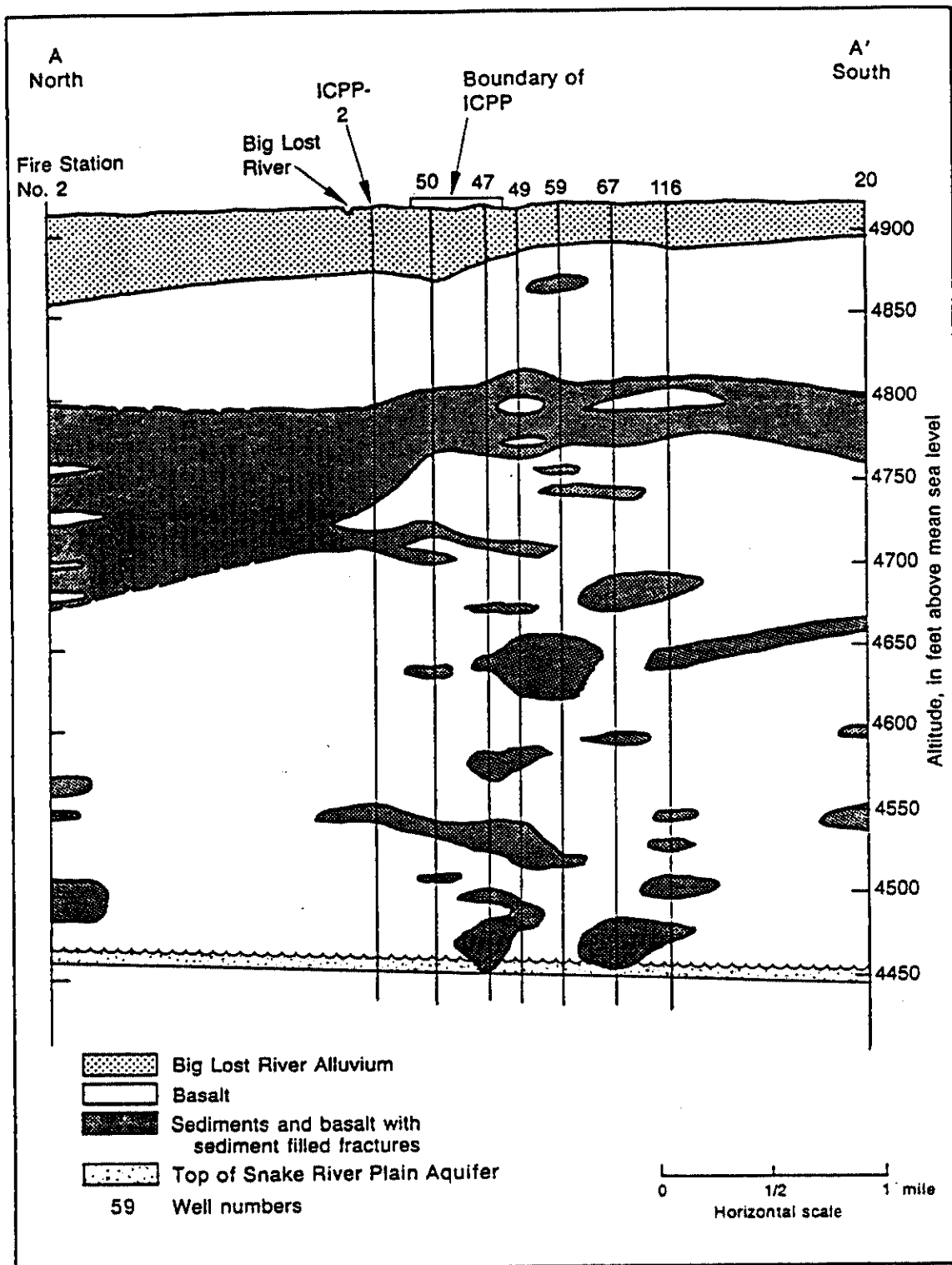


Figure 2-3a. Geologic Cross Section A to A', North to South

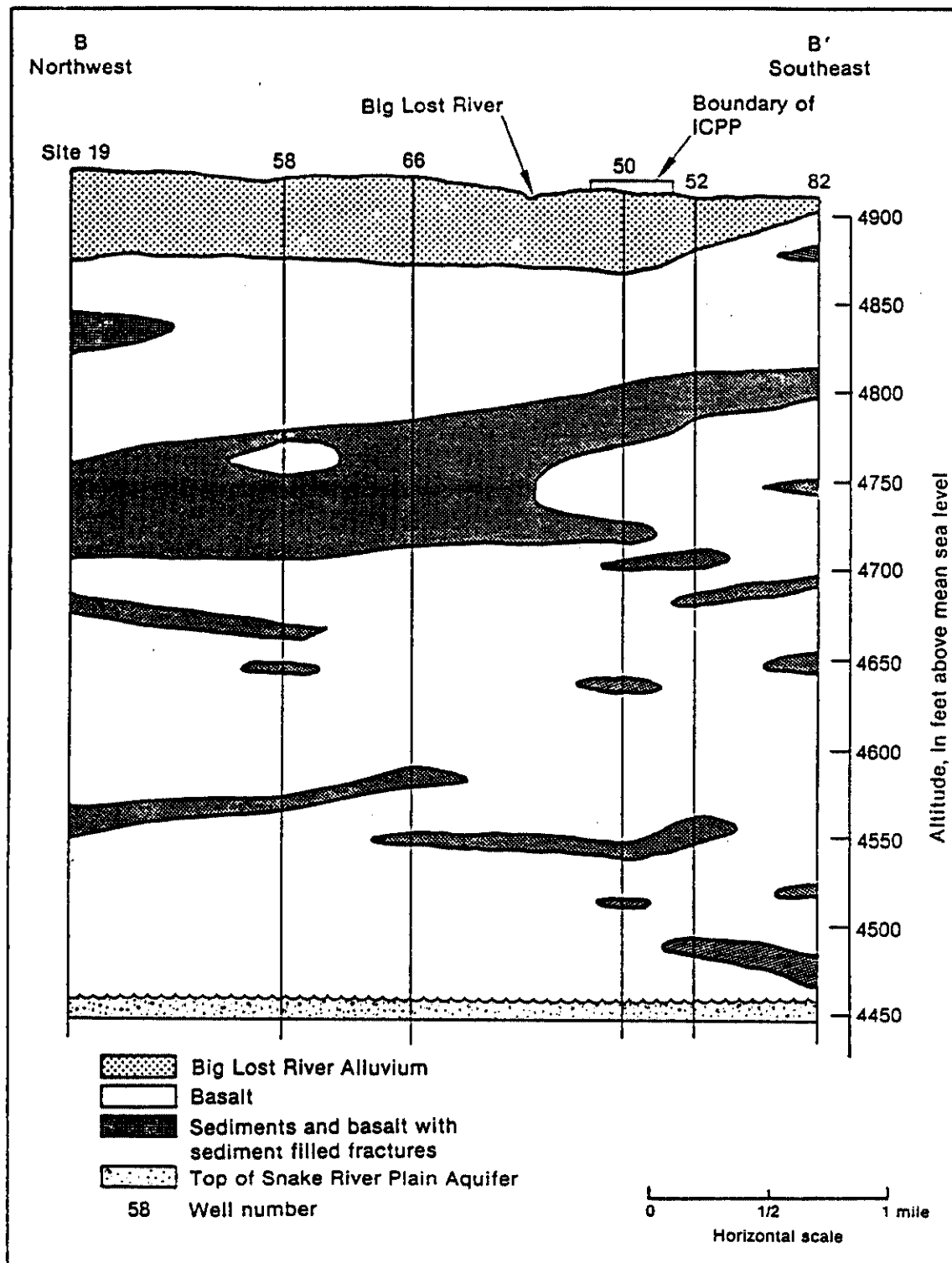


Figure 2-3b. Geologic Cross Section B to B', Northwest to Southeast

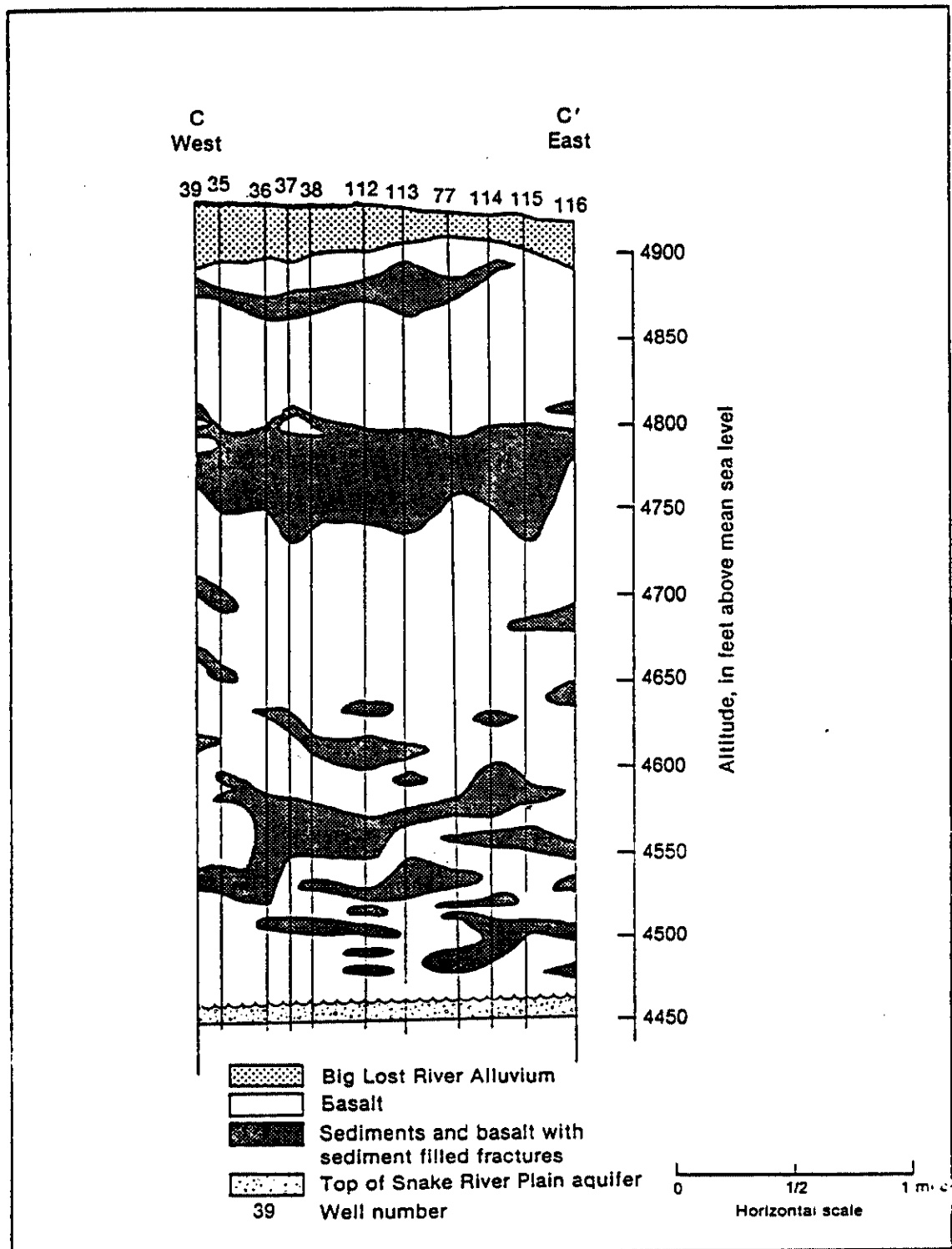


Figure 2-3c. Geologic Cross Section C to C', Semicircular Line of Wells South of ICPP

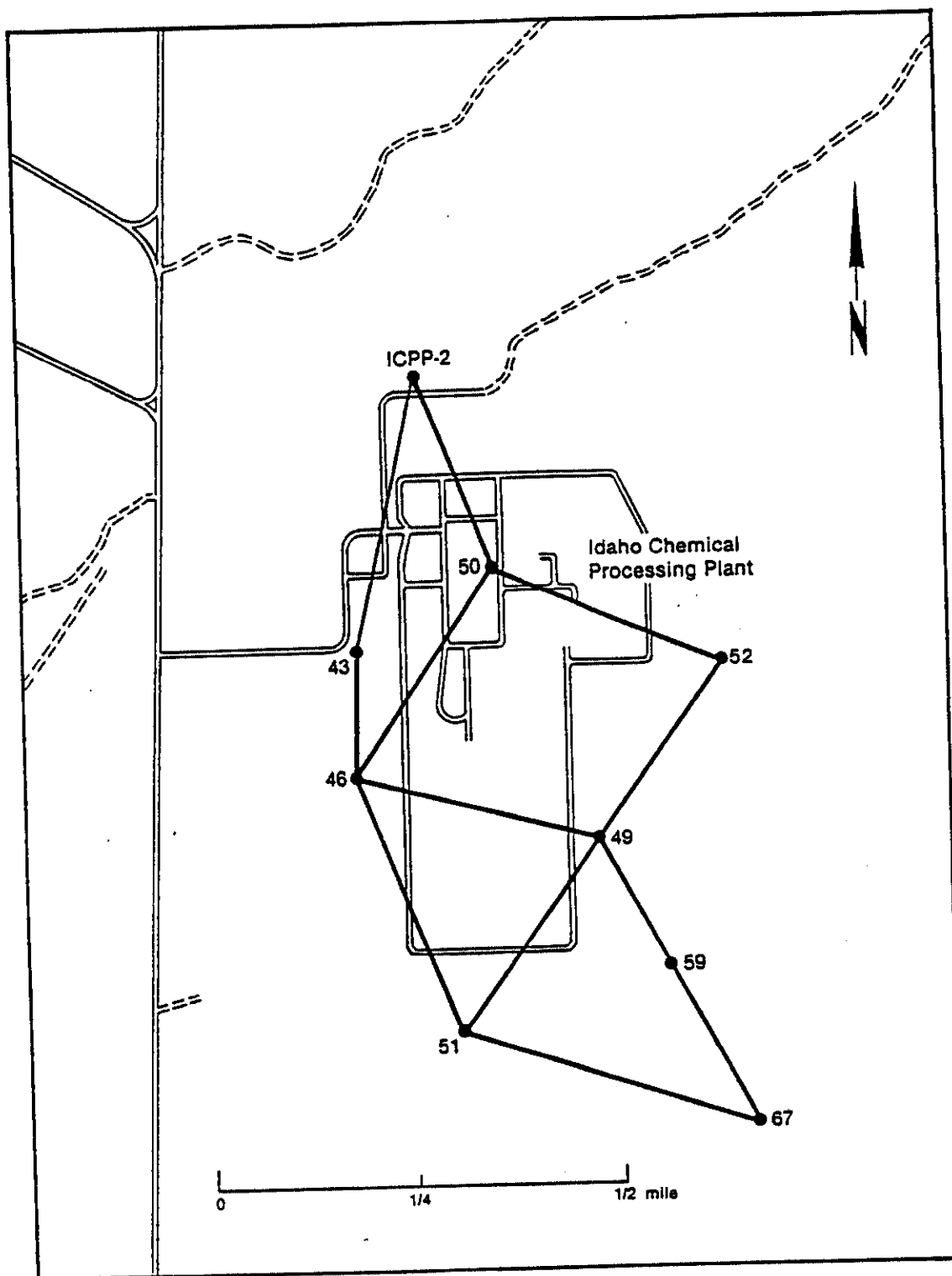


Figure 2-4. Location Map of Wells Used for Fence Diagram,  
Wells Which Surround ICPP



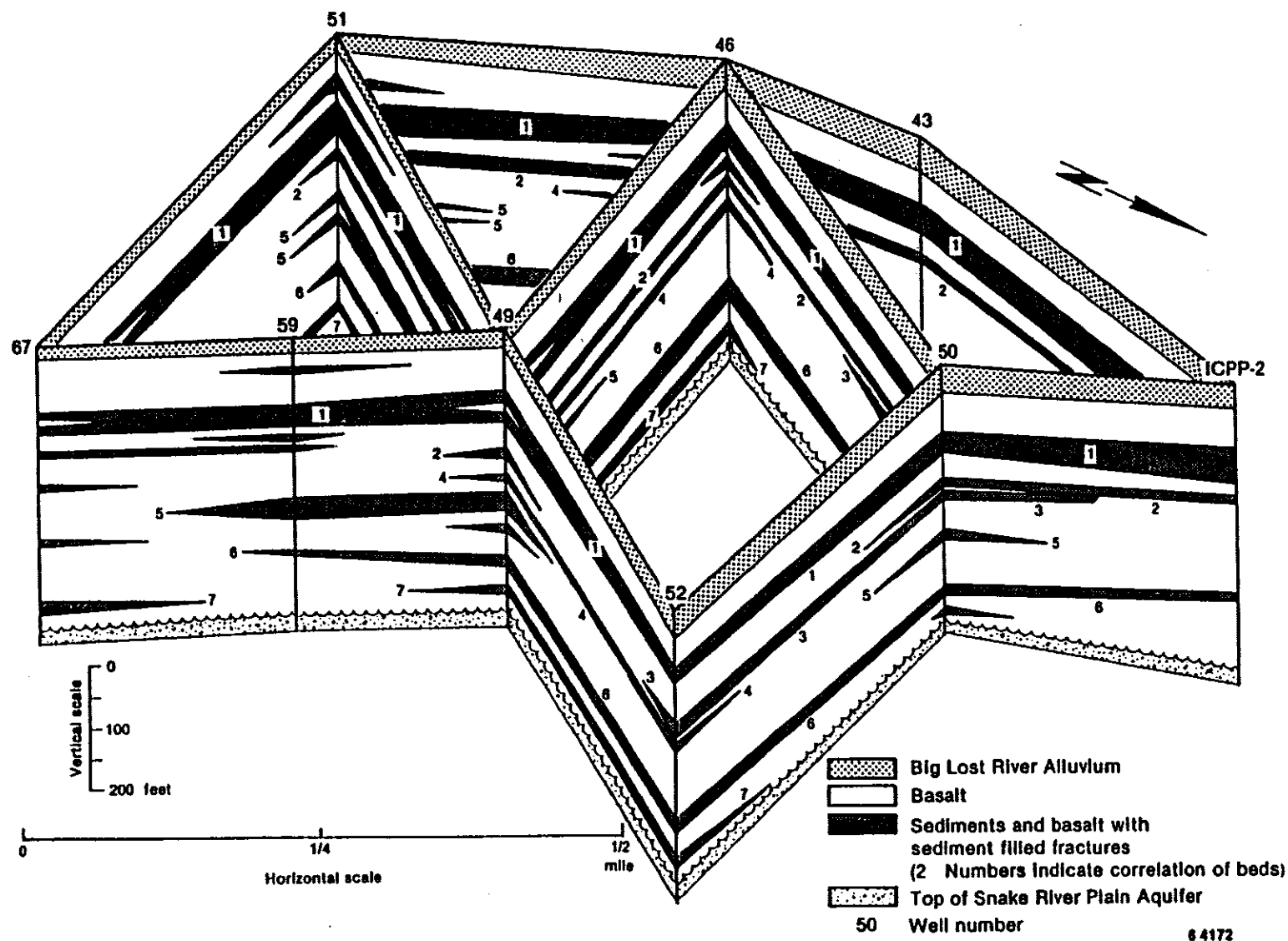


Figure 2-5. Geologic Cross Section Fence Diagram, Circular Line of Wells Which Surround the ICPP

Further evidence of continuous interbed layers at about the 30 and 115 m depths in the vadose zone comes from observation of perched water bodies on these layers since the early 1960's<sup>10</sup>. Figures 2-6 and 2-7 illustrate perched water bodies on the upper interbed for the Big Lost River near the TRA and ICPP and for the waste pond area at TRA. TRA is located about 2.4 km northwest of ICPP. Figure 2-7 illustrates a perched water body which formed on a lower interbed due to an acute break in the casing of the ICPP disposal well. The perched water bodies spread to about 1200 m in width on the upper interbed and 900 m on the lower interbed which indicates that these interbeds have low hydraulic conductivity and probably are continuous layers within the vicinity of TRA and ICPP. Where discontinuity may occur as indicated by lack of sediments in Figures 2-3a-c, in the lower interbed, the perched water body may encounter sediment-filled fractures and vesicular zones of basalt which have similar hydraulic conductivities to the sediments in the interbed.

The residence time of water in perched water bodies in the vadose zone is short. Based on measurements made on tritium migration from the TRA waste ponds to the aquifer, water is expected to move through the vadose zone in 6-12 months.<sup>10</sup>

### 3. AQUIFER UNDER THE CSSF

As indicated in Chapter II, Section 2, the aquifer lies about 136 m under the surface of the CSSF area; Section 1 provides general characteristics on the aquifer. Properties specific to the aquifer under the CSSF area include:

- (1) Depth available for dilution of radionuclides, based on measurement of vertical dispersion of contaminants from the ICPP injection well, is about 91 m<sup>10</sup>.
- (2) Porosity of the aquifer basalt ranges from 5 to 15% with an average of 10% used in this report<sup>10</sup>.

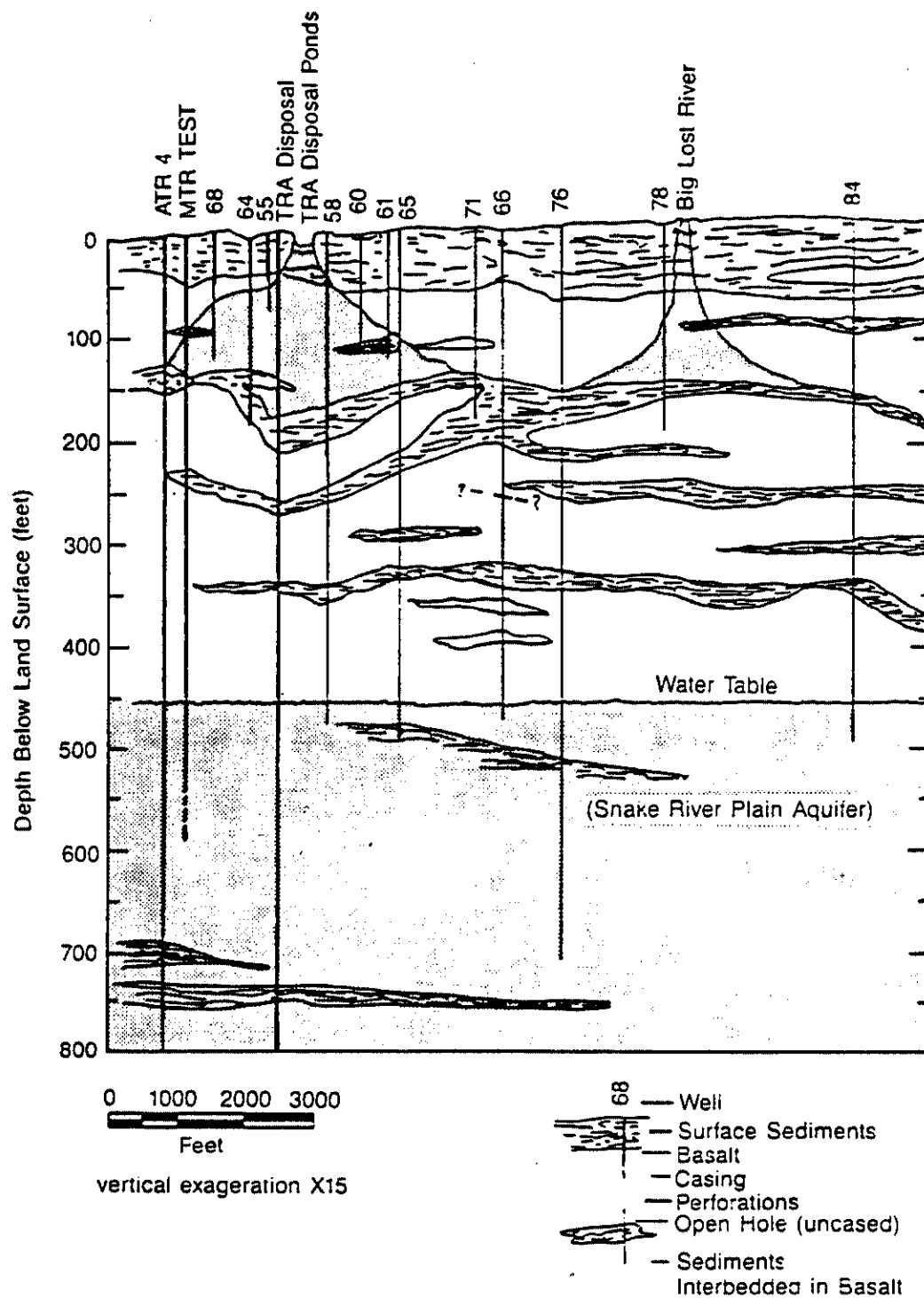


Figure 2-6. Geologic Cross Section of the Test Reactor Area Showing Wells, Interbeds, Perched Water Bodies, and the Aquifer

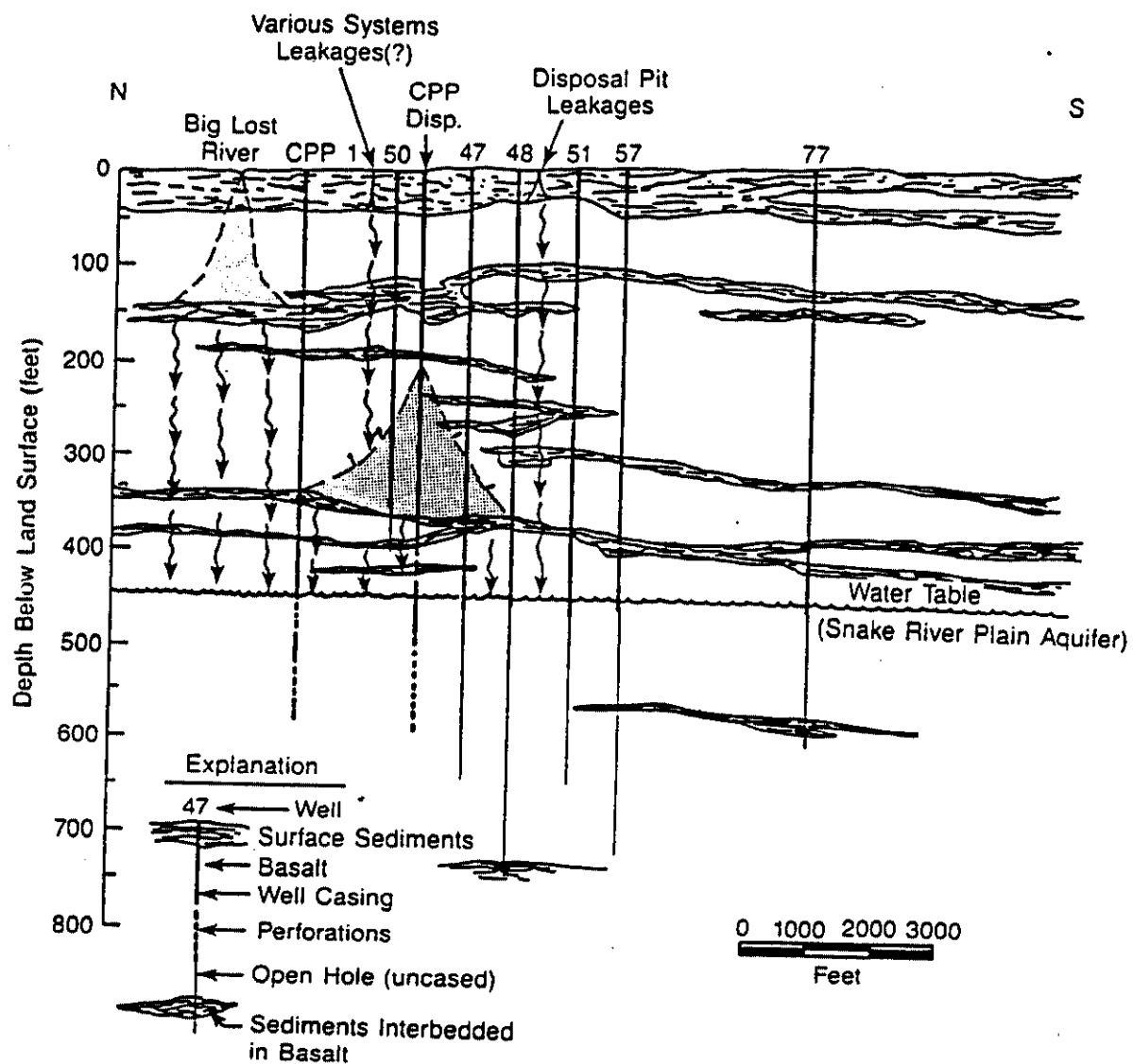


Figure 2-7. Geologic Cross Section of the ICPP Area Showing Wells, Interbeds, Perched Water Bodies, and the Aquifer

- (3) Density of the aquifer basalt is about  $2.7 \text{ g/cm}^3$ .
- (4) Measured flow velocity site-wide range from 1.5 to 8 m/d in the southwest direction<sup>13</sup>. Measured flow velocity based on tritium discharges from the ICPP injection well (no longer operational) to 3 km downgradient is about  $3.7 \text{ m/d}$ <sup>12</sup>.
- (5) Hydraulic conductivity is assumed to be 100 Darcy; a Darcy is equal to a hydraulic conductivity of  $9.1 \times 10^{-4} \text{ cm/s}$ . *~ 200 ft/day*
- (6) Longitudinal ( $a_L$ ) and transverse ( $a_T$ ) dispersivities are  $a_L = 91 \text{ m}$  and  $a_T = 137 \text{ m}$  based on best fits of digital modeling of tritium and chloride from the injection well<sup>13</sup>. These dispersion coefficients are the same ones used for modeling migration of radionuclides from the Radioactive Waste Management Complex on the INEL.<sup>16</sup> *Robinson*
- (7) The vertical dispersivity ( $a_V$ ) is assumed to be less than  $a_L$  and  $a_T$  but of the same order of magnitude; an estimate of 50 m is used.

#### 4. RAINFALL, RECHARGE AND % WATER SATURATION

Rainfall at the INEL is light and characteristic of a semiarid steppe area. Based on 22 years of records, the average annual precipitation is about  $22 \text{ cm/yr}$ <sup>2</sup>. The estimated rainwater recharge is 3.5% based on the amount of tritium remaining in the INEL surficial layer in 1965 and the amount of tritium which should have precipitated from fallout for the period 1951 through 1965<sup>17</sup>. Recharge to the vadose zone occurs mainly during the spring when combined snow melt and rain can cause temporary saturation. Maximum precipitation occurs during May and June and minimum precipitation occurs during July.

For modeling purposes, an average rainfall of 25 cm/yr and a 5% recharge was assumed which gave a recharge rate of 1.25 cm/yr. A second scenario of 10 times this recharge rate (12.5 cm/yr) was also modeled. The higher recharge rate was used as a bounding condition to any conceivable increase in rainfall and recharge rates over the next 10,000 years.

The TRACR3D Code was used to calculate % water saturation at equilibrium in the alluvium and interbeds based on assumed rainwater recharge rates and hydraulic conductivities. The code indicated only 1-2% greater moisture content for 12.5 cm/yr vs the 1.25 cm/yr recharge rate. The predicted water contents are about 47% saturation in the alluvium and 57% saturation in the interbeds. Observed levels of moisture in the INEL surficial layers average 29% of saturation with a standard deviation of  $\pm 16\%$ <sup>18</sup>. Observed levels of moisture in the INEL interbeds average 65 (upper 60 m) and 75% (below 60 m) of saturation with standard deviations of about  $\pm 25\%$ <sup>18</sup>. The calculated % saturation values are high for the surficial layer and low for the interbed layers when compared to the observed means, but are close to or within the standard deviation of the means.

## 5. HYDROGEOLOGIC PARAMETERS FOR MODELING

The hydrogeologic properties use for modeling in this study are summarized in Table 2.1. The values in Table 2.1 are nominal values only. Actual values vary depending on location and depth. A summary of hydraulic properties compiled by L. C. Hull of EG&G<sup>18</sup>, which was based on published reports<sup>11,19,20</sup>, indicates the following averages and standard deviations for numerous samples taken at the INEL:

(1) Densities (g/cm <sup>3</sup> ):	Alluvial	-	1.5 $\pm$ 0.2
	Upper Interbeds	-	2.0 $\pm$ 0.3
	Lower Interbeds	-	1.9 $\pm$ 0.2

Table 2.1

## Hydrogeological Parameters Used for Modeling

	Alluvial <u>Sediments</u>	Sedimentary <u>Interbeds</u>	Vadose <u>Basalt</u>	Aquifer <u>Basalt</u>
Bulk Density (g/cm <sup>3</sup> )	1.5	1.8	2.7	2.7
Porosity	0.43	0.35	0.10	0.10
Hydraulic Conductivity (Darcys) <sup>a</sup>	0.20 <small>9.1 x 10<sup>-4</sup> cm/s</small>	0.003 <small>0.0077 cm/s</small>	10 <small>25.8</small>	100 <small>258</small>
Accumulative Thickness (m)	12	16	108	91
Dispersion Coefficient (cm <sup>2</sup> /day) <sup>b</sup>	1.3	1.3	1.3	--
Water Saturation (%)	47	57	56	100
Flowrate (m/d)	--	--	--	3.7
Dispersivity Coefficient (m)				
Longitudinal (a <sub>L</sub> )		--	--	91
Transverse (a <sub>T</sub> )		--	--	137
Vertical (a <sub>V</sub> )		--	--	50

<sup>a</sup> At standard conditions of one atmosphere pressure and 20.2°C,  
a Darcy =  $9.1 \times 10^{-4}$  cm/s for water.

<sup>b</sup> Assumed to be equal to typical values for ionic diffusion.

(2) Porosity:	Alluvial	-	0.44 ± 0.09
	Upper Interbeds	-	0.34 ± 0.08
	Lower Interbeds	-	0.41 ± 0.06
(3) Hydraulic			
Conductivity (Darcy):	Alluvial	-	<sup>.57 ft/day</sup> 0.22 (0.02-3.7)
	Upper Interbeds	-	<sup>.018 ft/day</sup> 0.0070 (0.000019-2.7)
	Lower Interbeds	-	<sup>.0075 ft/day</sup> 0.0029 (0.000010-0.35)

The mean and standard deviation for hydraulic conductivity is based on a log normal distribution. This approach was taken because the data range is spread over eight orders of magnitude whereas density and porosity data range is within a factor of two. The hydrologic parameters for densities, porosities, and conductivities used for modeling in Table 2.1 are identical to or within the standard deviation of the values given above. The % water saturation of the alluvium, interbeds and basalt were calculated by the TRACR3D Code and as indicated in Chapter II, Section 4, are near or within the standard deviation of the average observed moisture contents at INEL.

The dispersion coefficient for the solutes in the vadose zone was assumed to be equivalent to the values typical for ionic diffusion of strong electrolytes (i.e.,  $1.5 \times 10^{-5} \text{ cm}^2/\text{sec}$  or  $1.3 \text{ cm}^2/\text{day}$ )<sup>21</sup>. Because of the slow vertical movement of water (i.e., a range of 0.1-0.7 cm/day for the 12.5 cm/yr recharge rate depending on porosity and % water saturation), dispersion by mechanical mixing is assumed to be insignificant.



### III. SOURCE TERM ASSUMPTIONS FOR MODELING

This chapter provides an assessment of soluble and insoluble species, distribution coefficients, effects of groundwater composition and initial concentrations assumed for modeling transport of chromium, cadmium and nitrates from the calcine. No attempt to construct a model for degradation of the CSSF integrity and rainwater infiltration vs time was made. The beginning of the modeling period is defined as time zero and is not predicated on a future time when rainwater infiltration into the CSSF might begin. The National Primary Drinking Water Regulations<sup>6</sup> are not based on beginning or ending or specified time periods. The regulations apply for all of time to any potential source of contamination. Assumptions made to simplify input parameters to the TRACR3D Code include:

- (1) Rainwater recharge is uniform at 1.25 cm/yr or 12.5 cm/yr for up to 10,000 years (i.e., two scenarios).
- (2) Rainwater infiltrating through the vadose zone has the same ionic composition as the aquifer.
- (3) At time zero, the % water saturation of the vadose zone and the calcine in the vadose zone are at equilibrium with the rainwater recharge rate.
- (4) The vault concrete wall and the bin steel walls of the CSSF offer no resistance to rainwater infiltration at time zero.
- (5) The vadose and aquifer zones are considered oxic environments due to the presence of adsorbed or dissolved oxygen.

#### 1. GROUNDWATER COMPOSITION

At the INEL, rainwater would contain very low levels of ionic constituents depending on washout of atmospheric contaminants during

precipitation. Once the rainwater infiltrates into the vadose below the CSSF, its ionic composition should rapidly approach that of the aquifer; the solubility of calcine constituents may be greater in pure rainwater, for example, but the controlling factors for solubility at equilibrium would be dictated by the final ionic composition of the vadose zone water and the distribution of the solute adsorbed on the alluvium and dissolved in solution.

The aquifer water is buffered at a pH of about 8.0 by the presence of the bicarbonate ion ( $\text{HCO}_3^-$ ); the hydrolysis of calcite ( $\text{CaCO}_3$ ) and dolomite ( $\text{CaCO}_3 \cdot \text{MgCO}_3$ ) minerals in the Snake River Plain cause the  $\text{Ca}^{+2}$ ,  $\text{Mg}^{+2}$ , and  $\text{HCO}_3^-$  ions to predominate. The dissolved  $\text{O}_2$  in the aquifer is near saturation and is assumed to create an oxic environment for solute transport. The ionic composition and oxygen content based on a 1988 analysis of water from an ICPP production well is given in Table 3.1<sup>22</sup>.

Table 3.1

Aquifer Composition under the ICPP Area

<u>Chemical Species</u>	<u>Concentration (mg/L)</u>
$\text{Na}^+$	8.5
$\text{K}^+$	2.1
$\text{Ca}^{+2}$	48
$\text{Mg}^{+2}$	18
$\text{Cl}^-$	12
$\text{SO}_4^{-2}$	24
$\text{HCO}_3^-$	206
$\text{O}_2$	7.6
$\text{SiO}_2$	.26

Extensive studies have been conducted on the  $\text{NO}_3^-$  levels and distribution in the aquifer. Throughout the INEL aquifer, the natural levels of  $\text{NO}_3^-$  range from 1-4 mg/L<sup>10</sup>. Levels as high as 20 mg/L (between 1952 and 1970) were observed within the eastern boundary of the INEL near the town of Terreton which are attributed to downgradient solute transport of nitrogenous fertilizers applied to the land or irrigation water. These levels can be compared to 44 mg/L which is the limit specified in the National Primary Drinking Water Regulations<sup>6</sup>.

## 2. INITIAL SOLUTE AND ADSORBED CONCENTRATIONS

The initial solute concentrations for modeling are based on the calcine inventory of the solutes, % water saturation in the surficial layer at equilibrium with rainwater recharge, possible solubility limitations, and the distribution of the solute between the water and alluvium. As indicated in Chapter I, Section 3, the nominal capacity of a single CSSF is assumed to be 2000 m<sup>3</sup> and the inventories of the nitrate, cadmium, and chromium ions in one CSSF were estimated to be  $2.8 \times 10^8$ ,  $1.7 \times 10^8$ , and  $2.8 \times 10^7$  g, respectively.

For modeling purposes, the calcine is assumed uniformly mixed with alluvium and contained in a surficial layer 20 m in diameter and 12 m deep. The vault and bin walls are assumed to be absent. This configuration is meant to approximate a CSSF stabilized-in-place with filler material packed around the bins, berm materials placed around and above the vault, and no resistance to rainwater infiltration caused by the bin and vault walls.

The alluvial source cylinder is assumed to occupy about 3800 m<sup>3</sup>, contain about 1600 m<sup>3</sup> of void space (i.e., 43% porosity), and contain 760 m<sup>3</sup> of water (based on equilibrium water saturation of 47% of void space from code calculations). The additional assumptions to calculate initial concentrations are given below:

## 2.1 NO<sub>3</sub><sup>-</sup> Solute

The complete inventory of nitrate ion is assumed to exist as the highly soluble NaNO<sub>3</sub>. Laboratory studies at the ICPP on solubility of various components in the calcine indicate that all of the nitrate inventory will dissolve. Based on total dissolution, the initial solute concentration of NO<sub>3</sub><sup>-</sup> would be 0.37 g/mL in the water contained by the 3800 m<sup>3</sup> alluvial source cylinder. This concentration corresponds to 0.51 g/mL of nitrates as NaNO<sub>3</sub> and would not exceed its solubility limit of 0.88 g/mL in distilled water<sup>23</sup>. Field soil leaching studies indicate that the nitrate ion is not retarded in solute transport<sup>24</sup>. Therefore, the distribution coefficient (K<sub>d</sub>) for the nitrate ion is assumed to be zero and because the modeling study deals with transport below the root zone, chemical or microbial reaction of the nitrate ion with the alluvium and interbeds is assumed to be insignificant. The initial solute concentration is assumed to be 0.37 g/mL.

## 2.2 Cr<sup>+6</sup> Solute

If the complete inventory of chromium existed as CrO<sub>3</sub> and were totally dissolved, the initial solute concentration of Cr<sup>+6</sup> would be 0.037 g/mL in the water contained by the 3800 m<sup>3</sup> alluvial source cylinder. This concentration corresponds to 0.071 g/mL of CrO<sub>3</sub> and would not exceed its solubility limit of 0.62 g/mL in distilled water<sup>23</sup>. Laboratory studies at the ICPP on the solubility of various components in the calcine indicate up to 62% of the chromium inventory will dissolve at 25°C in distilled water after 28 days and up to 100% will dissolve at 90°C after 7 days. This indicates that essentially all the chromium exists as the highly soluble CrO<sub>3</sub> which is assumed to be the case for this modeling study.

The K<sub>d</sub> for the Cr<sup>+6</sup> solute is assumed to be zero based on an extremely small K<sub>d</sub> of 0.03-0.04 reported in soil column studies<sup>25</sup>. The ionic composition of the vadose and aquifer water is not expected to cause reduction of Cr<sup>+6</sup> to lower oxidation states or the formation of

insoluble  $\text{Cr}^{+6}$  bicarbonates or hydroxides. Therefore, the initial solute concentration is assumed to be  $3.7 \times 10^{-2}$  g/mL and the adsorbed concentration is assumed to be zero. No retardation of  $\text{Cr}^{+6}$  is expected throughout the vadose and aquifer zones (i.e., it moves at the same velocity as the water).

### 2.3 $\text{Cd}^{+2}$ Solute

Leach-rate and dissolution tests on synthetic calcine made at ICPP indicate that the cadmium inventory is highly insoluble and probably exists as the oxide which hydrolyzes to the hydroxide in the presence of water. The cadmium concentration arising from  $\text{Cd}(\text{OH})_2$  as a function of hydrogen ion concentration (or pH) can be calculated from the hydroxide solubility product ( $K_{\text{sp}}$ )<sup>23</sup> and water ionization constant ( $K_{\text{w}}$ )<sup>26</sup> of  $2.5 \times 10^{-14}$  and  $1.0 \times 10^{-14}$ , respectively. Based on the relationships:

$$K_{\text{sp}} = 2.5 \times 10^{-14} = [\text{Cd}^{+2}][\text{OH}^{-}]^2$$

$$K_{\text{w}} = 1.0 \times 10^{-14} = [\text{H}^{+}][\text{OH}^{-}]$$

the equations can be rearranged to give:

$$[\text{Cd}^{+2}] = 2.5 \times 10^{14} [\text{H}^{+}]^2$$

In a geochemically buffered solution with a pH of 8.0, the equilibrium level of  $[\text{Cd}^{+2}]$  would be  $= 2.5 \times 10^{-2}$  moles/L ( $2.8 \times 10^{-3}$  g/mL) if no other equilibria were involved. This would be about two orders of magnitude less in concentration than if the total inventory of cadmium ( $1.7 \times 10^8$  g) were dissolved in the water contained by the  $3800 \text{ m}^3$  alluvial source cylinder.

When the distribution coefficient is taken into consideration, the adsorption of the  $\text{Cd}^{+2}$  on the alluvium and interbeds becomes more of a limiting factor than formation of the hydroxide on the maximum solute concentration. Soil column studies using Hanford sandy loam and trace

amounts of cadmium chloride and perchlorate solutions have indicated a  $K_d$  ranging between 88 and 140 in high ionic strength solutions (0.1 molar in the sodium salt of the anion)<sup>27</sup>. A previous literature survey<sup>3</sup> of  $Cd^{+2}$  distribution coefficients to use for modeling studies at ICPP assumed a  $K_d$  value of 100. Based on these two studies, a  $K_d$  value of 100 is assumed in this document. The equilibrium distribution of  $Cd^{+2}$  on the alluvium and in the water of the 3800 m<sup>3</sup> alluvial source cylinder is given by the equation:

$$(g\ Cd^{+2}/mL\ HOH) (mL\ HOH) + (g\ Cd^{+2}/g\ ALLU) (g\ ALLU) = g\ Cd\ INVT$$

where HOH = alluvial water, ALLU = alluvium, and INVT = inventory.

The ratio of adsorbed to dissolved cadmium is given by:

$$K_d = 100 = (g\ Cd^{+2}/g\ ALLU)/(g\ Cd^{+2}/mL\ HOH)$$

Substituting  $(g\ Cd^{+2}/mL\ HOH)$  in the first equation by the term  $[(g\ Cd^{+2}/g\ ALLU)/K_d]$  derived from the second equation yields:

$$[(g\ Cd^{+2}/g\ ALLU)/K_d] (mL\ HOH) + (g\ Cd^{+2}/g\ ALLU) (g\ ALLU) = g\ Cd\ INVT$$

Setting mL HOH = 760 mL, g ALLU =  $5.7 \times 10^9$  g (i.e., amount in 3800 m<sup>3</sup> at a density of 1.5 g/cm<sup>3</sup>), and g Cd INVT =  $1.7 \times 10^8$  g, yields an adsorbed concentration of 0.03 g  $Cd^{+2}$ /g ALLU. Since the amount in solution is the adsorbed concentration divided by 100, the initial solute concentration at equilibrium would be  $3 \times 10^{-4}$  g  $Cd^{+2}$ /mL HOH.

This solute concentration is a factor of ten less than that predicted by the solubility product for cadmium hydroxide. Therefore it is assumed that any hydroxide formed would be redissolved at equilibrium and the solute concentration of  $Cd^{+2}$  would be dictated by its distribution coefficient. An initial adsorbed concentration of 0.03 g  $Cd^{+2}$ /g ALLU and a solute concentration of  $3 \times 10^{-4}$  g  $Cd^{+2}$ /mL HOH is assumed.

#### IV. MODELING SOLUTE TRANSPORT

##### 1. SELECTION AND DESCRIPTION OF THE TRACR3D CODE

Selection of a code to model solute transport is complicated by the number and diversity of groundwater and contaminant transport codes that have been developed. A compilation of codes by the Oak Ridge National Laboratory<sup>28</sup> indicated 59 groundwater transport codes had been developed as of 1980. Many of the codes have limited application such as for saturated media, one- or two-dimensional analysis, a specific site or type solute. Most of the current emphasis in developing groundwater and contaminant transport codes for HLW repositories has dealt with water-saturated media. Transport in partially saturated fractured media is considered one of the most difficult problems in repository performance assessment.<sup>29</sup>

The TRACR3D code was selected for this modeling study based on an assessment by EG&G that it would be one of the best candidates for application to long-term transport of radionuclides from the buried waste at the INEL Radioactive Waste Management Complex<sup>30</sup>. The Nevada Nuclear Waste Storage Investigation Project (NNWSI) is conducting benchmarking tests among five codes, one of which is TRACR3D, for application to the proposed HLW repository at Yucca Mountain, Nevada<sup>31</sup>. Benchmarking involves the comparison of numerical solutions generated by codes when solving the same problem. The codes being examined are:<sup>31</sup>

TRACR3D: A three-dimensional, finite-difference, isothermal water-flow and contaminant-transport code developed at the Los Alamos National Laboratory (LANL) by Bryan Travis. The code has been modified extensively from its original form as an oil-shale analysis code to aid in the analysis of radioactive waste disposal.

- SAGURO: A finite-element code developed at Sandia National Laboratory (SNL) by Roger Eaton for the NNWSI Project to model water flow in variably saturated, porous medium. It is used to construct two-dimensional models of flow pathways in Yucca Mountain.
- FEMTRAN: A two-dimensional, finite-element isothermal radionuclide transport code that requires a hydrologic field as input. It was coupled with the SAGURO Code to provide this input.
- TRUST: A three-dimensional, isothermal water-flow code developed at Lawrence Berkeley Laboratory (LBL) by T. Narasimhan for application to unsaturated porous media. It is being applied to the NNWSI Project to determine water-flow mechanisms and to do site-scale modeling. It is also being used at Pacific Northwest Laboratory (PNL) to support DOE and NRC studies.
- TRUMP: Originally a three-dimensional, finite-difference solver for heat transfer. It was modified by T. Narasimhan at LBL to model advective-diffusive transport of radionuclides. It was coupled with TRUST which provides the hydrologic field input.

As indicated above, the water-transport and radionuclide-transport codes must be coupled. The coupled codes SAGURO plus FEMTRAN and TRUST plus TRUMP are reduced to two complete codes.

TRACR3D is a stand-alone code that calculates both water flow and mass transport of solutes. Solution is obtained by an implicit finite difference scheme for flow and an optional explicit or implicit scheme for transport. It operates in Cartesian or cylindrical coordinates in one, two, or three dimensions. Several transport mechanisms such as advection, diffusion, dispersion, adsorption, radioactive decay and chaining are included. An efficient matrix solver based on a preconditioned, incomplete factorization is used in conjunction with a modified Newton-Raphson iteration for nonlinear flow and transport terms.



A very important part of the selection process was the accessibility of the code for loading on the INEL CRAY computer and the accessibility of its author to assist in building input data files, running the code, and making contour plots of the results. The TRACR3D code does not incorporate chemical-equilibria and reaction-path models. Leach rates, solubilities, and distributions between the water and soil must be provided as input parameters for the solute source terms. The geochemical codes EQ3/6, MINEQL, and CHEMTRN are being examined for possible use or coupling with TRACR3D to incorporate geochemistry models.<sup>32</sup> Because TRACR3D was developed at the LANL, it can be considered an in-house code available for use at DOE facilities. A complete description of the code can be found elsewhere.<sup>33</sup>

## 2. GEOMETRY, SCALE, AND COMPUTATIONAL MESHES FOR MODELING

The geometry and scale used for modeling solute transport from the calcine to and through the aquifer is illustrated in Figure 4-1. The small cylinder on the rectangular section of the aquifer represents the section of the vadose zone (240 m diameter by 136 m depth) within which transport of the solute through the vadose zone was predicted to occur. The black dot in the top center of the cylinder represents the alluvial source cylinder (20 m diameter by 12 m depth) which contains the calcine. Cylindrical coordinates were used to model the vadose zone solute transport.

The large rectangle section, 6000 m on a side and 91 m thick, represents the volume of the aquifer within which transport of the solute was predicted to occur. The computational mesh size used for the aquifer was 200 x 200 m and is shown in the upper left hand corner. Three-dimensional Cartesian coordinates were used. The origin of the transverse and downgradient coordinates (0,0) lies directly below the center of the alluvial source cylinder and at this interface between the vadose and aquifer zones, the highest concentration of solute enters the aquifer.

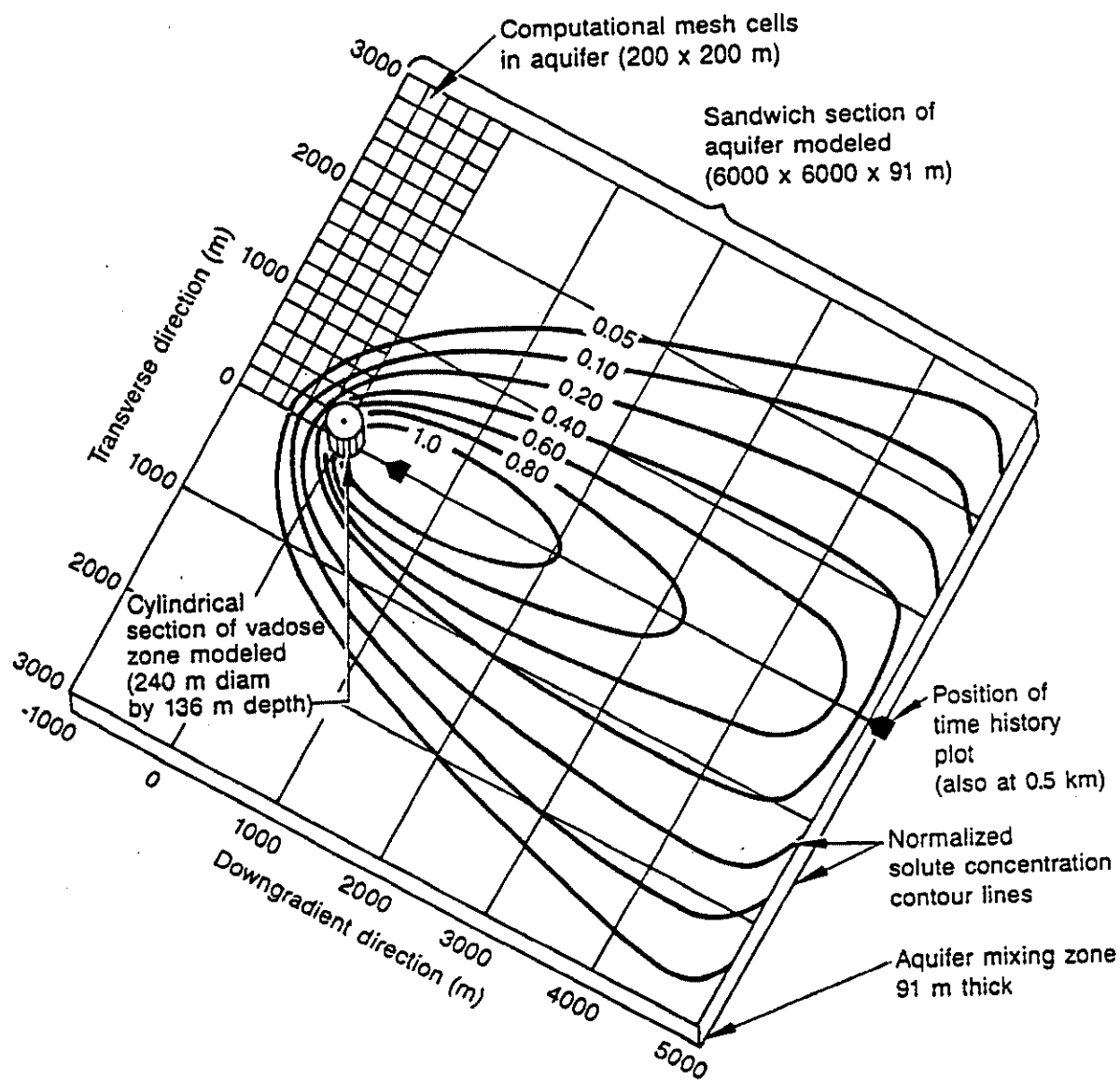


Figure 4-1. Geometrical Configuration for Modeling Solute Transport

The elliptical contour lines in the aquifer represent arbitrary solute concentration contour lines. The zero transverse direction axis represent the location of the highest solute concentrations in the aquifer vs down-gradient distance from the source. The black pentagons at 0.5 and 5.0 km downgradient positions represent the positions in which time history plot of solute concentration vs time were done.

The computational mesh used for the vadose zone is shown in Figure 4-2. A radial distance of 120 m and vertical distance of 136 m was used. Initially, a radial distance of 500 m was used but because of the limited amount of radial solute transport predicted and the longer computer time required, the radial distance was reduced to 120 m. The vadose zone is divided into 408 cells each 4 by 10 m. The alluvial source cylinder containing calcine is contained in three cells indicated by column 1 and rows 34-32. The surficial alluvium is contained in the first three rows, the clayey silt interbeds in rows 29-23 and row 5, and the basalt in the remaining rows.

The origin of the computational mesh (0,0) corresponds to the small dot in the top center of the vadose zone cylinder shown in Figure 4-1. Rotation of the computational mesh given in Figure 4-2 about the vertical axis at the origin of the radial axis would produce a cylindrical computational mesh within the vadose zone cylinder shown in Figure 4-1. Solute concentrations calculated for a cell at a given subsurface depth and radial distance are the same throughout a  $360^\circ$  rotation about the center vertical axis of the vadose zone cylinder.

The surface of the computational mesh used for the aquifer is shown in Figure 4-3. Only half of the mesh is shown which is symmetrical in the transverse direction (i.e., 0 to -3000 m in the y direction). Use of half of a symmetrical mesh provides more detail in the contour plots and avoids calculation of and print out of redundant numbers. Also not shown are two layers, each 45.5 m thick. from the top to the bottom of the aquifer (i.e., the vertical direction). Initially TRACER3D code calculations were



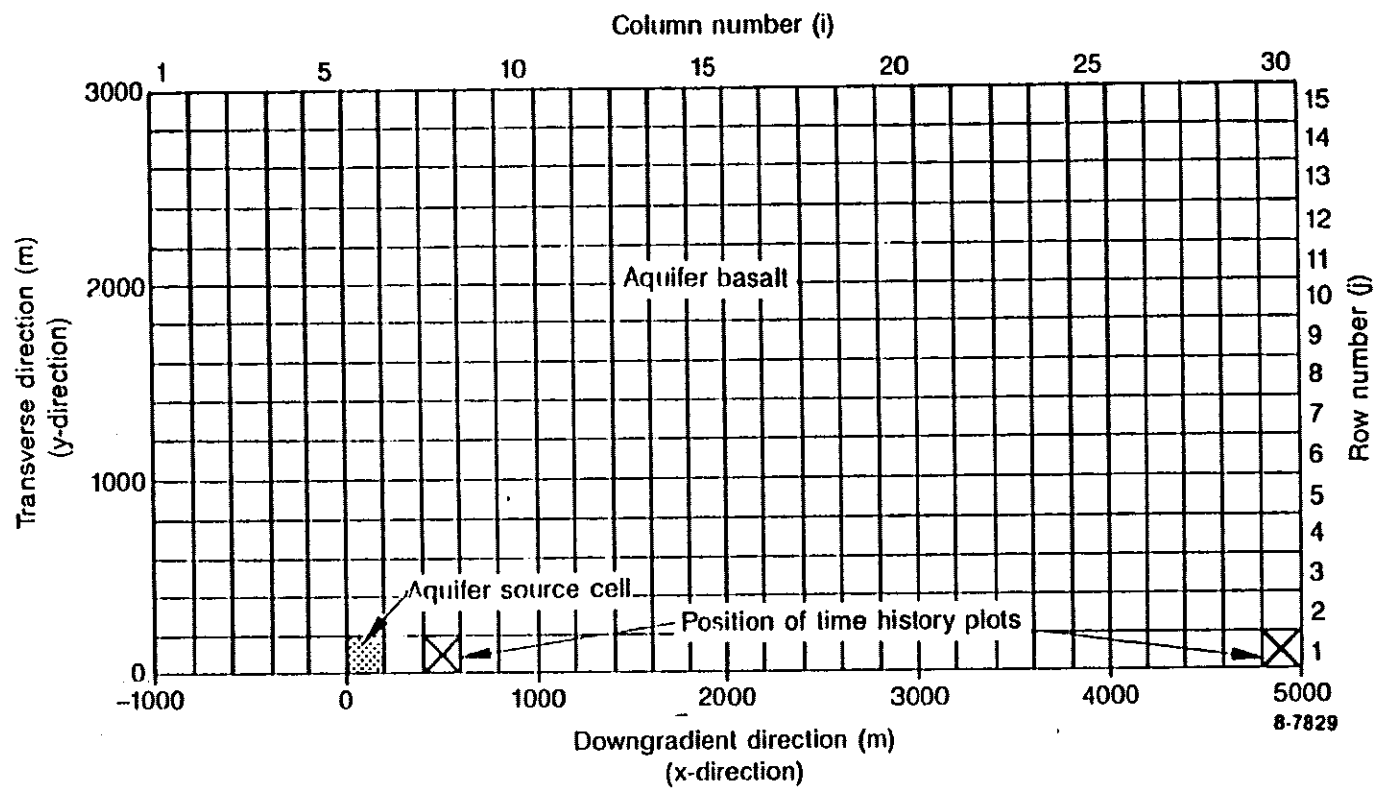


Figure 4-3. Computational Mesh for the ICPP Aquifer Zone

done using more layers, but the vertical concentration gradient was insignificant. Therefore, to reduce computational time and amount of data generated, only two layers were used as a check for possible vertical concentration gradients vs variation of the input parameters.

The computational mesh is square shaped with 6000 m in the transverse and downgradient directions. It includes 1000 m upgradient direction (i.e., -1000 m) for calculating upgradient dispersion of the solute against the aquifer flow. The mesh is divided into 200 x 200 m cells for a total of 450 cells in one 45.5 m layer or a total of 900 cells used for calculation in the two aquifer layers.

The black square at cell  $i,j = 6,1$  represents the source cell for contaminants from the vadose zone entering the aquifer. This cell should have an area comparable to the circular area which contains the solute transported through the vadose zone. Data generated from the vadose zone TRACR3D code calculations is stored for later use as the source term for the aquifer calculations. In effect, the code is run twice in an uncoupled mode.

*Is the vadose zone contribution halved for input into the saturated portion? Steven*

## V. TRACR3D CODE RESULTS

Because modeling and code results are subject to change as the assumptions for near-surface disposal are better defined, codes become more sophisticated, and hydrogeological parameters and geochemical reactions become better known, the results of this study are considered preliminary in nature. The intent was to assimilate the best available input data for the ICPP area and employ a state-of-the-art code to provide guidance for future studies and identify areas where more laboratory and field data are needed. Although the accuracy of the code predictions presented in this document cannot be verified without field testing, the trends and comparisons among the solutes and rainwater recharge scenarios modeled are considered valid.

The contour plots given below are based on the computational meshes illustrated in Figures 4-2 and 4-3. The solute source at time zero is located in the upper left corner of the vadose zone plots in an area enclosed by -12 m subsurface depth by 10 m radial distance. The vadose zone-aquifer interface occurs at -136 m subsurface depth. The 0,0 coordinate of the vadose zone plots given below corresponds to the position of the small alluvial cylinder on the aquifer illustrated in Figure 4-1. Only the upper half of the symmetrical aquifer contour lines illustrated in Figure 4-1 are shown in the vadose zone plots below.

### 1. NO<sub>3</sub><sup>-</sup> SOLUTE

#### 1.1 1.25 cm/yr Rainwater Recharge

Figures 5-1 through 5-3 illustrate the contour lines of the NO<sub>3</sub><sup>-</sup> concentration (log g/mL) over a 50 to 4000 yr period. As indicated in Chapter III, Section 2.1, the initial NO<sub>3</sub><sup>-</sup> concentration was 0.37 g/mL. A K<sub>d</sub> of zero was assumed for all vadose and aquifer media. The plots in Figure 5-1a indicate that the solute at the 10<sup>-11</sup> g/mL level reaches the aquifer after about 300 years. Between 50 and 600 years a concentrated plug of solute moves down the vertical axis but is diluted by about a factor of ten by the time it reaches the aquifer at -136 m.

Throughout the 50-4000 year period illustrated, a dilute solute front propagates in the radial distance out to about 100 m by 1000 years and then begins to withdraw. Simultaneously, concentrations of  $\text{NO}_3^-$  represented by the contour lines are passing into the aquifer. They progressively increase in concentration between 300-600 years and maintain a steady source depicted by the  $10^{-2}$  contour line 600-1000 years. The numerical data generated by the code indicates the most concentrated  $\text{NO}_3^-$  level to enter the aquifer is 0.045 g/mL at about 900 years. This indicates a dilution factor of about 8.2 is provided by the vadose zone. After 1000 years, the concentration begins to decrease until only very dilute lines are left by 4000 years. The 2000-4000 year plots show the  $\text{NO}_3^-$  solute being flushed from the top of the subsurface.

The wrap around of all the contour lines which reach the aquifer interface into one point (i.e., coordinates 0, -136 [radial, subsurface]) is an artifact of the plotting routine. For example, the contour lines in the 600 year plot do not actually wrap around but the  $10^{-11}$  line enters at the 80 m radial distance, the  $10^{-9}$  line enters at the 65 m radial distance, etc.

Figures 5-2a and 5-2b illustrate the contour lines of  $\text{NO}_3^-$  in the aquifer over a 300 to 4000 year period. The plots show that the concentration bands passing through the 5000 m downgradient points increase from  $10^{-16}$  to  $10^{-9}$  g/mL over a 300 to 1000 year period and then begin to decrease. A  $10^{-8}$  g/mL band forms between 700 and 1000 years but never extends beyond 3000 m downgradient. The plots show only two concentration bands which wrap around and the others going off-scale along the upper horizontal boundary of the plot. A larger transverse direction and downgradient distance for modeling would be required to see the complete profile of several contour lines in each plot. Another feature of the plotting routine is the dark vertical bands formed at the ends of some of the plots. Eleven contour lines ranging from  $10^{-18}$  to  $10^{-8}$  g/mL were used for plotting, some of which ended up being compressed into the dark bands because they are off-scale.



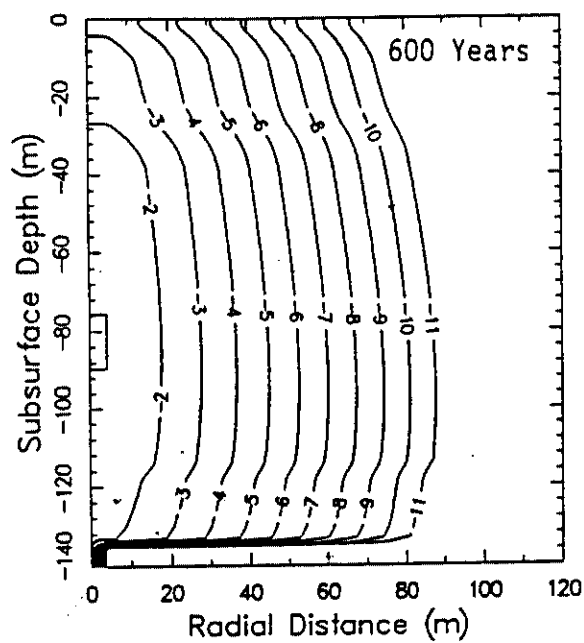
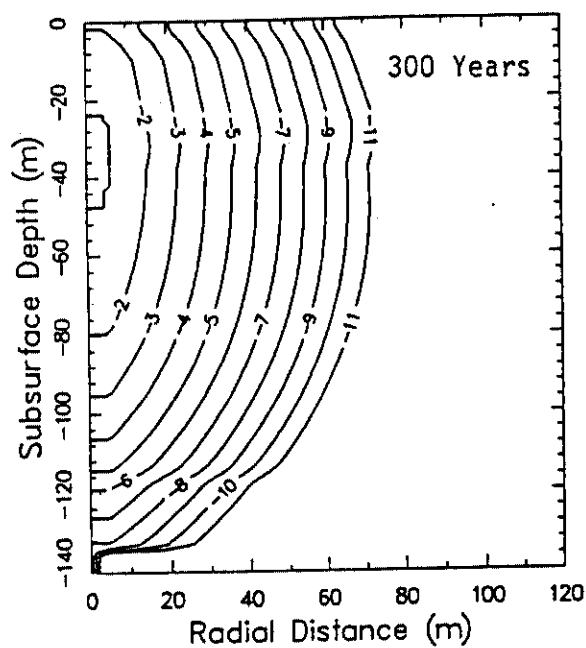
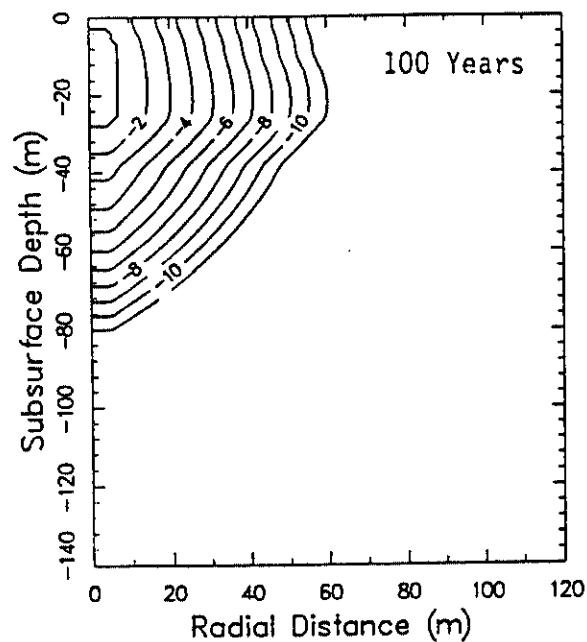
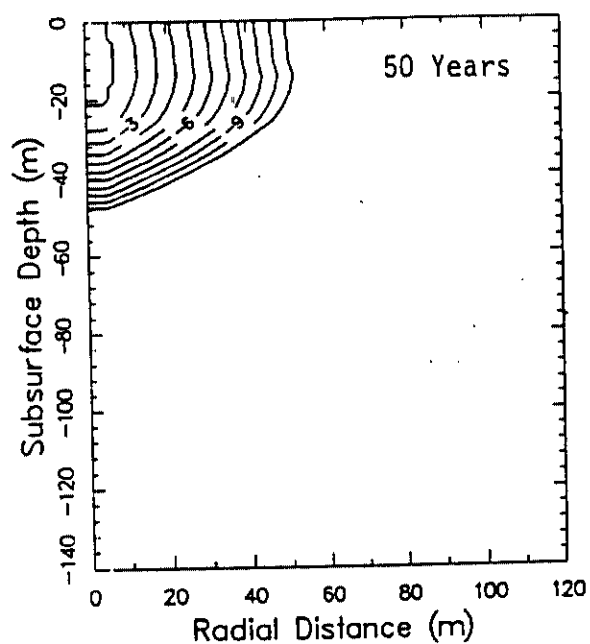


Figure 5-1a.  $\text{NO}_3^-$  Solute Transport (log conc. in g/mL) in the Vadose Zone 50-600 Years for 1.25 cm/yr Rainwater Recharge

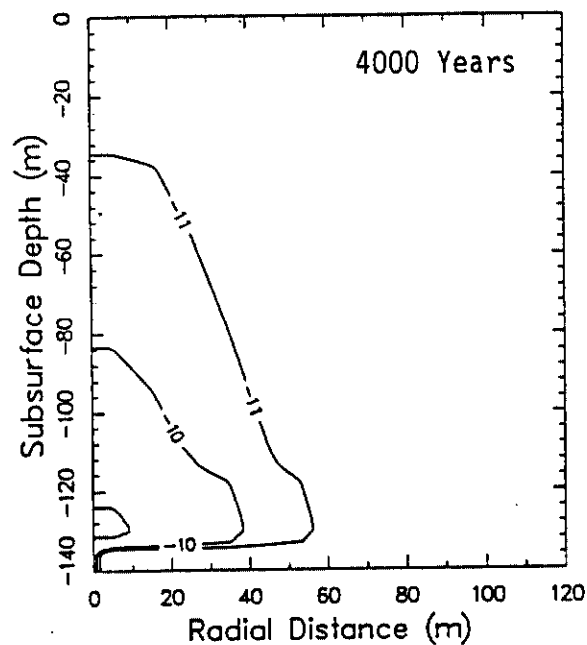
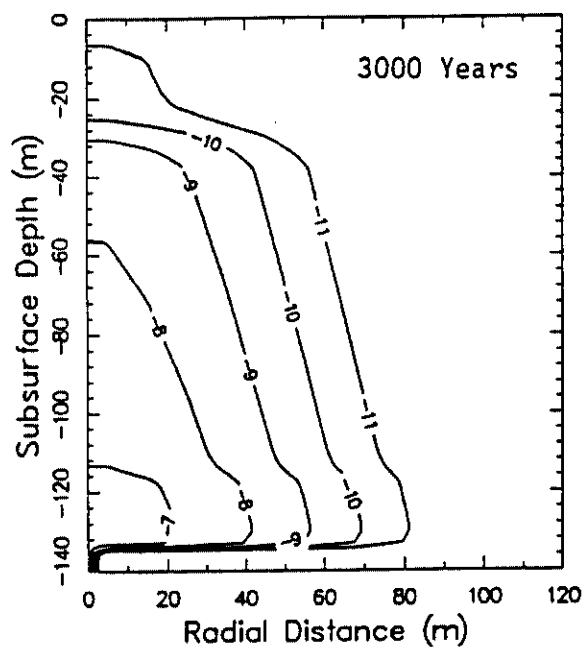
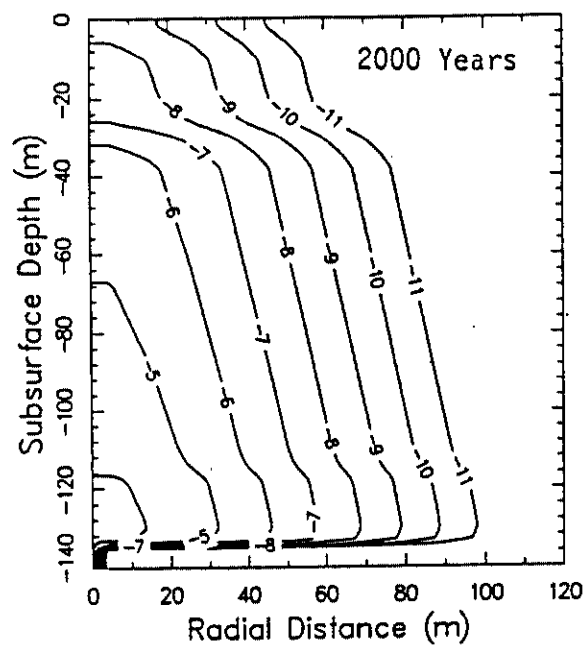
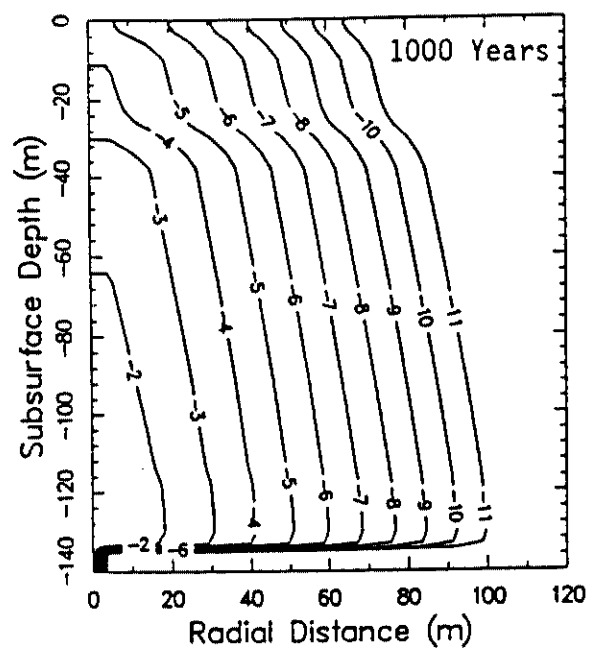


Figure 5-1b.  $\text{NO}_3^-$  Solute Transport (log conc. in g/mL) in the Vadose Zone 1000-4000 Years for 1.25 cm/yr Rainwater Recharge

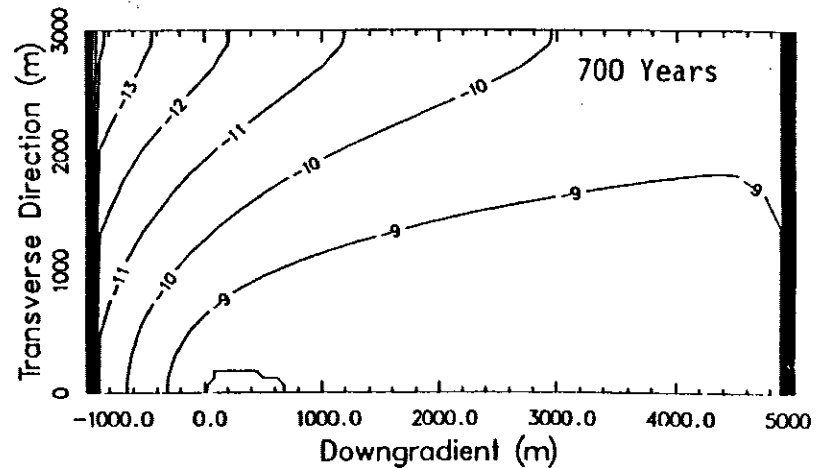
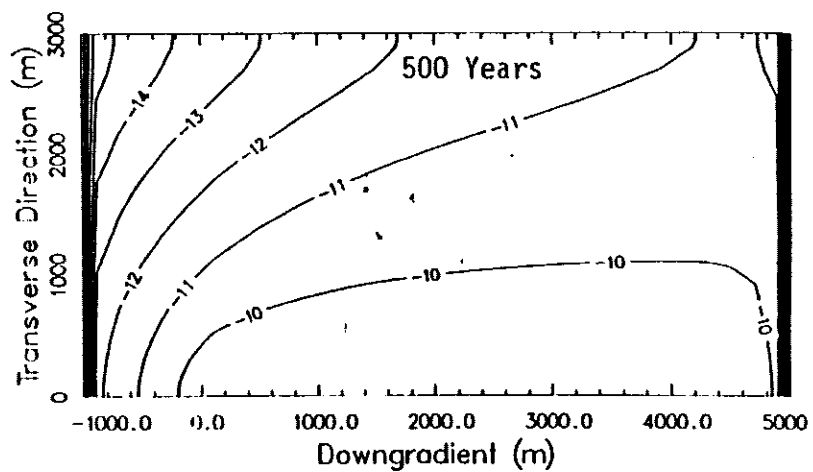
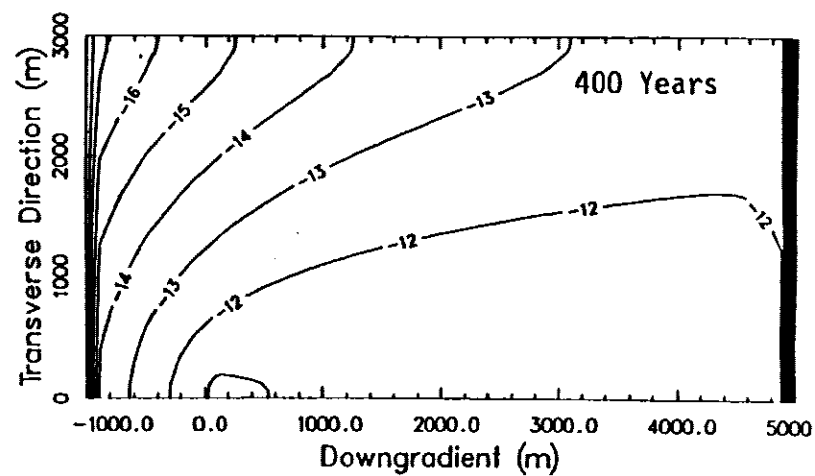
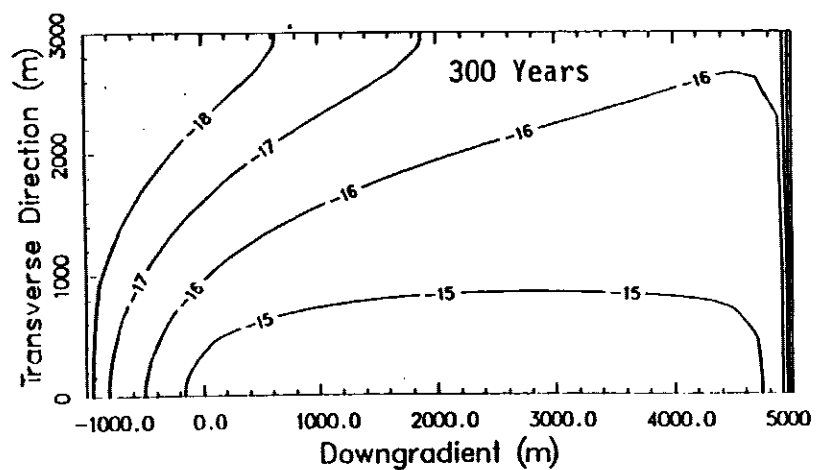


Figure 5-2a.  $\text{NO}_3^-$  Solute Transport (log conc. in g/mL) in the Aquifer  
300-700 Years for 1.25 cm/yr Rainwater Recharge

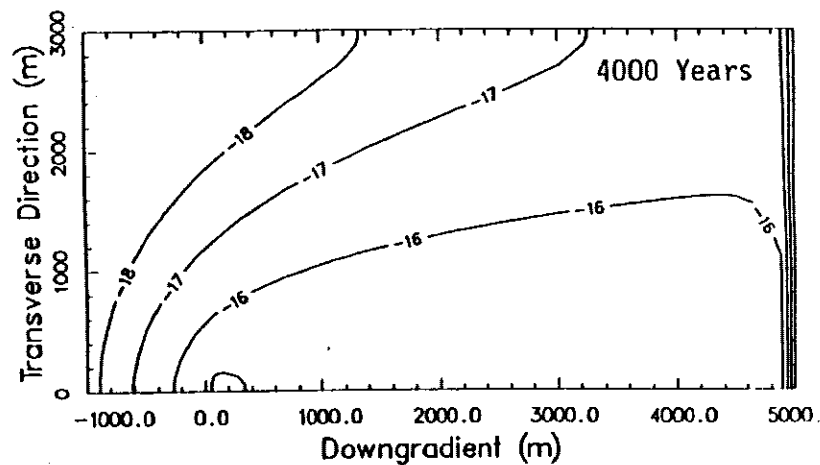
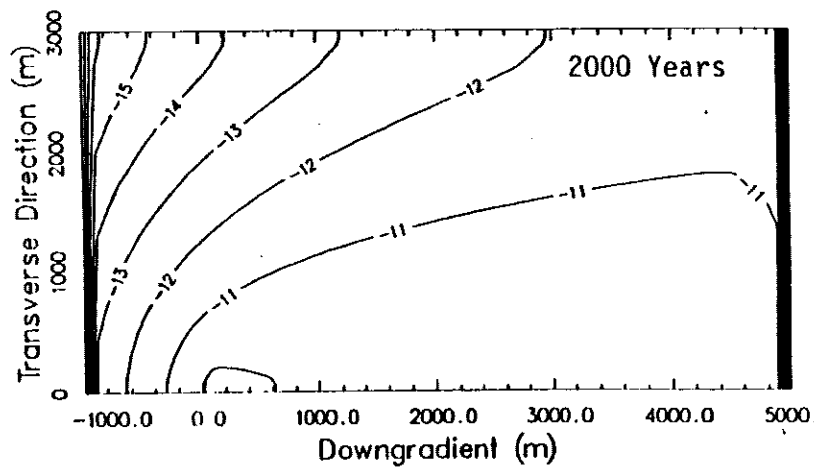
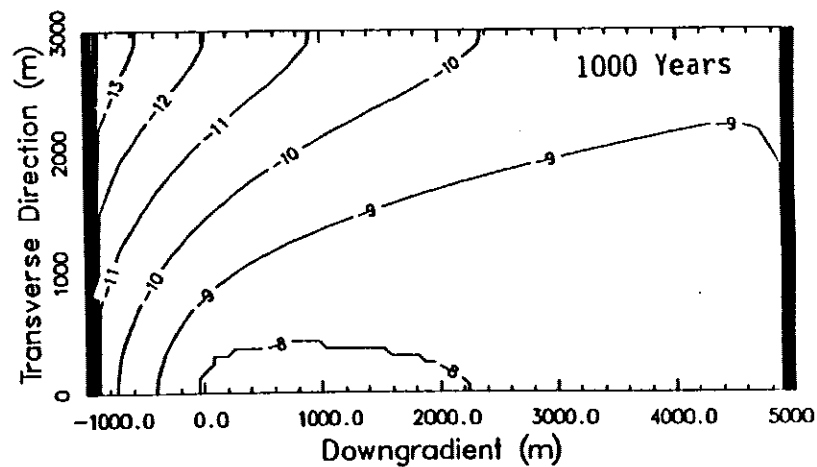
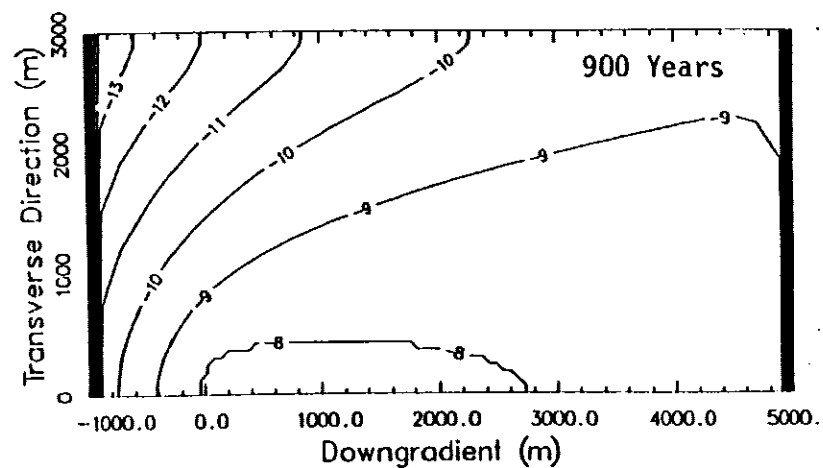


Figure 5-2b.  $\text{NO}_3^-$  Solute Transport (log conc. in g/mL) in the Aquifer  
900-4000 Years for 1.25 cm/yr Rainwater Recharge

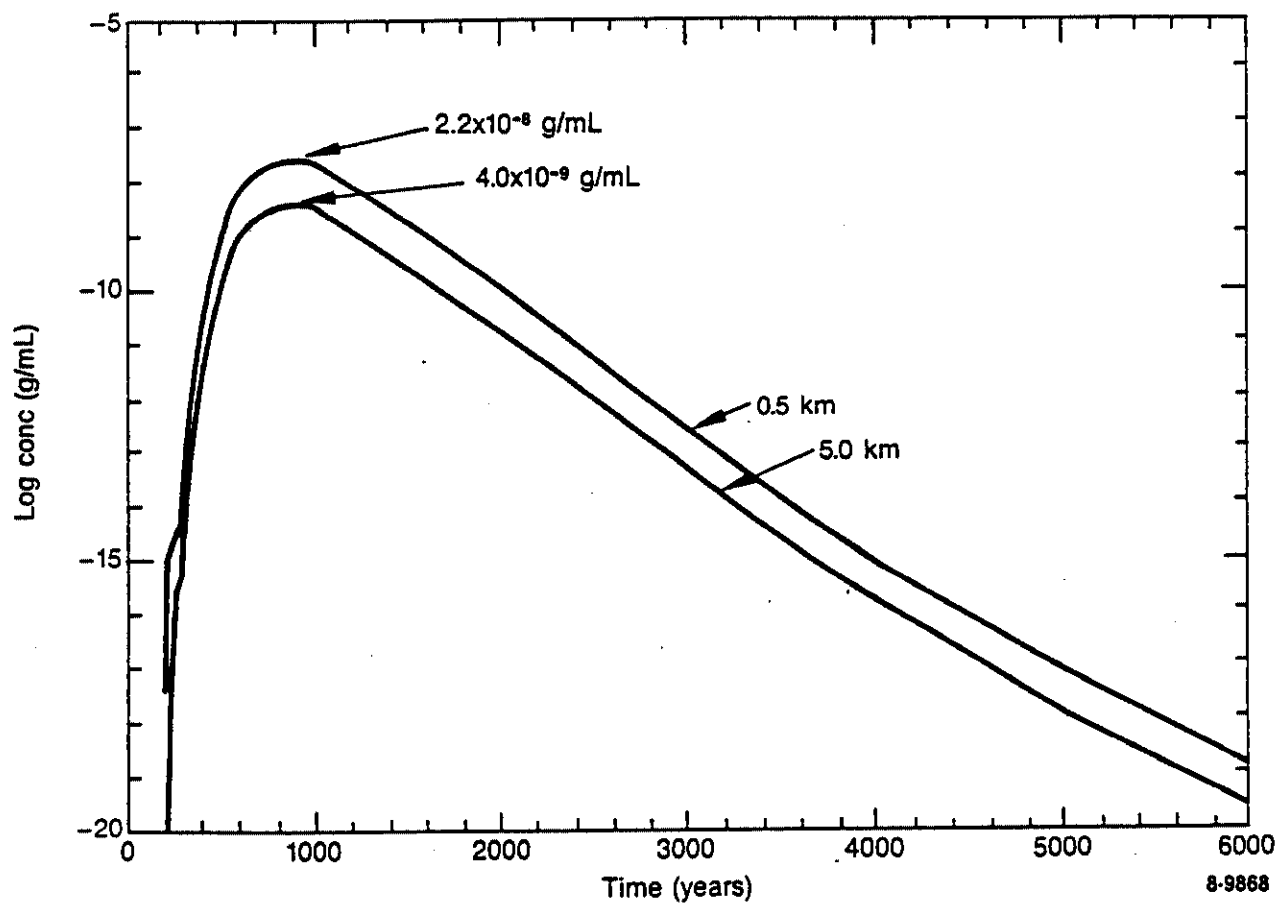


Figure 5-3. NO<sub>3</sub><sup>-</sup> Solute Concentration vs Time 0.5 and 5.0 km Down-gradient in the Aquifer for 1.25 cm/yr Rainwater Recharge

Figure 5-3 illustrates the  $\text{NO}_3^-$  concentrations vs time for two points directly downgradient of the vadose zone-aquifer interface where the most concentrated solute source enters. The solute concentration maximizes at about 900 years after the beginning of the modeling period with concentrations of  $2.2 \times 10^{-8}$  and  $4.0 \times 10^{-9}$  g/mL for the 0.5 and 5.0 downgradient positions, respectively.

From the original vadose zone source concentration (0.37 g/mL) to the 5.0 km downgradient aquifer concentration, the overall dilution factor is  $9.3 \times 10^7$ . The dilution factor between 0.5 km and 5.0 km downgradient positions is 5.5.

#### 1.2 12.5 cm/yr Rainwater Recharge

Figures 5-4 through 5-6 illustrate the solute transport of  $\text{NO}_3^-$  for ten times the rainwater recharge as in Figures 5-1 through 5-3. The vadose zone and aquifer plots all have the same shape and behavior as those for the 1.25 cm/yr rainwater recharge scenario but the solute moves through much faster. The solute is essentially flushed out of the vadose zone by 700 years compared to greater than 4000 years for the smaller rainwater recharge scenario.

As indicated in Figure 5-6, the maximum solute concentrations in the aquifer occur between 200 and 250 years after release with levels of  $8.4 \times 10^{-8}$  and  $1.5 \times 10^{-8}$  g/mL at 0.5 and 5.0 km downgradient, respectively. The dilution factor between the two downgradient positions is 5.6 which is the same observed with the 1.25 cm/yr rainwater recharge scenario. The 12.5 cm/yr rainwater recharge rate results in the solute concentration maxima occurring about 4 times earlier, increases the maximum aquifer concentrations by a factor of about 3.8, and produces a much sharper solute band shape relative to the 1.25 cm/yr recharge rate.

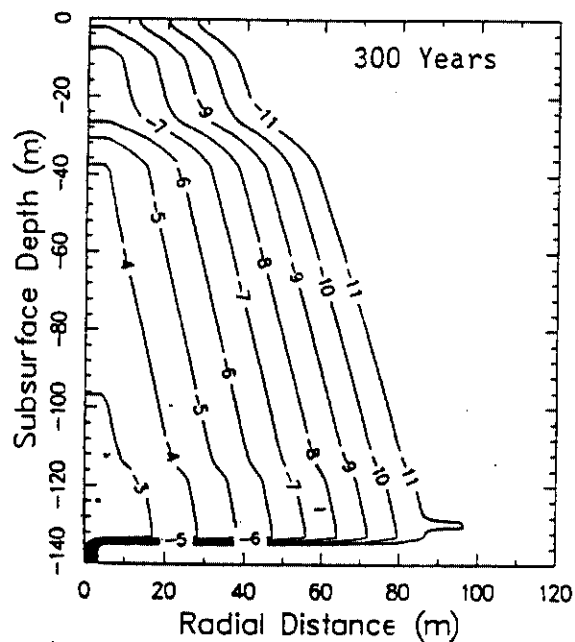
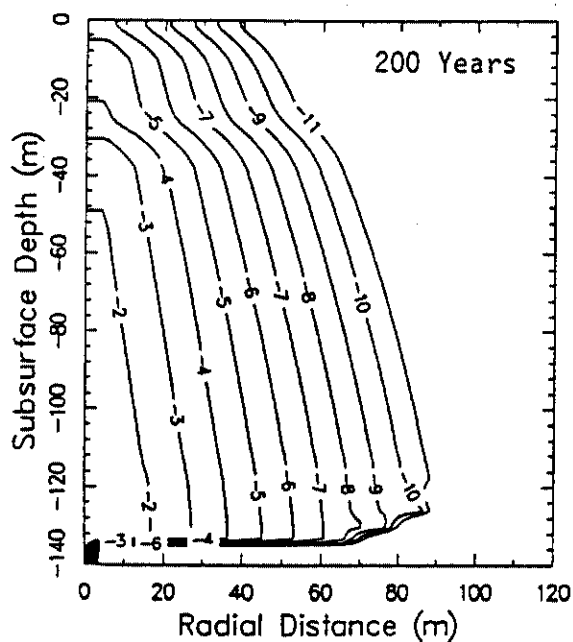
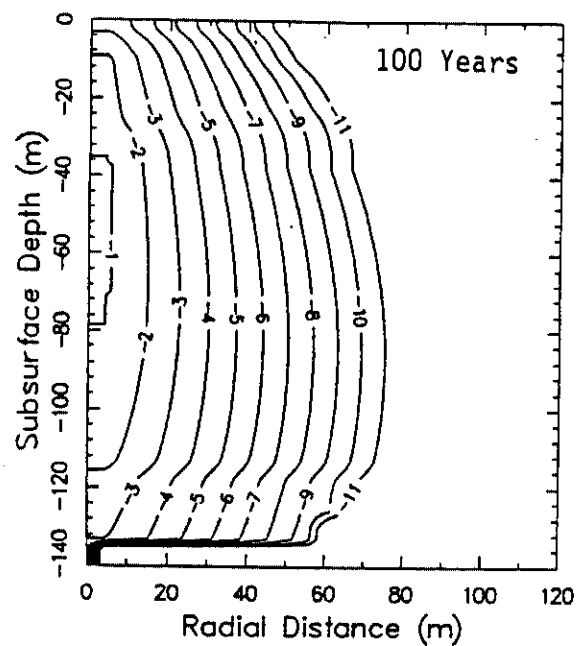
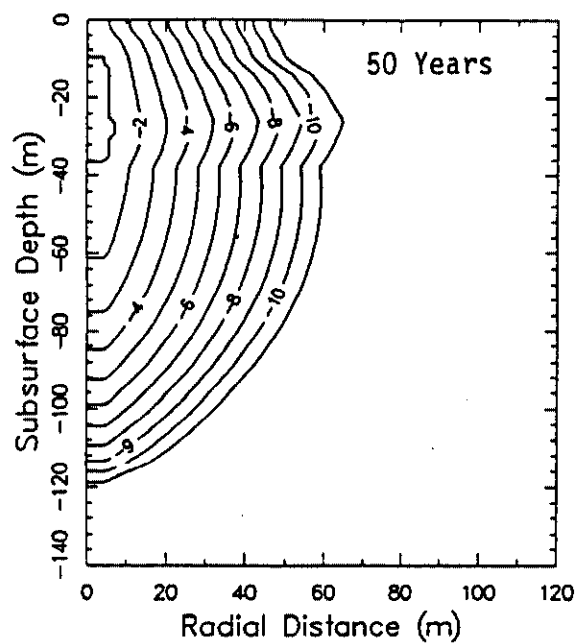


Figure 5-4a.  $\text{NO}_3^-$  Solute Transport (log conc. in g/mL) in the Vadose Zone 50-300 Years for 12.5 cm/yr Rainwater Recharge

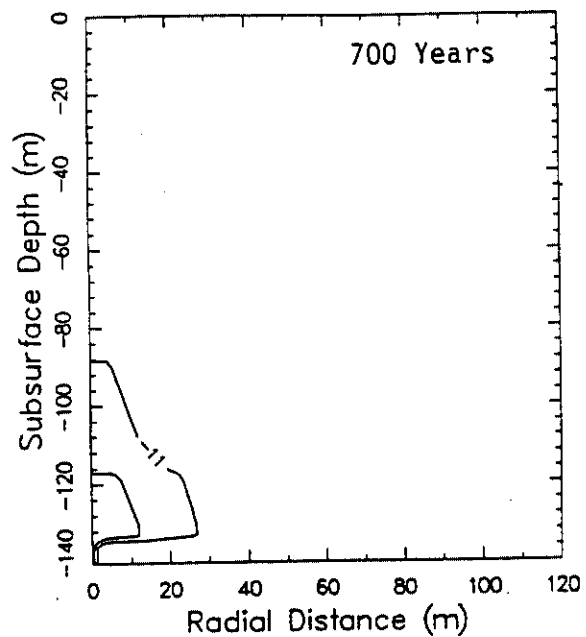
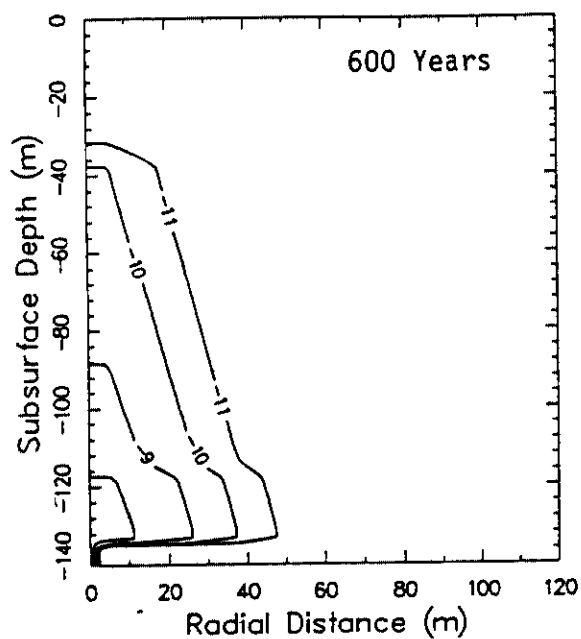
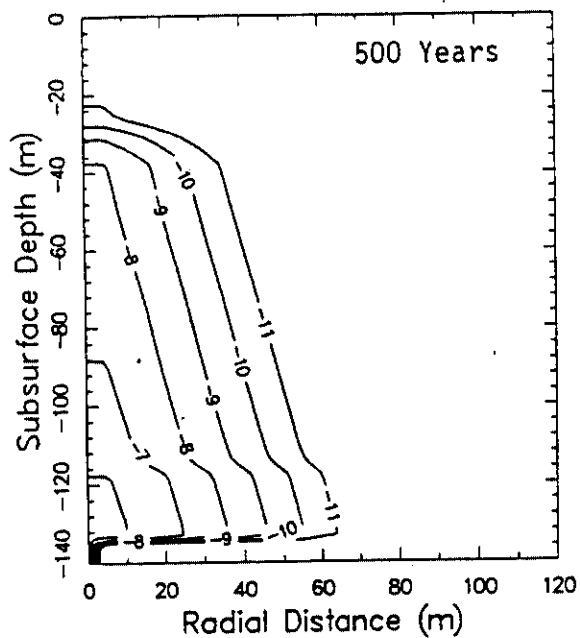
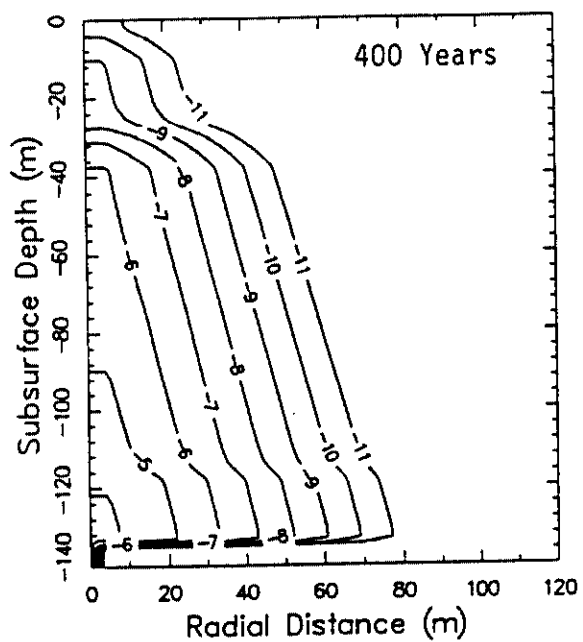


Figure 5-4b.  $\text{NO}_3^-$  Solute Transport (log conc. in g/mL) in the Vadose Zone 400-700 Years for 12.5 cm/yr Rainwater Recharge



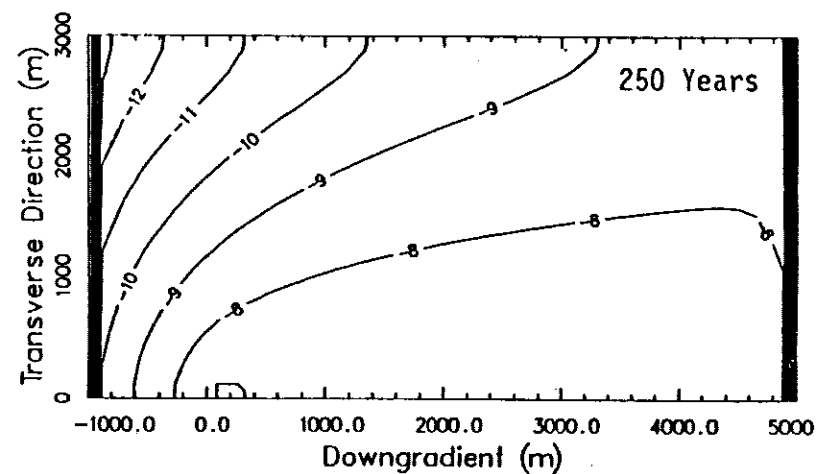
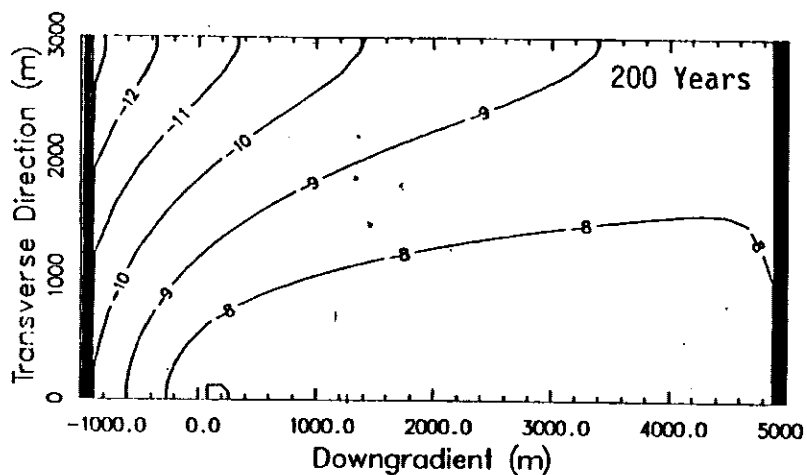
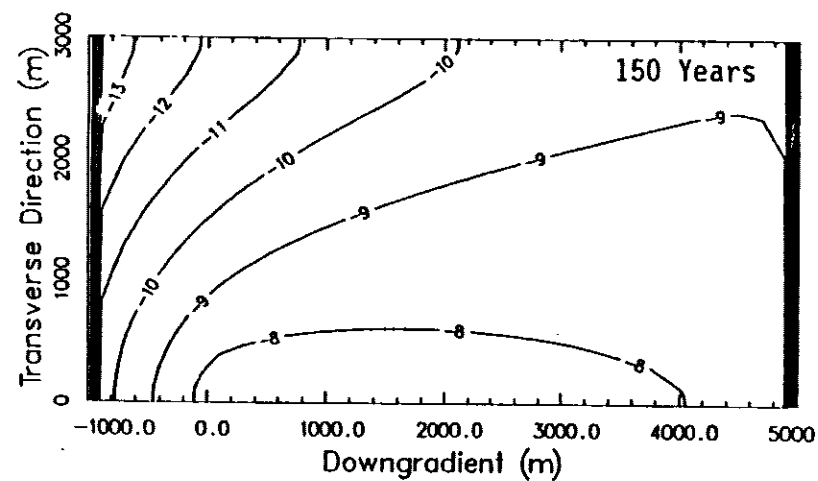
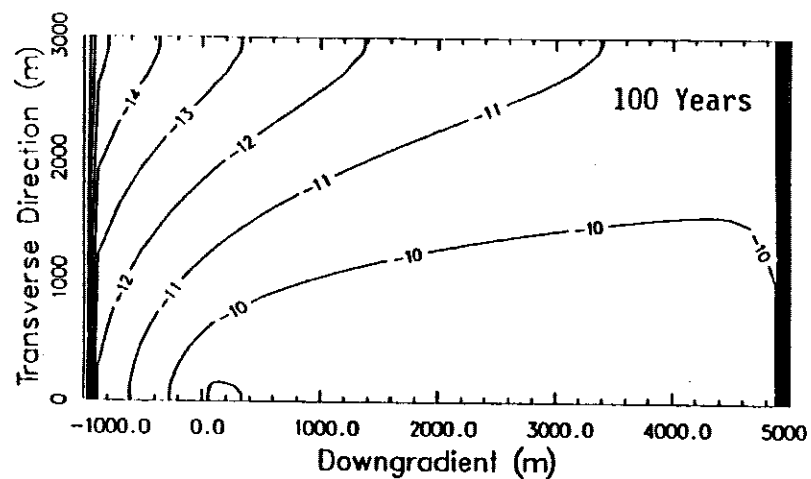


Figure 5-5a.  $\text{NO}_3^-$  Solute Transport (log conc. in g/mL) in the Aquifer  
100-250 Years for 12.5 cm/yr Rainwater Recharge

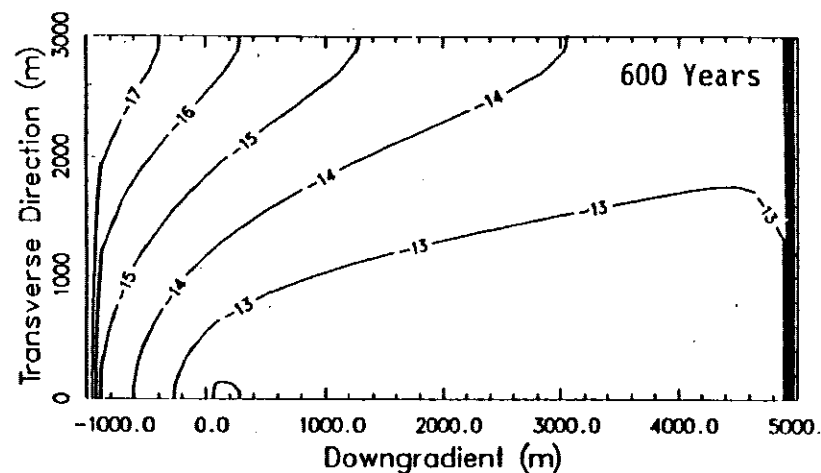
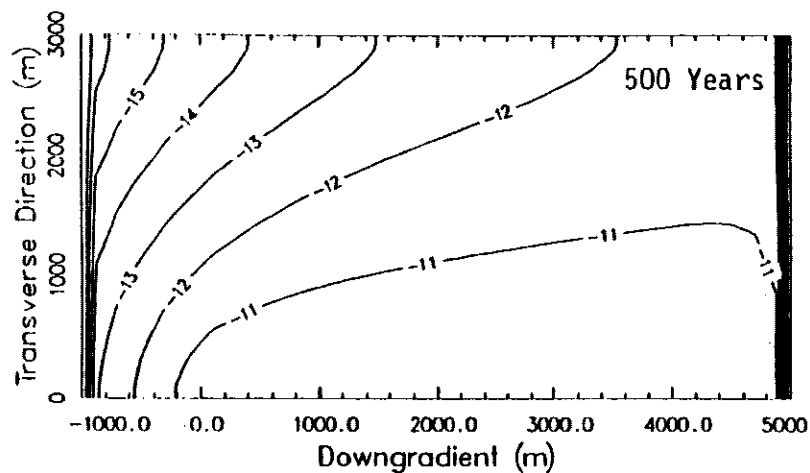
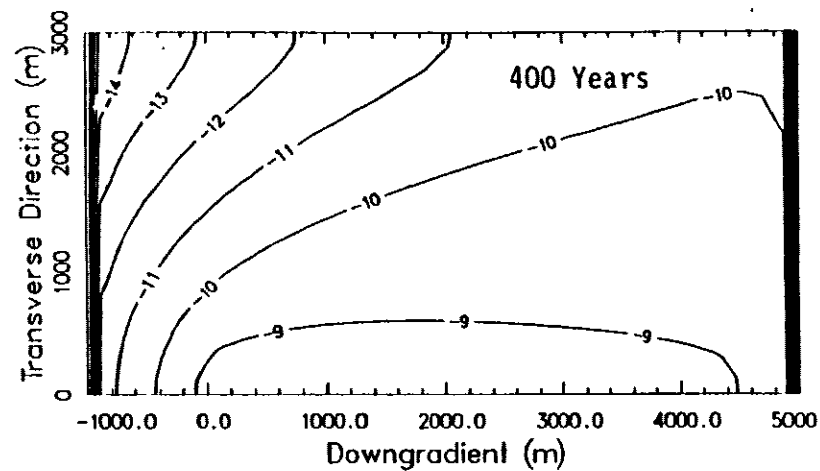
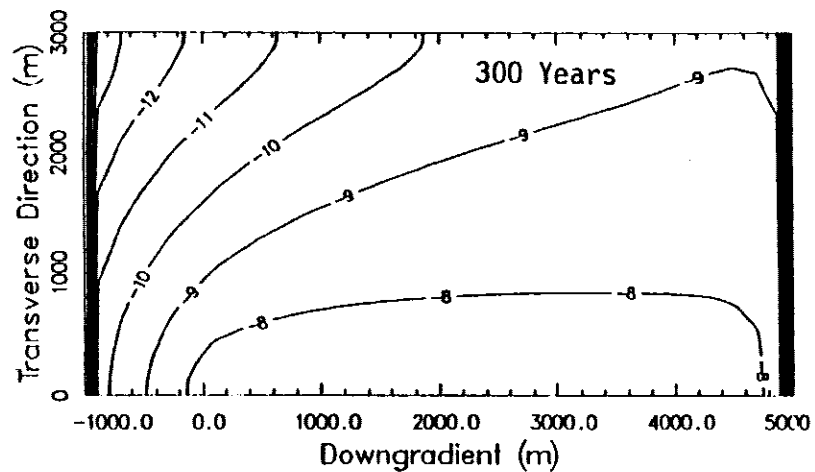


Figure 5-5b.  $\text{NO}_3^-$  Solute Transport (log conc. in g/mL) in the Aquifer  
300-600 Years for 12.5 cm/yr Rainwater Recharge

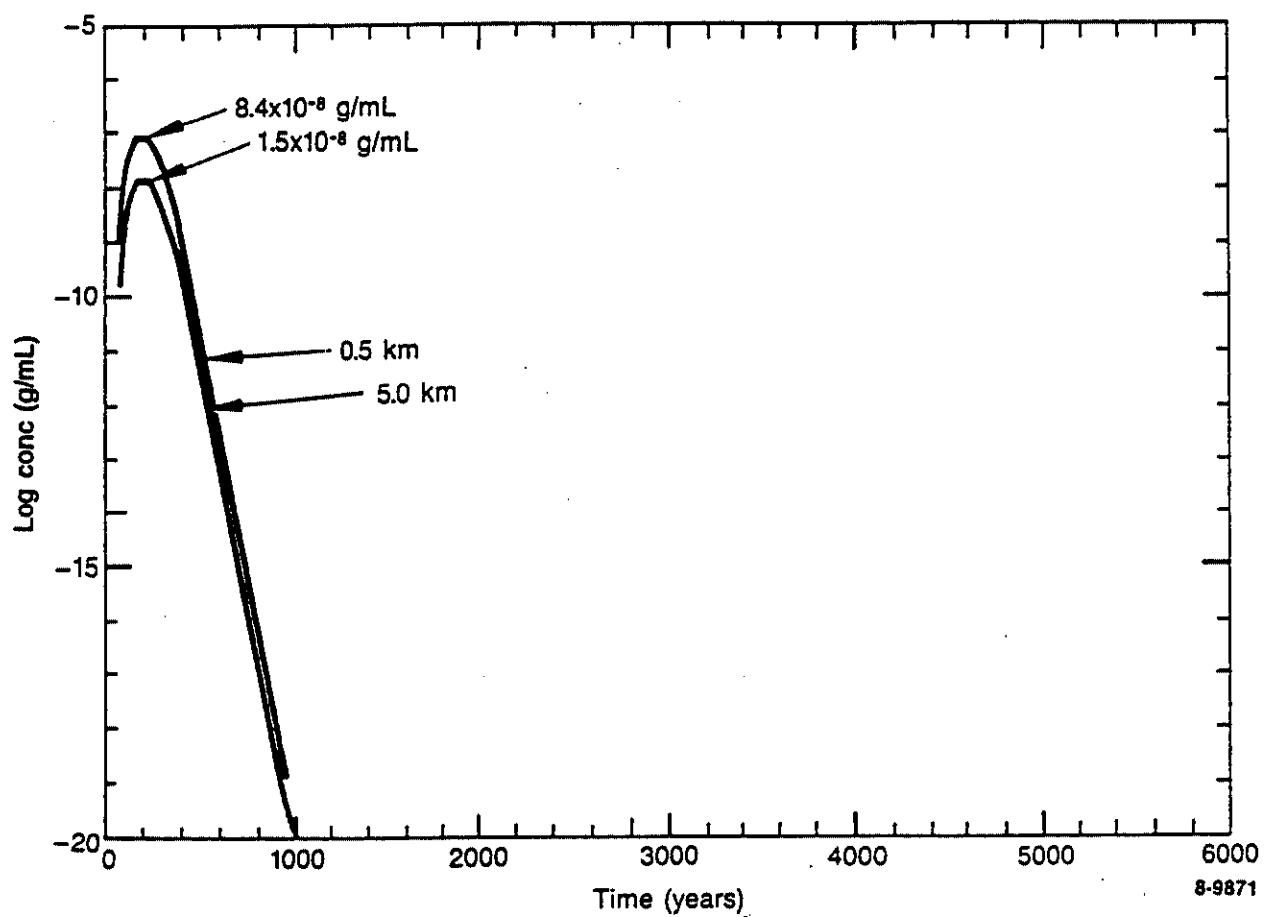


Figure 5-6.  $\text{NO}_3^-$  Solute Concentration vs Time 0.5 and 5.0 km Down-gradient in the Aquifer for 12.5 cm/yr Rainwater Recharge

## 2. Cr<sup>+6</sup> SOLUTE

As indicated in Chapter III, Section 2.2, the initial Cr<sup>+6</sup> concentration modeled was 0.037 g/mL. This is a factor of ten smaller than the initial NO<sub>3</sub><sup>-</sup> concentration. For both the NO<sub>3</sub><sup>-</sup> and Cr<sup>+6</sup> solute, no adsorption by the alluvium or interbeds in the vadose or aquifer zones was assumed. Therefore, the contour plots produced for the Cr<sup>+6</sup> solute are identical to those for the NO<sub>3</sub><sup>-</sup> solute except that the concentration profiles are a factor of ten less at any given time period for either rainwater recharge scenario. To avoid repetition, only the time history plots of Cr<sup>+6</sup> concentration vs time at 0.5 and 5.0 km downgradient in the aquifer are given below.

### 2.1 1.25 cm/yr Rainwater Recharge

Figure 5-7 illustrates that the maximum concentrations of Cr<sup>+6</sup> would be  $2.2 \times 10^{-9}$  and  $4.0 \times 10^{-10}$  g/mL at about 900 years 0.5 and 5.0 km downgradient in the aquifer for the 1.25 cm/yr rainwater recharge. The shape of the time history curves are identical to those in Figure 5.3 for the NO<sub>3</sub><sup>-</sup> solute except all points on the curves for the 5.0 or 0.5 km positions are a factor of ten less for the Cr<sup>+6</sup> solute.

### 2.2 12.5 cm/yr Rainwater Recharge

Figure 5-8 illustrates that the maximum concentrations of Cr<sup>+6</sup> are predicted to be  $9.2 \times 10^{-9}$  and  $1.6 \times 10^{-9}$  g/mL at about 200 years 0.5 and 5.0 km downgradient in the aquifer for the 12.5 cm/yr rainwater recharge. The maxima can be compared to maxima of  $8.4 \times 10^{-8}$  and  $1.5 \times 10^{-8}$  g/mL for the NO<sub>3</sub><sup>-</sup> solute in Figure 5-6. The Cr<sup>+6</sup> maxima are not quite a factor of ten less as would be expected. This may be due to a lack of data points calculated in a region of the time history curve which is changing rapidly. If 10- instead of 50-year intervals were used for computation near the maxima, this discrepancy should disappear.

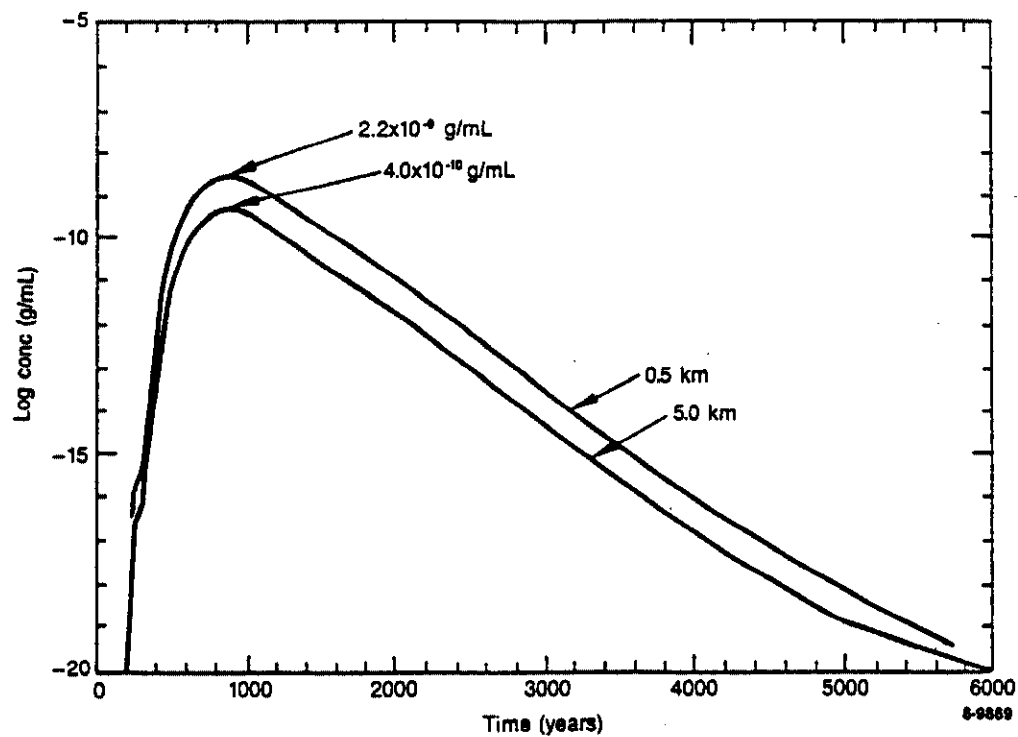


Figure 5-7.  $\text{Cr}^{+6}$  Solute Concentration vs Time 0.5 and 5.0 km Down-gradient in the Aquifer for 1.25 cm/yr Rainwater Recharge

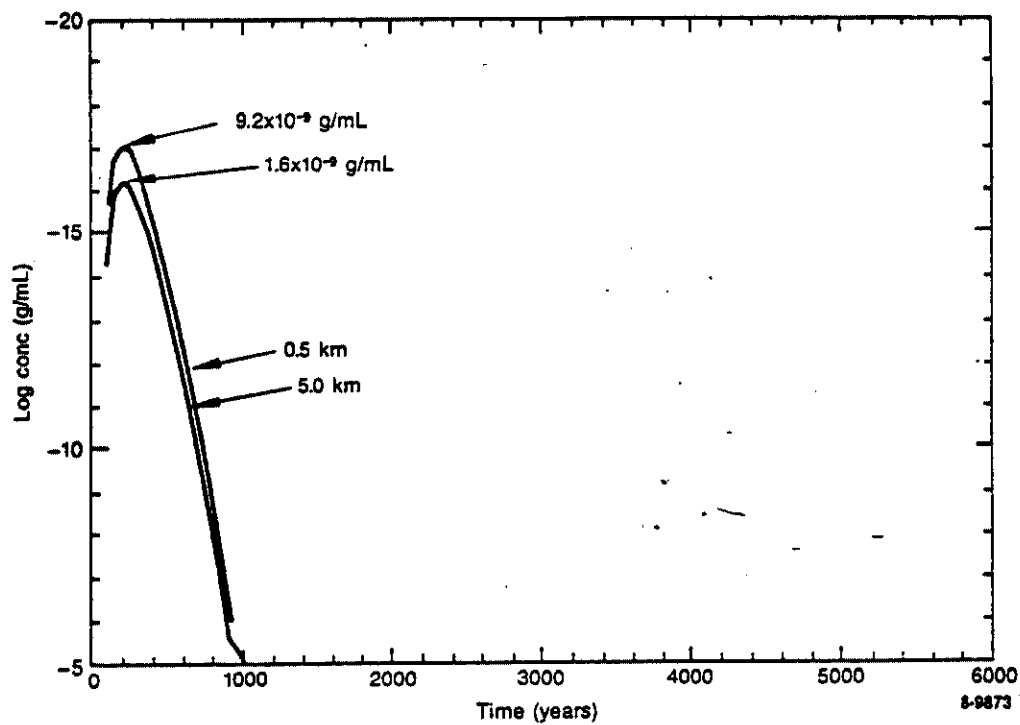


Figure 5-8.  $\text{Cr}^{+6}$  Solute Concentration vs Time 0.5 and 5.0 km Down-gradient in the Aquifer for 12.5 cm/yr Rainwater Recharge

### 3. Cd<sup>+2</sup> SOLUTE

As indicated in Chapter III, Section 2.3, the initial solute concentration of Cd<sup>+2</sup> was assumed to be  $3 \times 10^{-4}$  g/mL. But unlike the NO<sub>3</sub><sup>-</sup> and Cr<sup>+6</sup> solute, for which K<sub>d</sub> was assumed to be zero, a K<sub>d</sub> of 100 was assumed for Cd<sup>+2</sup> in the vadose zone alluvial and interbed layers. This results in the adsorbed concentration being 100 times greater (i.e., 0.03 g Cd<sup>+2</sup>/g alluvium) than that in solution. Because there is approximately ten times more soil than water per unit volume in the scenarios modeled, the actual equilibrium distribution of Cd<sup>+2</sup> is about 0.1% in solution and 99.9% adsorbed. These assumptions dramatically alter the appearance of the vadose contour lines for Cd<sup>+2</sup> and the amount of the solute which finally reaches the aquifer.

#### 3.1 1.25 cm/yr Rainwater Recharge

Figures 5-9a and 5-9b illustrate the Cd<sup>+2</sup> solute and adsorbed distribution in the vadose zone between 200 and 10,000 years. The solute contour lines are spaced by a factor of 10 whereas the adsorbed contour lines are spaced by a factor of 100 apart to make them legible. The solute contour lines show distinctive bulging and retraction at the top and bottom of the interbeds, respectively. Only a very small portion of the solute is transported over the 10,000 year period modeled. At 10,000 years, the  $10^{-4}$  g/mL solute contour line is still present in the alluvial layer while the most concentrated contour line reaching the aquifer is  $10^{-10}$  g/mL.

In Figure 5-9b, contour lines for the adsorbed species occur within the first 200 years and grow radially over the 10,000 year period. Very little of the Cd<sup>+2</sup> is transferred to the lower interbed (at -116 to -120 m) which has a  $10^{-10}$  g/g contour line and can be compared to a  $10^{-4}$  g/g line in the higher interbed and a  $10^{-2}$  g/g line in the alluvium. The numerical printout of the contour data indicated that after 10,000 years, 95.9 and 2.7% of the original Cd<sup>+2</sup> inventory resided in the alluvial layer and first interbed, respectively.

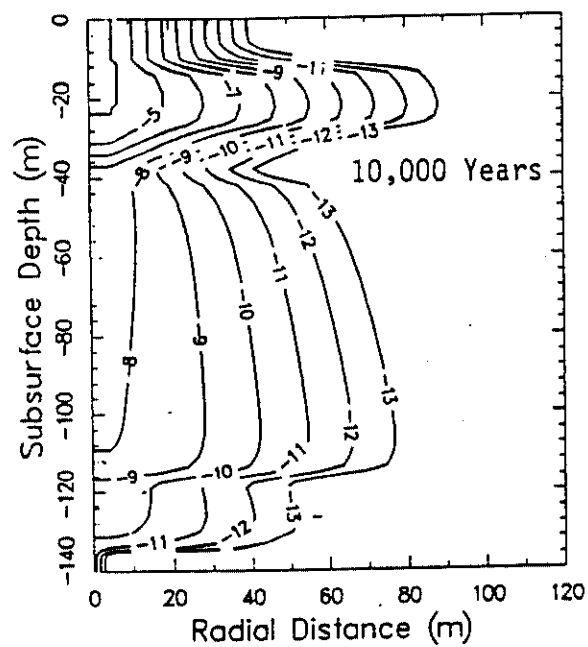
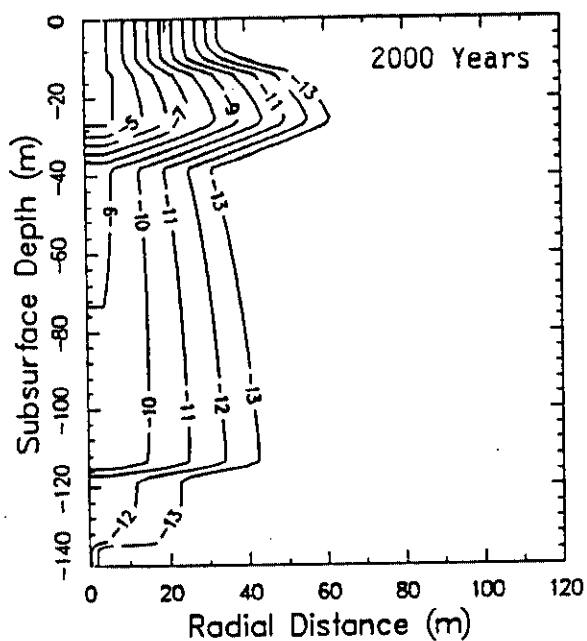
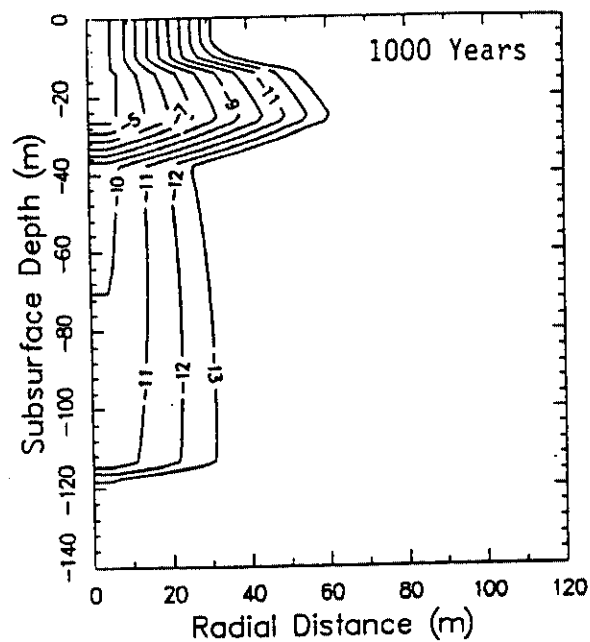
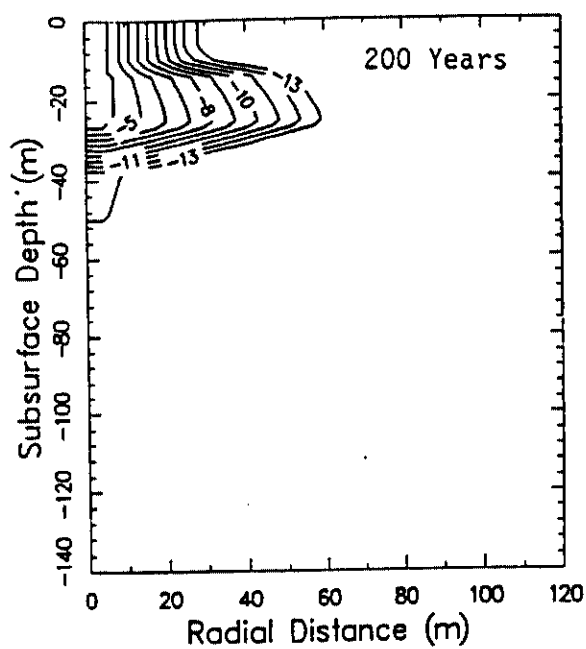


Figure 5-9a.  $\text{Cd}^{+2}$  Solute Transport (log conc. in g/mL) in the Vadose Zone 200-10,000 Years for 1.25 cm/yr Rainwater Recharge

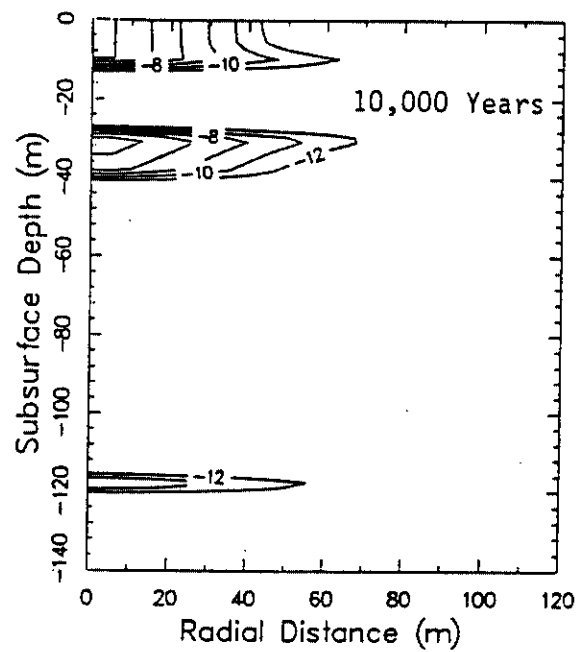
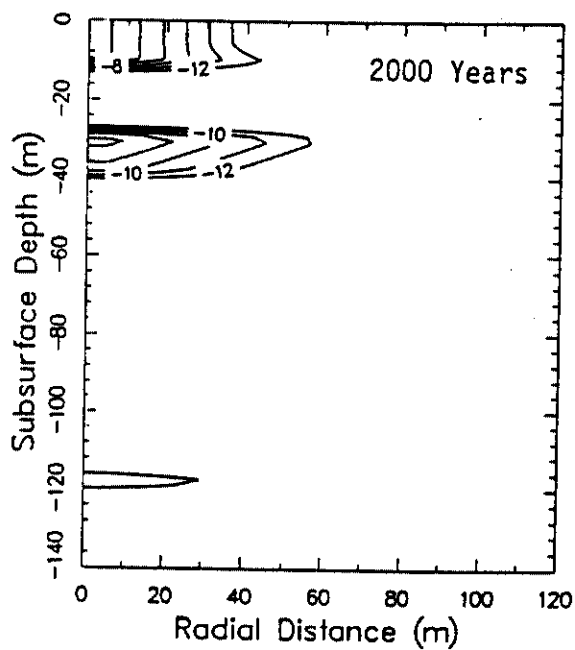
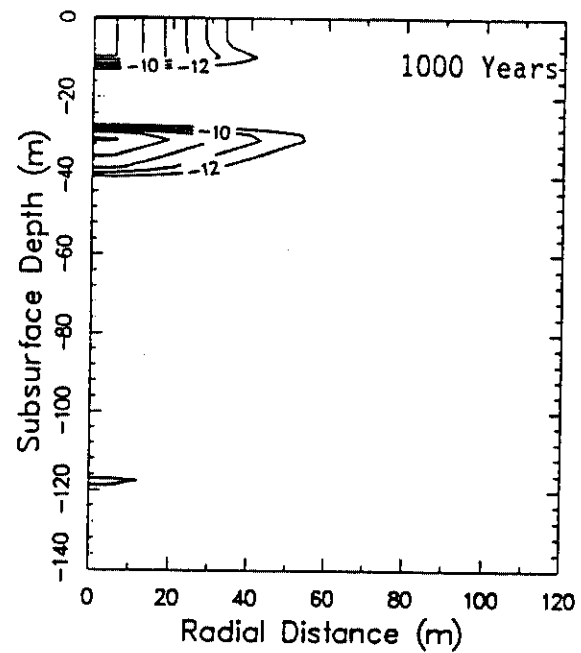
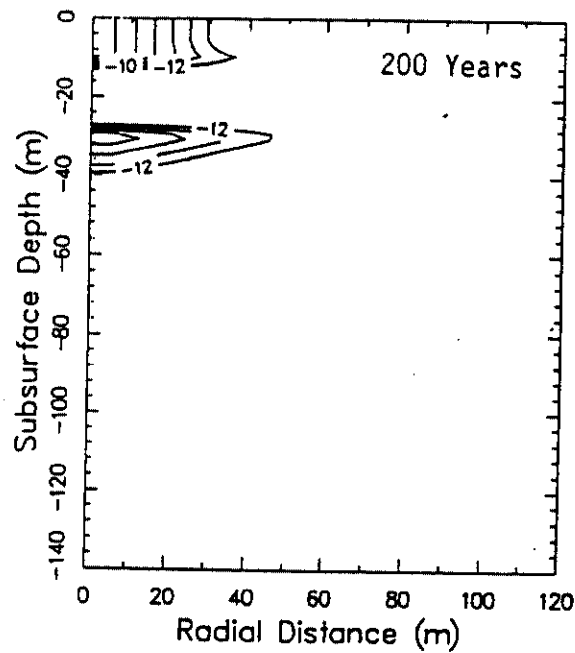


Figure 5-9b.  $\text{Cd}^{2+}$  Adsorbed Distribution (log conc. in g/g) in the Vadose Zone 200-10,000 Years for 1.25 cm/yr Rainwater Recharge



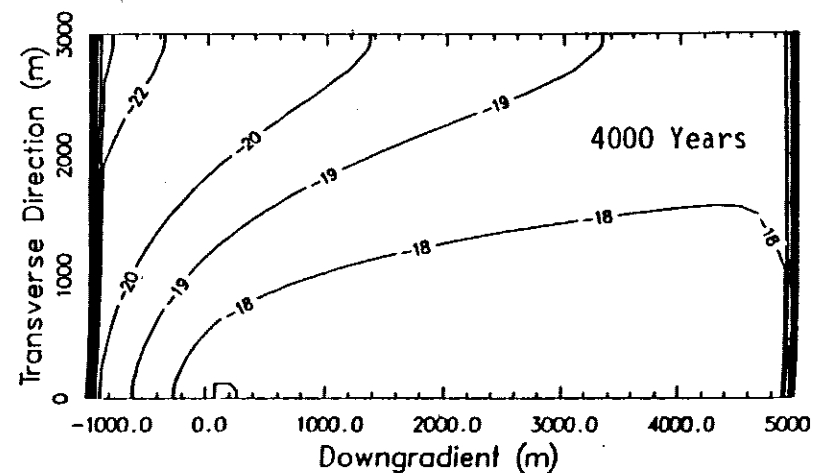
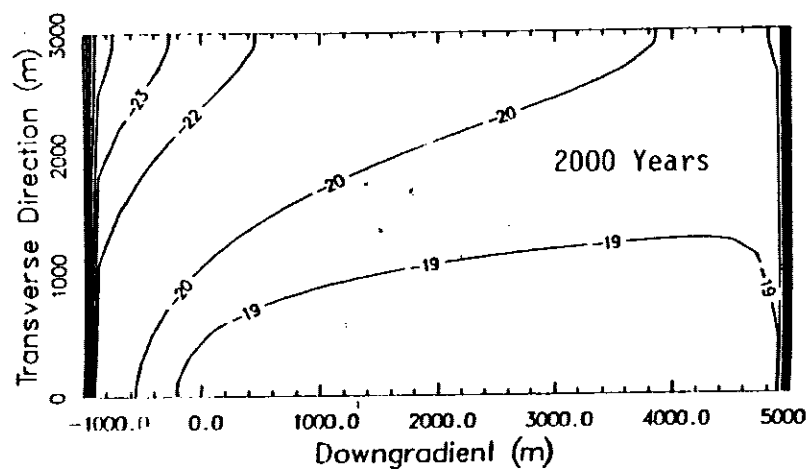
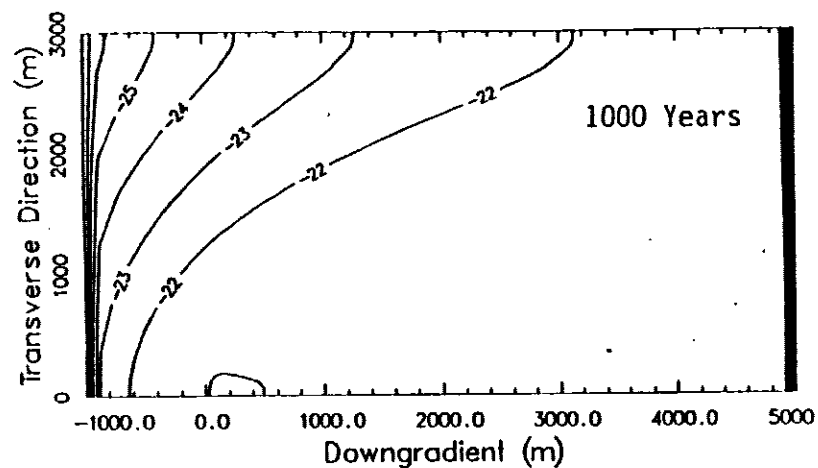
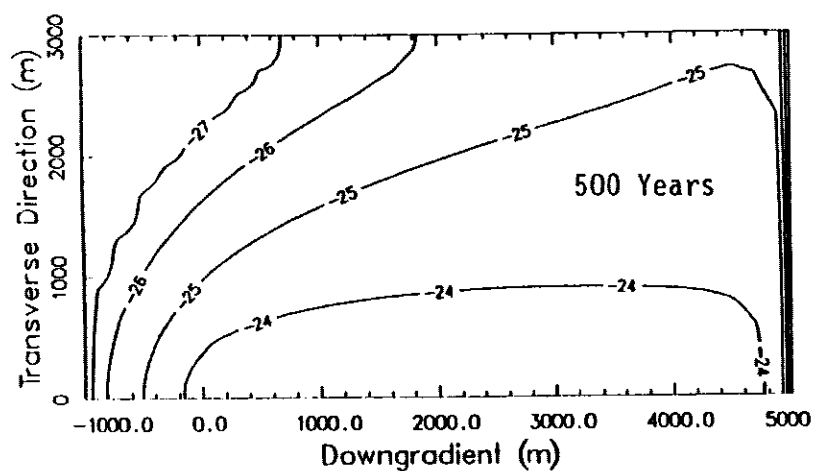


Figure 5-10a.  $\text{Cd}^{+2}$  Solute Transport (log conc. in g/mL) in the Aquifer  
500-4000 Years for 1.25 cm/yr Rainwater Recharge

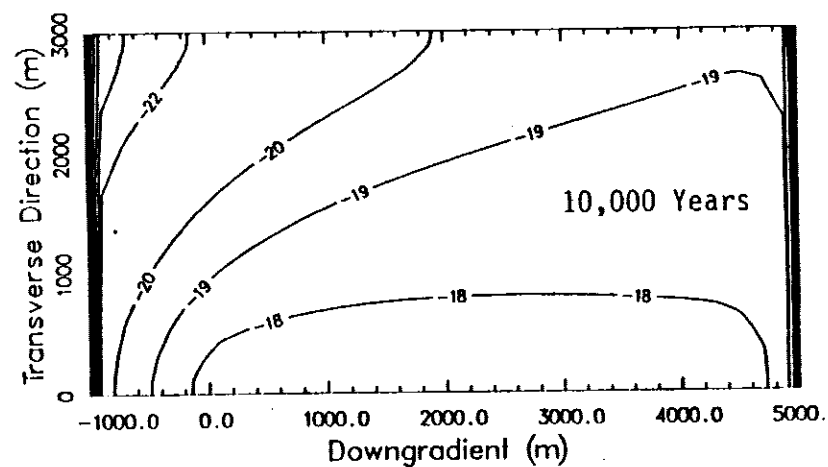
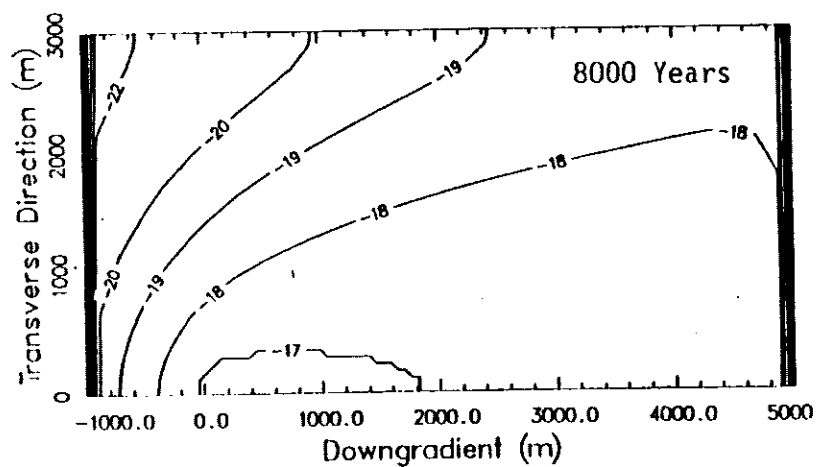
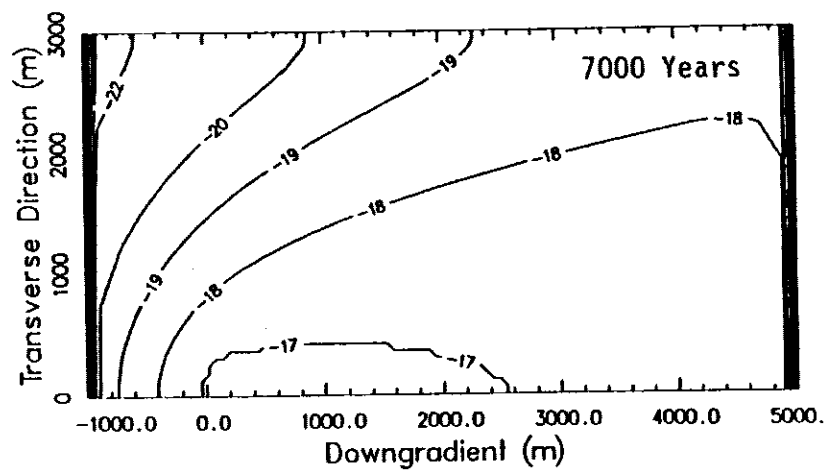
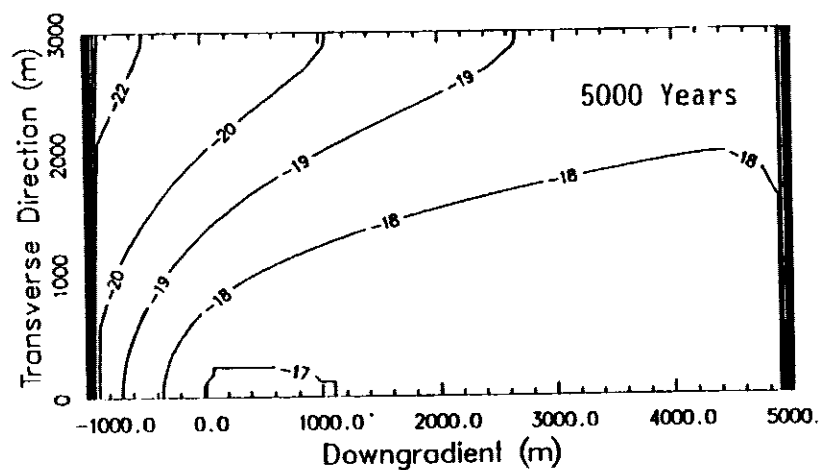


Figure 5-10b.  $\text{Cd}^{+2}$  Solute Transport (log conc. in g/mL) in the Aquifer  
5000-10,000 Years for 1.25 cm/yr Rainwater Recharge

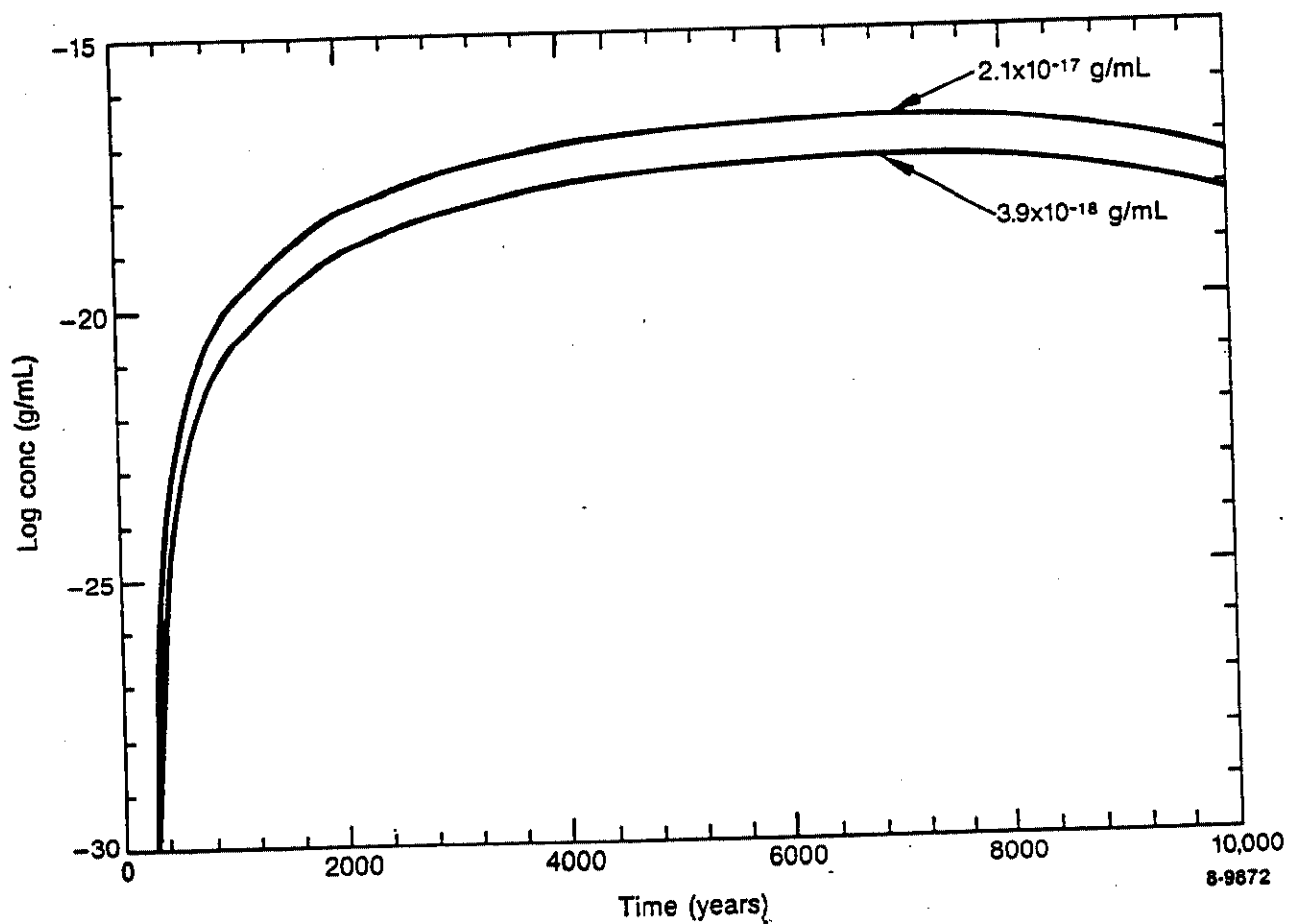


Figure 5-11. Cd<sup>2+</sup> Solute Concentration vs Time 0.5 and 5.0 km Down-gradient in the Aquifer for 1.25 cm/yr Rainwater Recharge

Figures 5-10a and 5-10c illustrate the contour lines of  $\text{Cd}^{+2}$  in the aquifer over a 500 to 10,000 year period. As with  $\text{NO}_3^-$  and  $\text{Cr}^{+6}$ , a  $K_d$  of zero was assumed for  $\text{Cd}^{+2}$  in the aquifer basalt. Therefore, the contour lines have the same shape and propagation patterns as the previous solutes. However, whereas an overall dilution factor of about  $10^6$  was observed from the alluvial source to 5.0 km downgradient in the aquifer for  $\text{NO}_3^-$  and  $\text{Cr}^{+2}$  in the 1.25 cm/yr rainwater recharge scenario, an overall dilution factor of about  $10^{14}$  is observed for  $\text{Cd}^{+2}$ . The much greater dilution factor is due to the hold up of  $\text{Cd}^{+2}$  in the vadose zone causing it to act like a constant source of solute to the aquifer rather than a pulse source.

Figure 5-11 indicates that between 3000 and 10,000 years the solute concentrations in the aquifer remain within a factor of 10 of their maxima. The maximum concentrations are  $2.1 \times 10^{-17}$  and  $3.9 \times 10^{-18}$  g/mL at about 7000 years. A mass balance check on the numerical printout of the plots indicates that less than 1.4% of the original  $\text{Cd}^{+2}$  inventory passes into the aquifer over the 10,000 year period modeled.

### 3.2 12.5 cm/yr Rainwater Recharge

Figures 5-12a and 5-12b illustrate the effect of ten times more rainwater recharge on the solute transport of  $\text{Cd}^{+2}$ . By 10,000 years, the most concentrated contour line reaching the aquifer is  $10^{-7}$  g/mL or three orders of magnitude greater than for the 1.25 cm/yr rainwater recharge scenario. The profile of the vadose contour lines for both recharge scenarios are about the same at 2000 and 10,000 years except the larger recharge results in two or three additional contour lines extending deeper into the vadose zone.

Figure 5-12b indicates a greater amount of  $\text{Cd}^{+2}$  is transported from the alluvial layer to the first and second interbeds than in Figure 5-9b for the 1.25 cm/yr rainwater recharge scenario. However, the additional

transport is not large. An analysis of the numerical printout data indicates that at 10,000 years 82.1, 13.6, and 0.03% of the original  $\text{Cd}^{+2}$  inventory is still contained in the alluvium, the first interbed, and the second interbed, respectively. About 4.3% of the  $\text{Cd}^{+2}$  reaches the aquifer which can be compared to 1.4% for the smaller recharge scenario.

A comparison of Figures 5-13b and 5-10b show that at least three orders of magnitude larger concentrations show up in the aquifer contour plots for the 12.5 cm/yr rainwater recharge scenario. In Figure 5-13b, the maximum contour line is  $10^{-14}$  while in Figure 5-10b the maximum line is  $10^{-17}$ . A comparison of the time history plots for the two recharge scenarios (i.e., Figures 5-11 and 5-14) show the same broad plateau for both scenarios. However the larger rainwater recharge rate produces maxima which are about 3000 times greater than the smaller recharge rate (c.f.,  $1.1 \times 10^{-14}$  in Figure 5-14 to  $3.9 \times 10^{-18}$  g/mL in Figure 5-11).

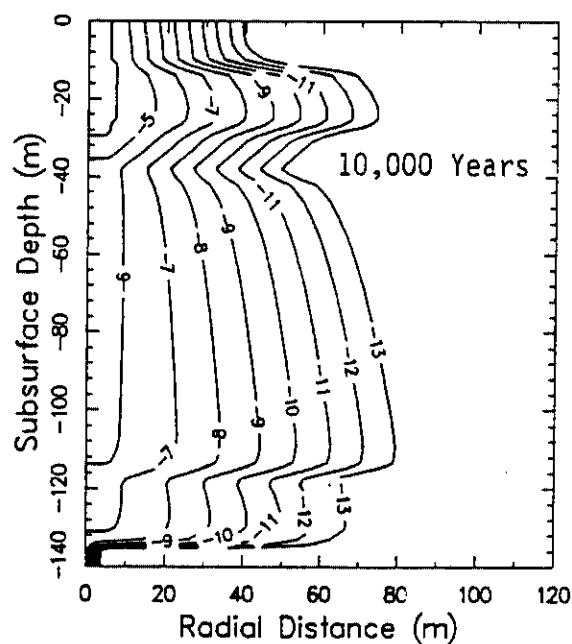
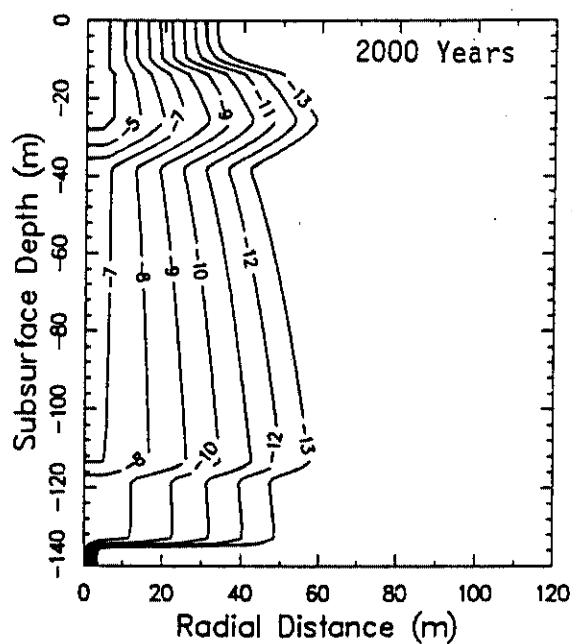
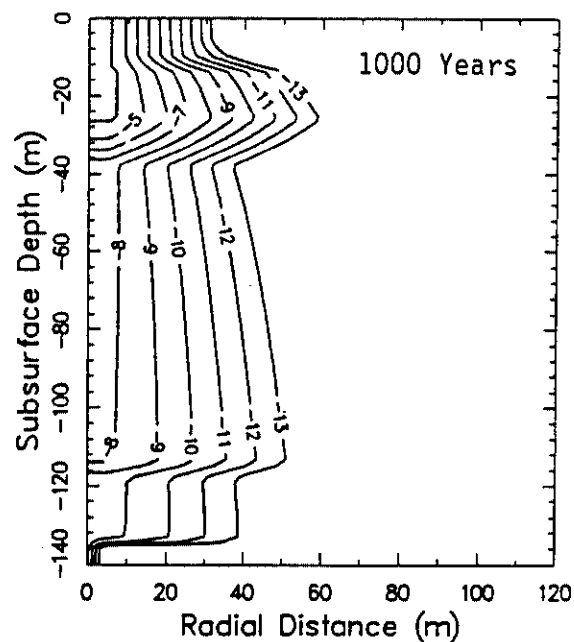
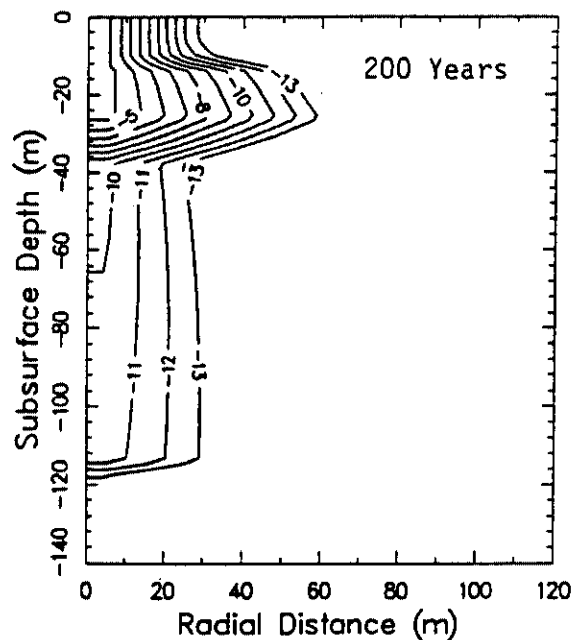


Figure 5-12a.  $\text{Cd}^{+2}$  Solute Transport (log conc. in g/mL) in the Vadose Zone 200-10,000 Years for 12.5 cm/yr Rainwater Recharge

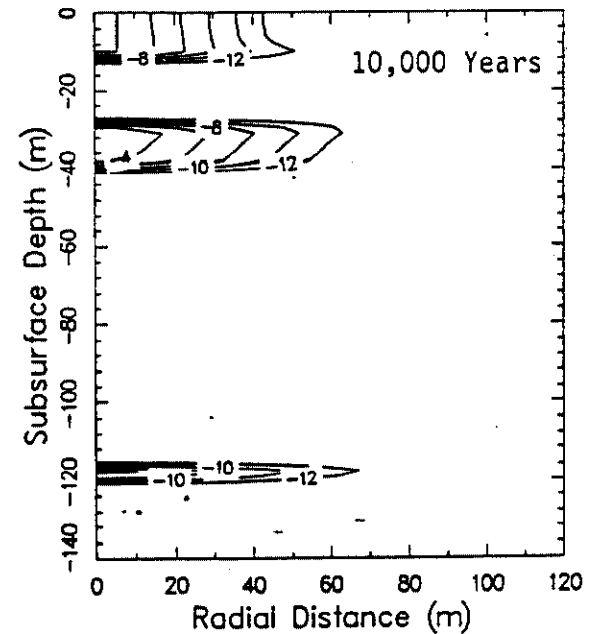
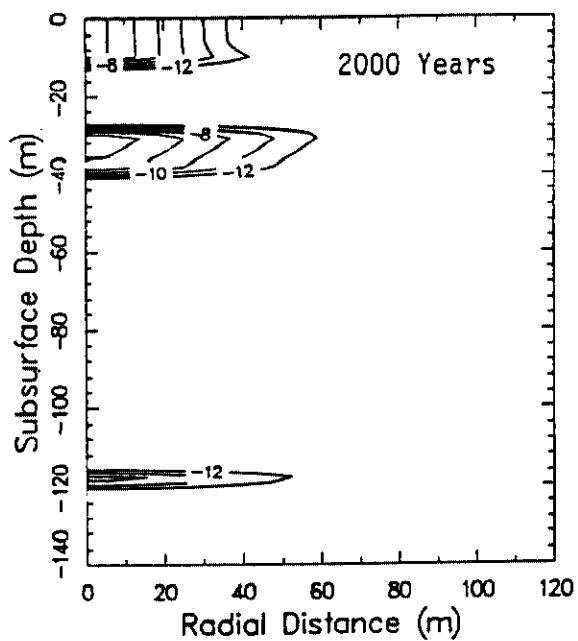
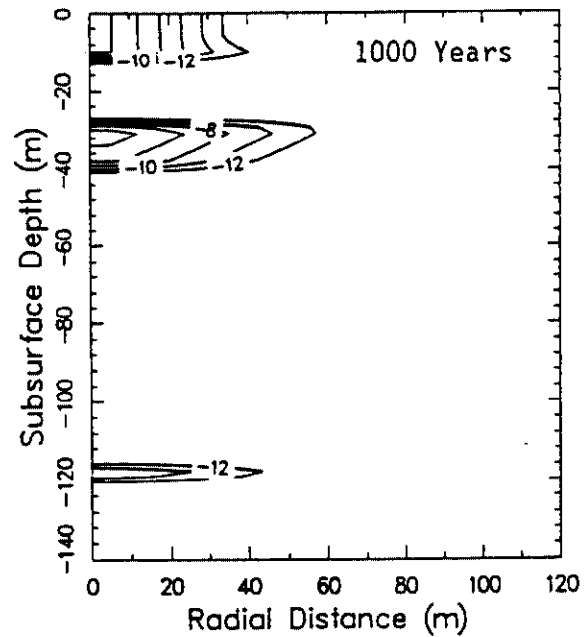
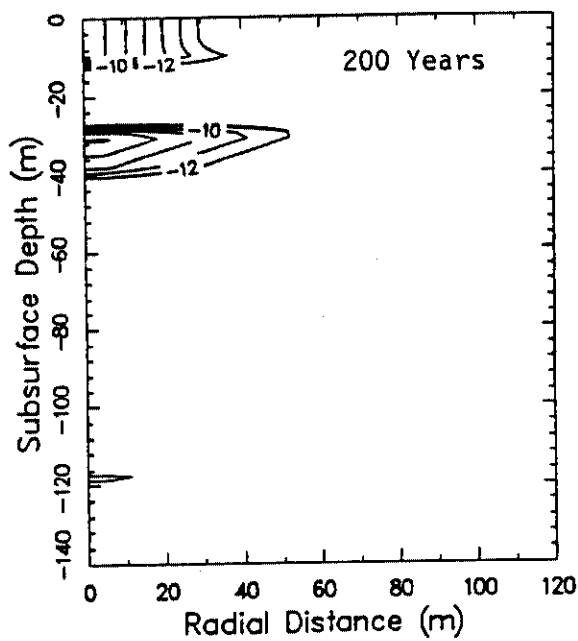


Figure 5-12b.  $\text{Cd}^{+2}$  Adsorbed Distribution (log conc. in g/g) in the Vadose Zone 200-10,000 Years for 12.5 cm/yr Rainwater Recharge

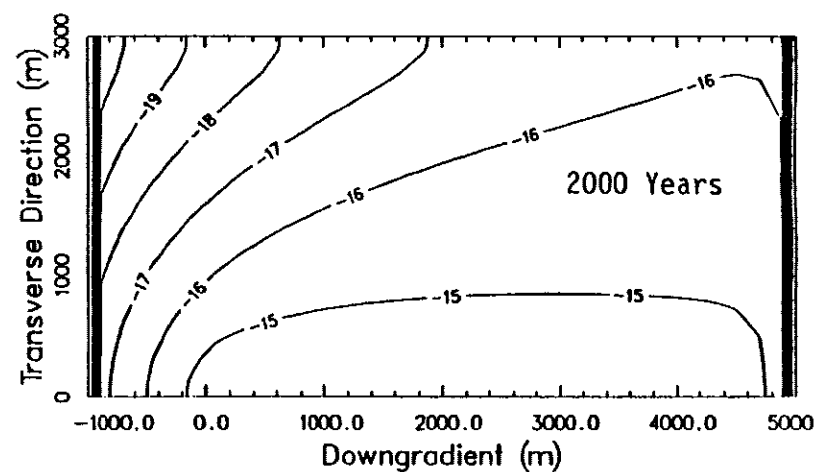
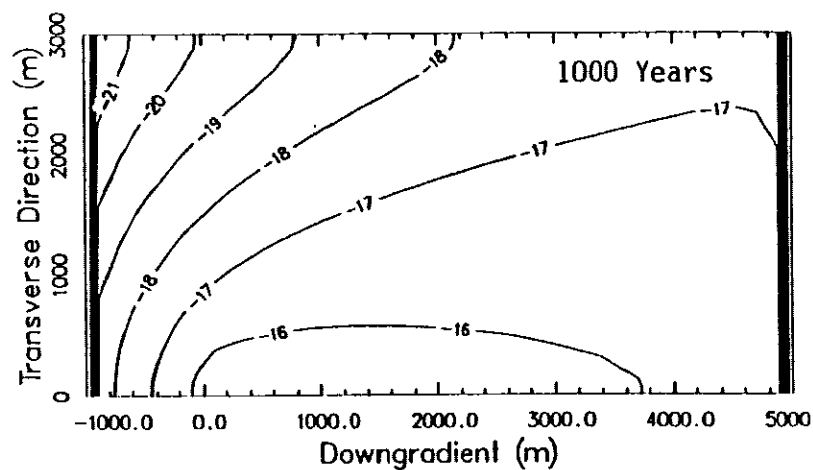
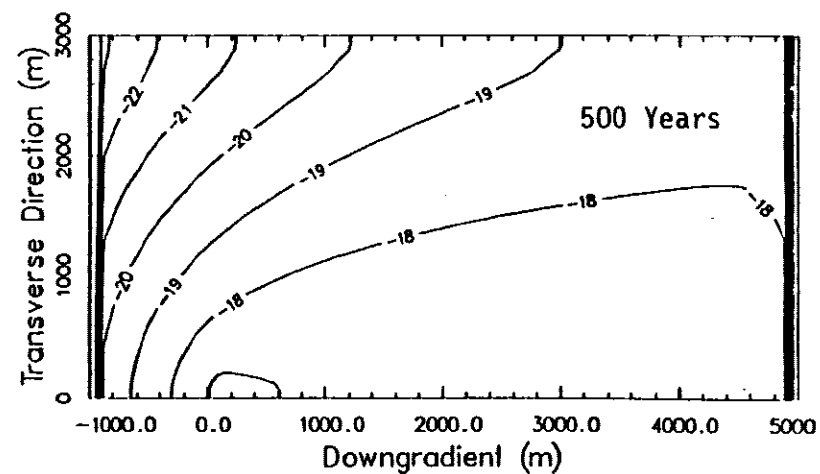
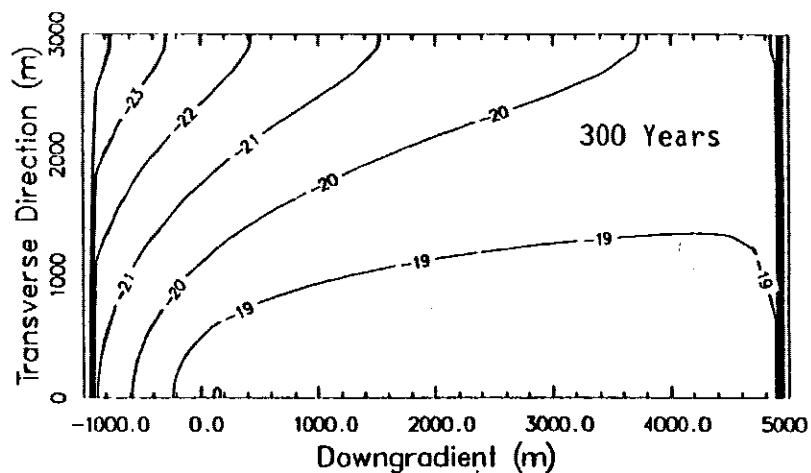


Figure 5-13a.  $\text{Cd}^{2+}$  Solute Transport (log conc. in g/mL) in the Aquifer  
300-2000 Years for 12.5 cm/yr Rainwater Recharge



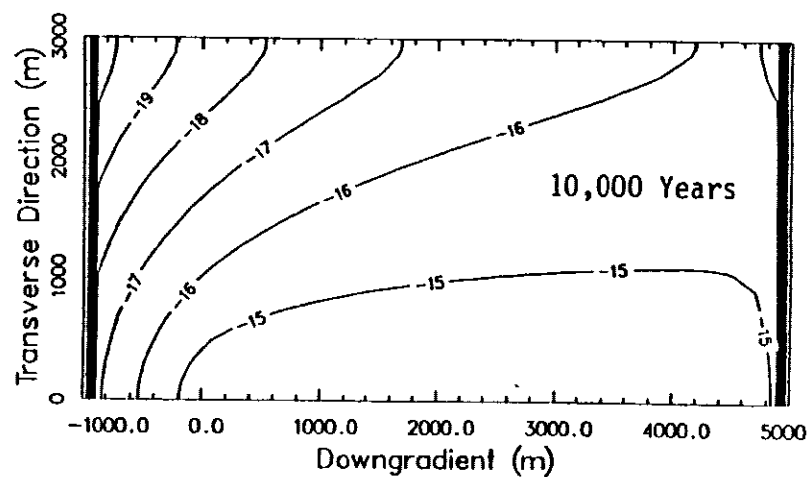
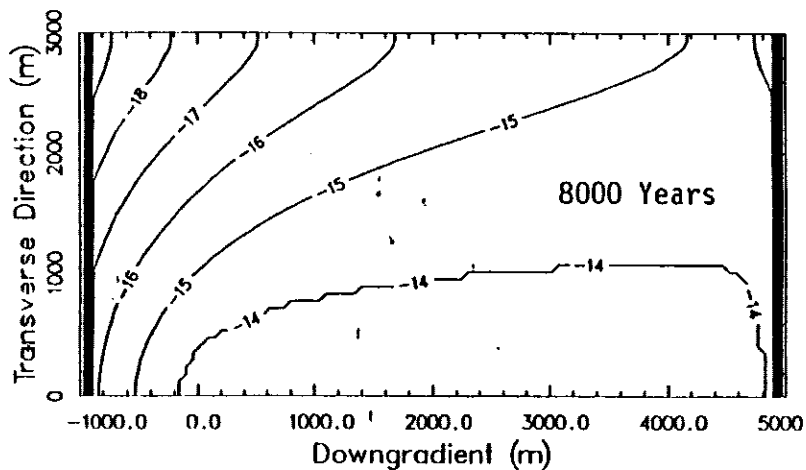
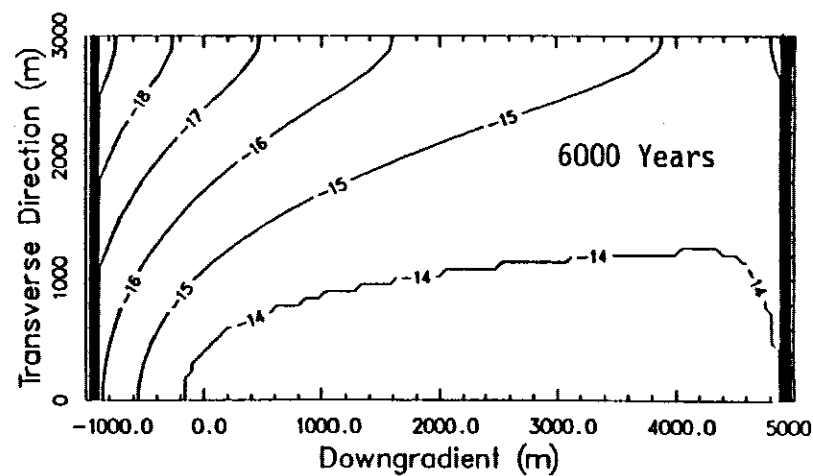
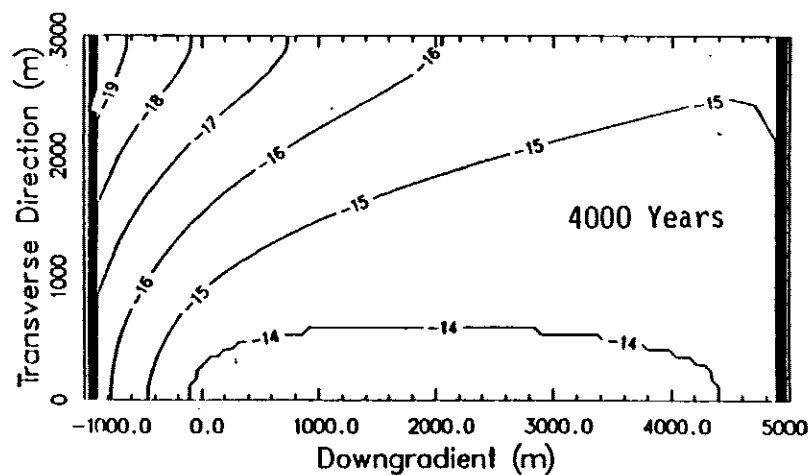


Figure 5-13b.  $\text{Cd}^{+2}$  Solute Transport (log conc. in g/mL) in the Aquifer  
4000-10,000 Years for 12.5 cm/yr Rainwater Recharge

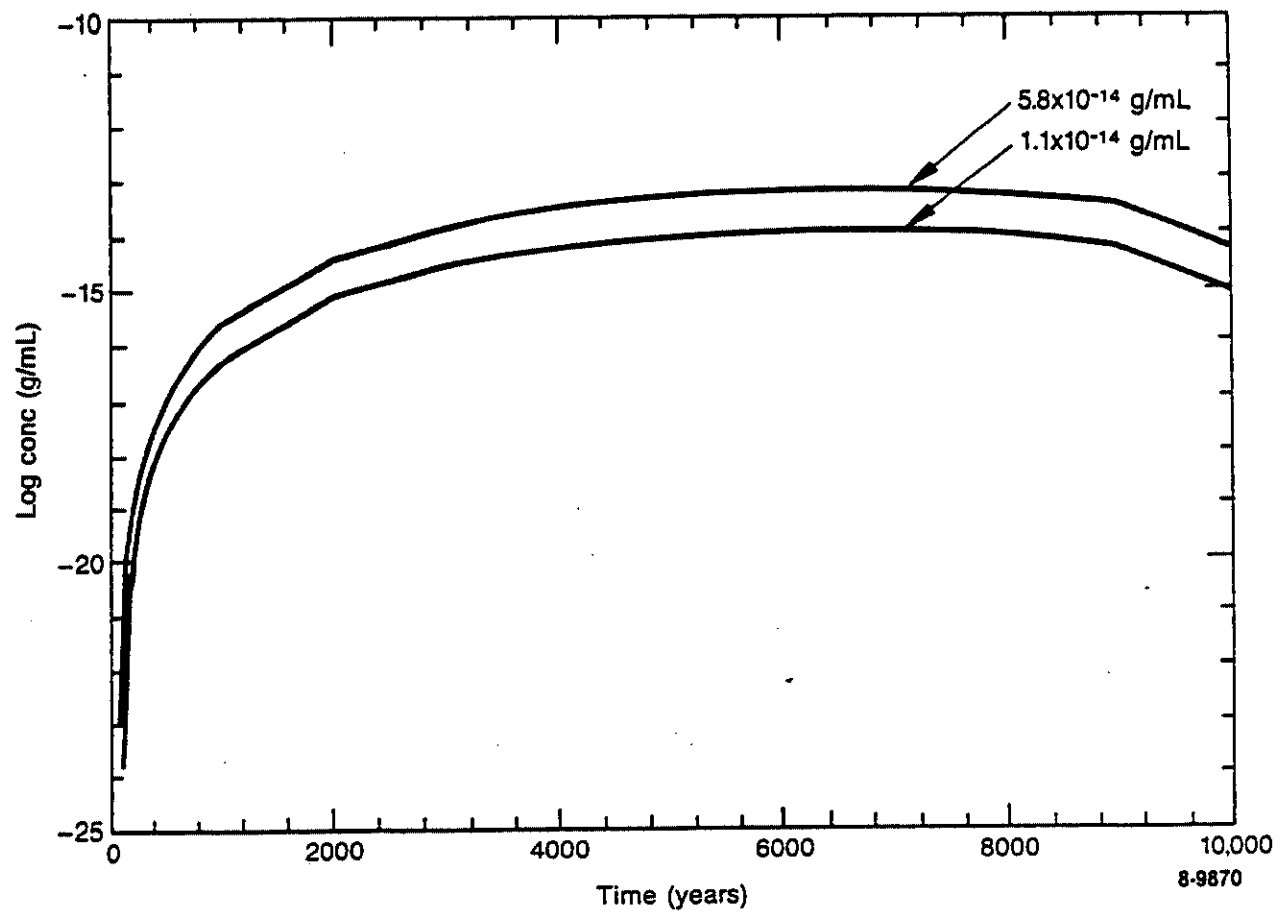


Figure 5-14.  $\text{Cd}^{+2}$  Solute Concentration vs Time 0.5 and 5.0 km Down-gradient in the Aquifer for 12.5 cm/yr Rainwater Recharge

## VI. COMPARISON OF CODE RESULTS TO DRINKING WATER STANDARDS

The maximum contaminant levels allowed in public water systems for nitrate (as N), chromium, and cadmium are 10, 0.05, and 0.01 mg/L as stipulated by the National Primary Drinking Water Regulations<sup>6</sup>. Since the nitrogen is only 14/62 parts of the nitrate ion, the drinking water standard would allow 44 mg/L of nitrate (i.e.,  $10 \times [62/14]$ ). To compare these limits to the TRACR3D code results (which are in units of g/mL) the above limits are multiplied by  $10^{-6}$  to give  $4.4 \times 10^{-5}$ ,  $5 \times 10^{-8}$ , and  $1 \times 10^{-8}$  g/mL, for nitrate, chromium, and cadmium, respectively.

The two positions modeled for comparison to the standards were 0.5 and 5.0 km directly downgradient in the aquifer (see Figure 4.1). Both positions represent locations where peak concentrations of the solutes would occur. The 5.0 km position was chosen for modeling because it is defined as the maximum distance allowed in 40 CFR 191 from waste emplacement to the boundary of a high-level waste repository.<sup>34</sup> At the boundary, the public would have access to well water. The 0.5 km position was modeled to examine the dilution capacity of the aquifer due to vertical and transverse mixing over a 10-fold downgradient distance near the point of solute entry into the aquifer.

Table 6.1 compares the drinking water standards to the peak concentrations of the solutes in the source-term alluvial cylinder, the vadose zone-aquifer interface directly below the cylinder, and the 0.5 and 5.0 km downgradient aquifer positions. The results indicate that  $\text{Cd}^{+2}$  solute concentrations at 5 km downgradient in the aquifer would be a factor of about  $10^9$  and  $10^6$  below the drinking water standards for the smaller and larger rainwater recharge rates, respectively. Based on the hydrogeological parameters used in this model, the solute transport for any element from the ICPP calcine with a  $K_d$  of 100 or greater would not be significant when compared to drinking water standards.

Table 6.1

Comparison of Model Results<sup>a</sup> Drinking Water Standards

<u>Peak Solute Concentrations (g/mL)</u>			
<u>1.25 cm/yr RAINWATER RECHARGE</u>	<u>NO<sub>3</sub><sup>-</sup></u>	<u>Cr<sup>+6</sup></u>	<u>Cd<sup>+2</sup></u>
Initial vadose source term	$3.7 \times 10^{-1}$	$3.7 \times 10^{-2}$	$3.0 \times 10^{-4}$
Vadose-aquifer interface	$4.5 \times 10^{-2}$	$4.5 \times 10^{-3}$	$8.2 \times 10^{-11}$
Aquifer 0.5 km downgradient	$2.2 \times 10^{-8}$	$2.2 \times 10^{-9}$	$2.1 \times 10^{-17}$
Aquifer 5.0 km downgradient	$4.0 \times 10^{-9}$	$4.0 \times 10^{-10}$	$3.9 \times 10^{-18}$
Drinking Water Limits	$4.4 \times 10^{-5}$	$5.0 \times 10^{-8}$	$1.0 \times 10^{-8}$
<u>Factor Below Drinking Water Limits</u>			
	<u>NO<sub>3</sub><sup>-</sup></u>	<u>Cr<sup>+6</sup></u>	<u>Cd<sup>+2</sup></u>
Aquifer at 0.5 km downgradient	$2.0 \times 10^3$	$2.3 \times 10^1$	$4.8 \times 10^8$
Aquifer at 5.0 km downgradient	$1.1 \times 10^4$	$1.3 \times 10^2$	$2.6 \times 10^9$
<u>Peak Solute Concentrations (g/mL)</u>			
<u>12.5 cm/yr RAINWATER RECHARGE</u>	<u>NO<sub>3</sub><sup>-</sup></u>	<u>Cr<sup>+6</sup></u>	<u>Cd<sup>+2</sup></u>
Initial vadose source term	$3.7 \times 10^{-1}$	$3.7 \times 10^{-2}$	$3.0 \times 10^{-4}$
Vadose-aquifer interface	$7.2 \times 10^{-2}$	$7.2 \times 10^{-3}$	$1.1 \times 10^{-7}$
Aquifer 0.5 km downgradient	$8.4 \times 10^{-8}$	$9.2 \times 10^{-9}$	$5.8 \times 10^{-14}$
Aquifer 5.0 km downgradient	$1.5 \times 10^{-8}$	$1.6 \times 10^{-9}$	$1.1 \times 10^{-14}$
Drinking Water Limits	$4.4 \times 10^{-5}$	$5.0 \times 10^{-8}$	$1.0 \times 10^{-8}$
<u>Factor Below Drinking Water Limits</u>			
	<u>NO<sub>3</sub><sup>-</sup></u>	<u>Cr<sup>+6</sup></u>	<u>Cd<sup>+2</sup></u>
Aquifer at 0.5 km downgradient	$5.2 \times 10^2$	5.4	$1.7 \times 10^5$
Aquifer at 5.0 km downgradient	$2.9 \times 10^3$	$3.1 \times 10^1$	$9.1 \times 10^5$

<sup>a</sup> Based on one 2000 m<sup>3</sup> capacity CSSF

The peak  $\text{NO}_3^-$  levels predicted are about a factor of  $10^4$  and  $10^3$  below the drinking water standards at 5.0 km downgradient in the aquifer. These results indicate that based on the hydrogeological parameters assumed, the  $\text{NO}_3^-$  levels would not exceed the drinking water standards even for a cluster of CSSF containing 13 times the amount of solute inventory modeled from which a superposition of the contaminant plumes might conceivably increase the peak levels by a factor of ten.

Of the three solutes modeled,  $\text{Cr}^{+6}$  is the only one which potentially could approach drinking water standards in the aquifer based on the assumed parameters. The peak  $\text{Cr}^{+6}$  levels predicted are a factor 130 and 31 below drinking water standards 5.0 km downgradient in the aquifer for 1.25 and 12.5 cm/yr rainwater recharge rates, respectively. If a cluster of CSSF were modeled with a configuration that would cause superposition of the contaminant plumes to increase solute concentrations by a factor of 10 (i.e., line them up parallel to the aquifer flow direction), the predicted factors would decrease to 13 and 0.31, respectively.

## VII. CONCLUSIONS AND RECOMMENDATIONS

Of the three solutes modeled,  $\text{Cr}^{+6}$  is the only one for which further sensitivity studies are recommended. Variation of assumed hydrogeological parameters (e.g., interbed thickness, porosity, % water saturation, hydraulic conductivity, etc.) within conceivable bounding limits would not result in predicted values of  $\text{NO}_3^-$  or  $\text{Cd}^{+2}$  concentrations that would approach drinking water standards in the aquifer. The sensitivity of rainwater recharge was examined in this study and found not to be crucial for the latter solutes. The transport of  $\text{Cd}^{+2}$  is extremely sensitive to  $K_d$ , but a  $K_d$  of about zero would be required (as is the case with  $\text{Cr}^{+6}$ ) for predicted values of  $\text{Cd}^{+2}$  to approach drinking water standards. This would not be a realistic bounding parameter.

Depending on assumptions, predicted levels of  $\text{Cr}^{+6}$  could approach drinking water standards for a cluster of CSSF containing 13 times the amount of solute modeled. For a given inventory and rainwater recharge rate, the most sensitive parameter for a highly soluble and non-adsorbing solute would be its release rate. Since an instantaneous release scenario was used for this study, further modeling should incorporate realistic release rates based on assumed rainwater infiltration rates to the calcine which start slowly and increase with time. Based on corrosion data given in Chapter I, Section 2.3, the time for rainwater infiltration (i.e., recharge) to the calcine to equal that in the surrounding alluvium might take several hundred years once the integrity of the bin wall was breached by a pinhole leak. Therefore, more realistic release rate scenarios (i.e., other than instantaneous) should be modeled to determine their effect on predicted  $\text{Cr}^{+6}$  levels compared to the drinking water standards.

A second recommendation is to use a geochemical code to check for speciation or solubility limitations specific to the INEL groundwater. Further geochemical evaluation would probably have little impact on the

conclusions of this particular study as neither the  $\text{NO}_3^-$  or  $\text{Cr}^{+6}$  solute should have a tendency to form other species in the oxic environment of the INEL ground waters. And even if a geochemical code were to predict higher solubilities and a smaller  $K_d$  for  $\text{Cd}^{+2}$ , it still would not be expected to reach levels of concern in the aquifer. However, for future modeling studies involving elements that could form solubility limited carbonates, bicarbonates or hydroxides or undergo speciation (e.g., Sr, Cs, Pu, and Am), a geochemical code could predict which species and concentrations to model.

## VIII. REFERENCES

1. D. A. Knecht and J. R. Berreth, Strategy Planning for the Long-Term Management of ICPP High-Level Radioactive Waste, WINCC-11392 (January 1988).
2. U.S. DOE, Environmental Evaluation of Alternatives for Long-Term Management of Defense High-Level Radioactive Wastes at the Idaho Chemical Processing Plant, IDO-10105 (September 1982).
3. ERDA (U.S. Energy Research and Development Administration), Final Environmental Impact Statement, Waste Management Operations, Idaho National Engineering Laboratory, P II-95, ERDA-1536, (September 1977).
4. T. L. Hoffman, "Corrosion Monitoring of Storage Bins for Radioactive Calcines", Materials Performance, Vol. 15, p 40 (January 1976).
5. Nickel Co. Inc., Corrosion Resistance of the Austenitic Chromium-Nickel Stainless Steels in Chemical Environments, Bulletin by the International Nickel Company, Inc., New York, NY (1963).
6. Environmental Protection Agency, 40 CFR Part 141, National Primary Drinking Water Regulations, Code of Federal Regulations, Vol 40, p 526 (July 1, 1987).
7. B. D. Lewis and R. G. Jensen, Hydrologic Conditions at the Idaho National Engineering Laboratory, Idaho: 1979-1981 Update, U. S. Geological Survey Open-File Report 84-230, IDO-22066 (June 1984).
8. J. T. Barraclough, et.al., Hydrologic Conditions at the Idaho National Engineering Laboratory, Idaho Emphasis: 1974-1978, U.S. Geological Survey Water-Resources Investigation Open File Report 81-526, IDO-22060 (April 1981).
9. J. T. Barraclough and R. G. Jensen, Hydrological Data for the Idaho National Engineering Laboratory Site, Idaho 1971 to 1973, U.S. Geological Survey Water Resources Division Open-File Report 75-318, IDO-22055 (January 1976).
10. J. D. Robertson, et.al., The influence of Liquid Waste Disposal on the Geochemistry of Water at the National Reactor Testing Station Idaho: 1952-1970, U.S. Geological Survey Water Resources Division, IDO-22053 (February 1974).
11. D. A. Morris, et.al., Hydrology of Subsurface Waste Disposal National Reactor Testing Station Idaho, Annual Progress Report 1964, U.S. Department of the Interior Geological Survey, IDO-22047 (May 1965).
12. J. T. Barraclough et.al., Hydrology of the National Reactor Testing Station Idaho 1966, U. S. Geological Survey Water Resources Division, IDO-22049 (October 1967).



13. J. B. Robertson, Digital Modeling of Radioactive and Chemical Waste Transport in the Snake River Plain Aquifer at the National Reactor Testing Station, Idaho, U.S. Geological Survey National Reactor Testing Station Open-File Report, IDO-22054 (May 1974).
14. G. H. Chase, et.al., Completion Report for Observation Wells 1 through 49, 51, 54, 55, 56, 80, and 81 at the National Reactor Testing Station, Idaho, U.S. Geological Survey, ID-22045 (1964).
15. W. S. Keys, Completion Report for Contracts AT(10-1)-1054 and AT(10-1)-1122. Drilling, Casing, and Cementing Observation Wells at the National Reactor Testing Station, Idaho, USAEC, IDO-12022 (1963).
16. F. J. Keneshea and T. H. Smith, "Risk Analysis for Transuranic Waste at the Idaho National Engineering Laboratory", Nuclear and Chemical Waste Management, Vol 4, pp. 63-79 (1983).
17. B. L. Schmalz and W. L. Polzer, "Tritiated Water Distribution in Unsaturated Soil", Soil Science, Vol. 108, pp. 43-47 (1969).
18. L. C. Hull, Hydrogeologic Assessment of Land Disposal Unit, CPP-37 ICPP Gravel Pit #2, no report number (February 1987).
19. J. T. Barraclough, J. B. Robertson, and V. J. Janzer, Hydrology of the Solid Waste Burial Ground, as Related to the Potential Migration of Radionuclides, U. S. Geological Survey Open-File Report 76-471, IDO-22056 (1976).
20. D. A. Morris et.al., Hydrology of Waste Disposal, National Reactor Testing Station, Idaho, Annual Progress Report, 1962, U. S. Geological Survey, IDO-22044 (1963).
21. R. C. Weast and M. J. Astle, Eds., CRC Handbook of Chemistry and Physics, 63th Edition, Chemical Rubber Publishing Co., p. F-51 (1982-1983).
22. J. A. Del Debbio and T. R. Thomas, "Determination of Technetium and Selenium Transport Properties in Laboratory Soil Columns," Twelfth International Symposium on the Scientific Basis of Nuclear Waste Management, West Berlin, October 10-13 (1988).
23. D. C. Stewart, Data for Radioactive Waste Management and Nuclear Applications, John Wiley & Sons, Publishers, pp. 130-134 (1985).
24. J. W. Bigger and D. R. Nielsen, Spatial Variability of the Leaching Characteristics of a Field Soil, Water Resources Research, Vol 12, pp. 75-84 (1976).
25. M. Th. Van Genuchten, Determining Transport Parameters from Solute Displacement Experiments, U. S. Department of Agriculture Science and Education Administration, U. S. Salinity Laboratory Riverside, CF, Research Report No. 118 (April 1980).

26. R. C. Weast and M J. Astle, Eds., CRC Handbook of Chemistry and Physics, 63th Edition, Chemical Rubber Publishing Co., p. D-174 (1982-1983).
27. H. E. Doner, Chloride as a Factor in Mobilities of Ni(II), Cu(II), and Cd(II) in Soil, Soil Science Society American Journal, Vol. 42, pp. 882-885 (1978).
28. J. E. Mosier, et.al., Low Level Waste Management: A Compilation of Models and Monitoring Techniques, ORNL/SUB-79/13617/2 (April 1980).
29. J. A. Lieberman, et.al., Performance Assessment National Review Group, RFW-CRWM-85-01, (no date) by Weston Consultants, 2301 Research Boulevard, Rockville, MD.
30. J. M. Hubbell, et.al., Annual Progress Report: FY-1986, Subsurface Investigations Program at the Radioactive Waste Management Complex of the Idaho National Engineering Laboratory, DOE/ID-10153, p. 53 (January 1987).
31. N. K. Hayden, Nevada Nuclear Waste Storage Investigations Project. Benchmarking NNWSI Flow and Transport Codes: Cove 1 Results, SAND-84-0996, (June 1985).
32. J. F. Kerrisk, "Applications of Geochemical Modeling to Site Characterization and Radionuclide Transport in the NNWSI Project," Proceedings of the Conference on the Application of Geochemical Models to High-Level Nuclear Waste Repository Assessment, NUREG/CP-0062, ORNL/TM-9585 (May 1985).
33. B. J. Travis, TRACR3D: A Model of Flow and Transport in Porous/Fractured Media, LA-9667-MS, (May 1984).
34. Environmental Protection Agency, 40 CFR Part 191, Environmental Standards for the Management and Disposal of Spent Nuclear Fuel. High-Level and Transuranic Radioactive Wastes: Final Rule, Federal Register, Vol. 50, No. 182, p 38077, column 3, (September 19, 1985).